# The influence of horizontal resolution and boundary forcing in simulating hurricanes over the South Atlantic Ocean using WRF

Gemma Kendall Pelton Bluff
*BSc in Environmental and Geographical Science*
*BSc (HONS) in Atmospheric Science*

Dissertation presented for the degree of Master of Science in the Department of Environmental and Geographical Science




University of Cape Town

June 2017

Supervisor: Dr Babatunde J. Abiodun

# Content's Page

## Plagiarism Declaration

I know that plagiarism is wrong. Plagiarism is to use another's work and pretend that it is one's own. Allowing another to copy my work and use it as their own is also plagiarism.

This dissertation is my own work.

I have not allowed and will not allow anyone to copy my work with the intention of passing it off as his or her own work.

I acknowledge that working with someone on my dissertation is allowed, but only if a mutual effort is made and different examples and, where necessary, wordings are used.

Name: Gemma Kendall Pelton Bluff
Student No: BLFGEM001

"I acknowledge that plagiarism (any other attempt to pass another's work as one's own) is both unethical and against university rules. I hereby confirm that I have not plagiarised in the preparation of this thesis and have not allowed anyone to copy my work."

# Acknowledgements

I would like to thank first and foremost Dr Babatunde Abiodun for his constant and unwavering supervision and help throughout my Master's degree, and for his constant faith in me and in my ability. Thank you to the University of Cape Town for providing me with this opportunity to further my studies and to grow in my academic field. Thirdly, I would like to thank the University for awarding me the *Masters Research Scholarship*, Dr Abiodun for awarding me the *Top-Up Studies Bursary*, and the NRF for awarding me the *Masters Freestanding Scholarship;* without which this degree would not have been possible. Fourthly, to Roland Takong, who kindly and patiently provided many vital months of technical assistance and support – you made part of this thesis a reality! Furthermore, to Shakirudeen Lawal, Linda Maoyi, Stephen Ogungbenro, and Mariam Nguvava for their on-going and unwavering support. Thank you to Myra Naik and Sabina Abba Omar for proofreading my thesis. Lastly, to my family – Mom and Dad, thank you for affording me the time to complete my Master's and supporting me unconditionally, and Kyla Bluff, thank you for the time put in proofreading my thesis on such short notice. And to my friends (Bethany Wright you were my rock through all the difficult times, Matthew Rosenberg you were there when I needed you most, and Kirsty Nefdt, thank you for your constant support and motivation) – you got me through this year. Without you this degree would have been impossible.

# List of Acronyms

| | |
|---|---|
| ACW03 | WRF simulation of Hurricane Anita forced with CFSR at a resolution of 3.3 km |
| ACW10 | WRF simulation of Hurricane Anita forced with CFSR at a resolution of 10 km |
| ACW30 | WRF simulation of Hurricane Anita forced with CFSR at a resolution of 30 km |
| AEW03 | WRF simulation of Hurricane Anita forced with ERAINT at a resolution of 3.3 km |
| AEW10 | WRF simulation of Hurricane Anita forced with ERAINT at a resolution of 10 km |
| AEW30 | WRF simulation of Hurricane Anita forced with ERAINT at a resolution of 30 km |
| CFSR | National Centers for Environmental Prediction Climate Forecast System Reanalysis |
| CCW03 | WRF simulation of Hurricane Catarina forced with CFSR at a resolution of 3.3 km |
| CCW10 | WRF simulation of Hurricane Catarina forced with CFSR at a resolution of 10 km |
| CCW30 | WRF simulation of Hurricane Catarina forced with CFSR at a resolution of 30 km |
| CEW03 | WRF simulation of Hurricane Catarina forced with ERAINT at a resolution of 3.3 km |
| CEW10 | WRF simulation of Hurricane Catarina forced with ERAINT at a resolution of 10 km |
| CEW30 | WRF simulation of Hurricane Catarina forced with ERAINT at a resolution of 30 km |

| | |
|---|---|
| ECMWF | European Centre for Medium-Range Weather Forecasts |
| ENSO | El Niño–Southern Oscillation |
| ERAINT | European Centre for Medium-Range Weather Forecasts ERA-Interim reanalysis |
| GFS | global forecast system |
| GOES | Geostationary Operational Environmental Satellite system |
| IBT | International Best Track and Archive for Climate Stewardship data |
| IPCC | Intergovernmental Panel on Climate Change |
| ITCZ | Intertropical Convergence Zone |
| MLC | mid-latitude cyclone |
| MSLP | mean sea level pressure |
| NCAR | National Center for Atmospheric Research |
| NCEP | National Centers for Environmental Prediction |
| NCEP/DOE | NCEP/Department of Energy |
| NH | Northern Hemisphere |
| NNRA | NCAR Reanalysis |
| NOAA | National Oceanic and Atmospheric Administration |
| SACZ | South Atlantic Convergence Zone |
| SAO | South Atlantic Ocean |
| SH | Southern Hemisphere |
| ST | subtropical cyclones |
| SST | sea-surface temperatures |

| | |
|---|---|
| TC | tropical cyclone |
| TRMM | Tropical Rainfall Measuring Mission |
| WCRs | warm core rings |
| WRF | Weather Research and Forecasting |

# List of Figures

# List of Tables

## Abstract

A hurricane is a threat to socio-economic activities in coastal communities bordering the South Atlantic Ocean (SAO). Hurricanes rarely form over this region and as such these communities are not prepared for them. Previous studies have suggested that anthropogenic warming may lead to more frequent hurricanes over the region and have demonstrated the capability of the Weather Research and Forecasting model (WRF) in capturing the impacts of the warming on hurricanes. However, none of the studies have investigated how the model's horizontal resolution and boundary forcing could alter the characteristics of simulated hurricanes. The present study used WRF to perform a series of experiments to simulate two hurricanes (Hurricane Catarina and Hurricane Anita) over the SAO at three horizontal resolutions (3.3 km, 10 km, and 30 km), using two reanalysis datasets (ERA-Interim (hereafter ERAINT) and NCEP CFSR (hereafter CFSR)) as the boundary forcing data. The performances of the reanalysis and WRF are compared with observational data from the International Best Track and Archive for Climate Stewardship.

The results show that both reanalyses datasets give a good representation of the two hurricanes, but they grossly underestimate the intensity thereof. CFSR gives a better representation than that of ERAINT. However, both reanalyses also suggest that the South Atlantic Convergence Zone may be the moisture belt for hurricane formation over the SAO. WRF gives a credible simulation of the hurricanes. In simulating Hurricane Catarina, WRF performs best at a 10 km resolution; but in reproducing Hurricane Anita, the model performs best at a 3.3 km resolution. For both cases, the model performs better when forced with ERAINT than with CFSR. Hence, the study shows that increasing the resolution of the model may not necessarily improve the simulated hurricane over the SAO, and that, the quality of the simulated hurricane depends on the dataset that provides the boundary forcing. The results of the study have improved the understanding of hurricane characteristics in the SAO, and have shown the potentials of WRF to forecast and project future events as well as for downscaling the potential impacts of future climate change on hurricanes over the SAO.

# 1 Introduction

## 1.1 What is a tropical cyclone?

A tropical cyclone (TC) is a small intense rotating low-pressure system with bands of cloud spiralling away from the core (Figure 1.1). This warm-cored, non-frontal system is about 550 km wide (Pidwirny, 2006a) and is often associated with wind gusts (in excess of 25 m $s^{-1}$), low surface pressure (approximately 950 hPa), thunderstorms, heavy rain squalls, and tornadoes (Bureau of Meteorology, 2017; Smithson et *al.*, 2008; Pidwirny, 2006a). As their name suggests, TCs only form in the tropics (*i.e.* within 25° North and South of the Equator). TCs are also called hurricanes or typhoons depending on the location of their development. They are called typhoons over the western North Pacific Ocean and hurricanes in the western Atlantic and eastern North Pacific Oceans (Emanuel, 2003; NOAA, 1999; Pezza and Simmonds. 2006; Landsea, 2011a). TCs usually require warm oceanic waters with temperatures greater than 26°C, which means that they form during each hemisphere's summer and autumn seasons, and dissipate over land when the warm moist water-source is depleted and surface friction dominates.

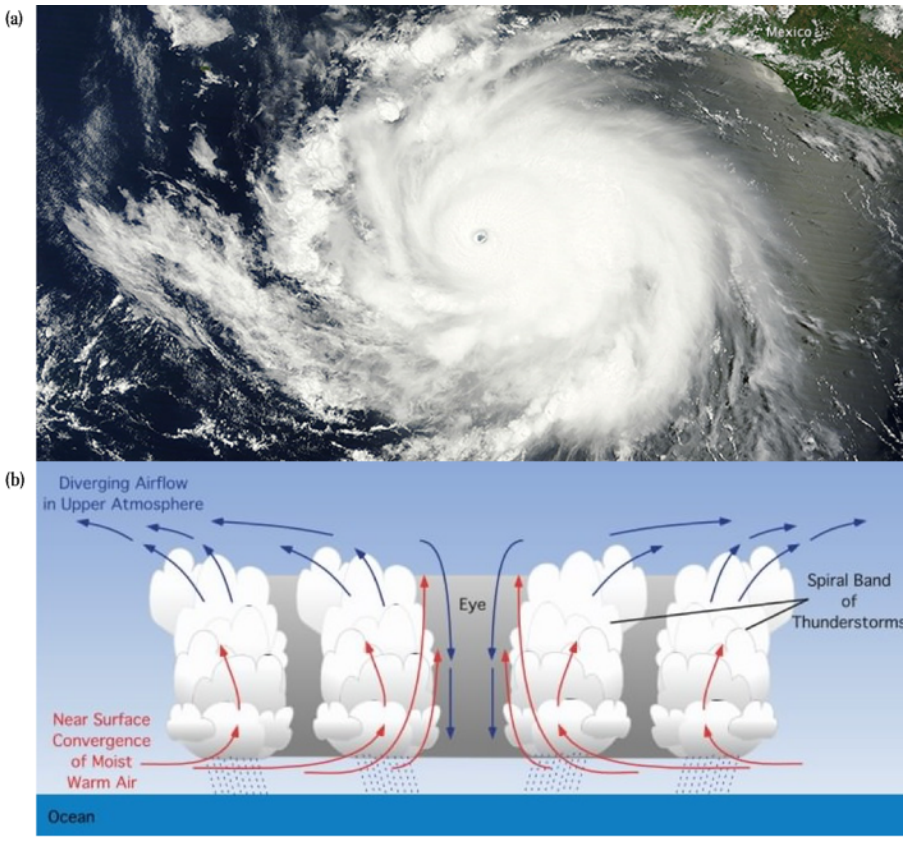


**Figure 1.1**: The spatial and vertical structure of a tropical cyclone, panel (a) and (b) respectively *(NASA: Earth Observatory, 2014; Pidwirny, 2006a)*

### 1.1.1 The difference between a tropical cyclone and a mid-latitude cyclone

A TC differs from a mid-latitude cyclone (MLC; also known as an extra-tropical cyclone; Figure 1.2). A MLC is a low-pressure system that forms in the mid-latitudes ($30^{o}$ – $55^{o}$N and $30^{o}$ – $55^{o}$S). Although both TCs and MLCs are low-pressure systems, a TC is warm-cored while a MLC is cold-cored. A TC is a non-frontal system whereas a MLC is associated with frontal systems (warm, cold, and occluded fronts), which may reach 970 hPa at the surface (Pidwirny, 2006b). TCs are generally smaller but more intense than MLCs, which can reach 2000 km in diameter. Lastly, TCs and MLCs trajectories follow different directions. While TCs generally propagate westerly, the MLC, which follows the Rossby Wave, propagates eastward in both the Northern and Southern Hemisphere (hereafter NH and SH; Marshak, 2008).

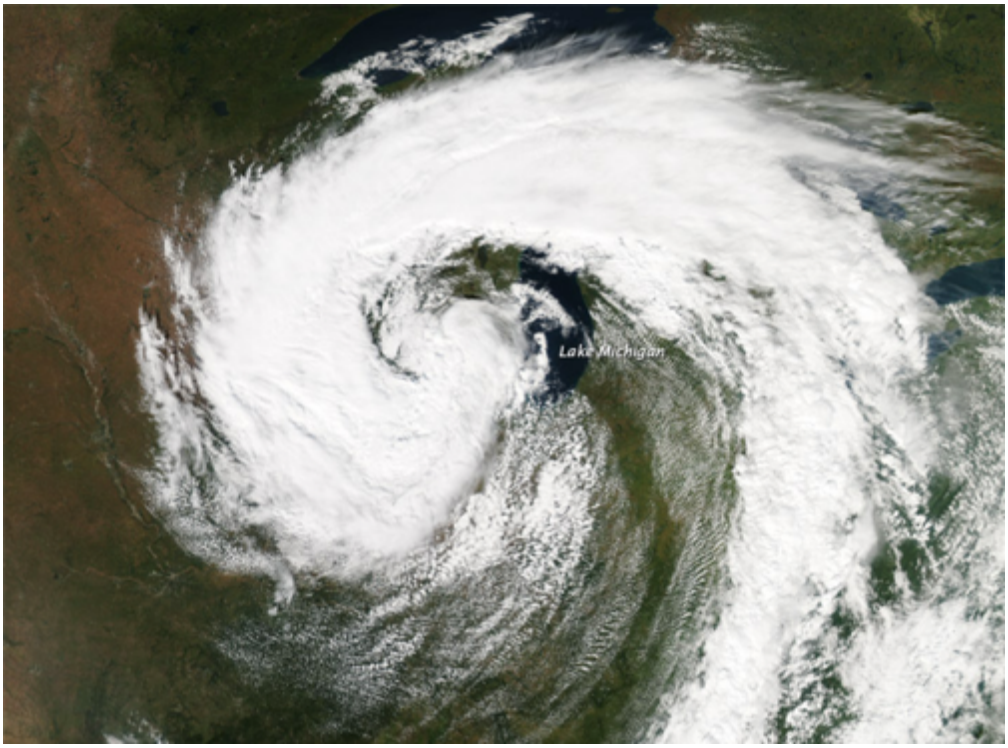


**Figure 1.2**: The spatial structure of a mid-latitude cyclone *(Schmaltz, 2011)*

### 1.1.2 Subtropical cyclones

It is important to know that some cyclone systems have some characteristics of TCs and MLCs. These are subtropical cyclones (ST), formerly MLCs transitioning into TCs. They form when a deep cold-core MLC drops into the subtropics (over the North and South Atlantic, and the southwest Indian Ocean basins) and loses its frontal boundaries. However, STs only require sea-surface temperatures (SST) of $23^{o}$C, compared to TCs that need SST

exceeding 26°C (Evans and Braun, 2012). There are two types of STs: the first is an upper-level, cold-cored, low-pressure system with the extension of its circulation to the surface; while the second is a mesoscale cyclone that begins near, or in, the horizontal wind shear frontolyzing zone, and that is a short-lived, cold- or warm-cored, marine system (Evans and Braun, 2012). STs have characteristics of both TCs (in that convective clouds provide much of their energy as they do for TCs) and MLCs (in that there is "a weak to moderate horizontal temperature gradient region like MLCs") (Landsea, 2011b).

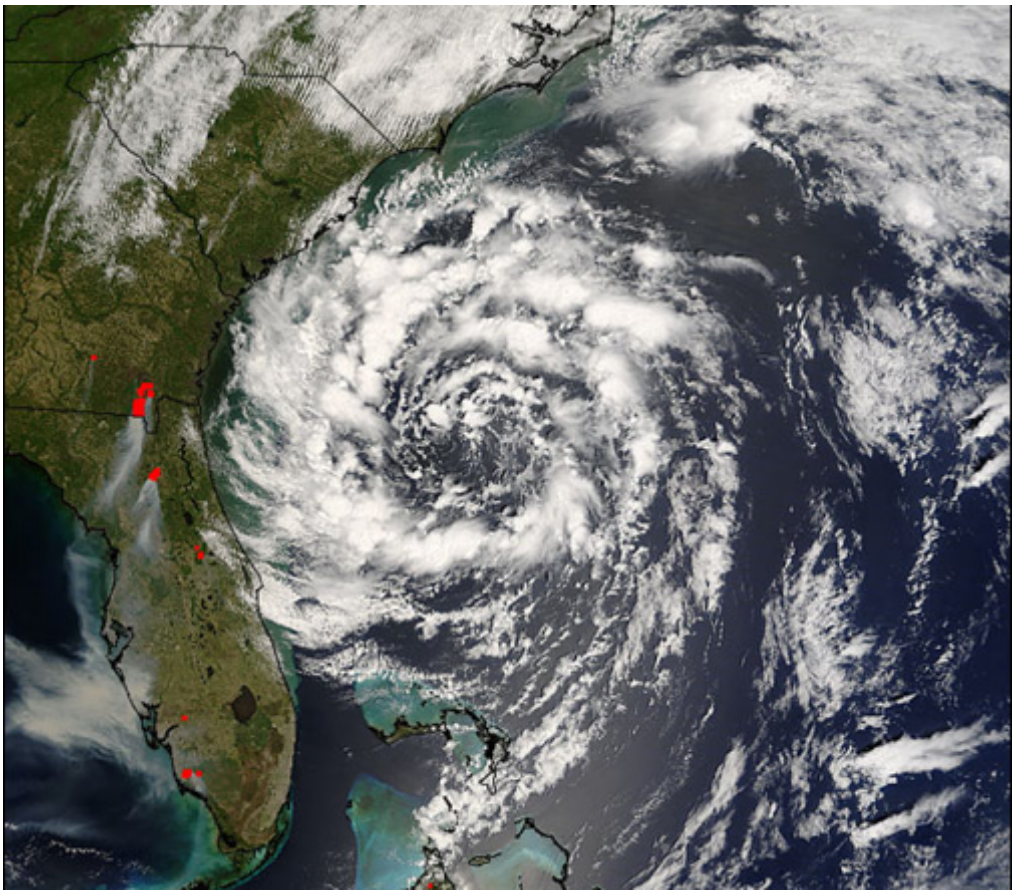

**Figure 1.3**: The spatial structure of a subtropical cyclone *(Schmaltz, 2007)*

## 1.2 Favourable conditions for the formation of tropical cyclones

According to the NASA: Earth Observatory (2000), the following four criteria are important for the formation of TCs:

- warm SSTs exceeding 26°C;
- deep moisture at the low levels while light winds dominate the tropopause;
- a trigger such as the Intertropical Convergence Zone (ITCZ) or Easterly Waves; and
- maximum sustained surface winds of 33 m $s^{-1}$ or more.

TCs form in areas where the absolute vorticity of the air flow has a nonzero value; in other words, rotational airflow is necessary for TC formation (Emanuel, 2003). These conditions generally occur over the tropical oceans. The regions of the world that satisfy these conditions are shown in Figure 1.4. Note that TCs are scarce near the equator due to the negligible Coriolis Effect.

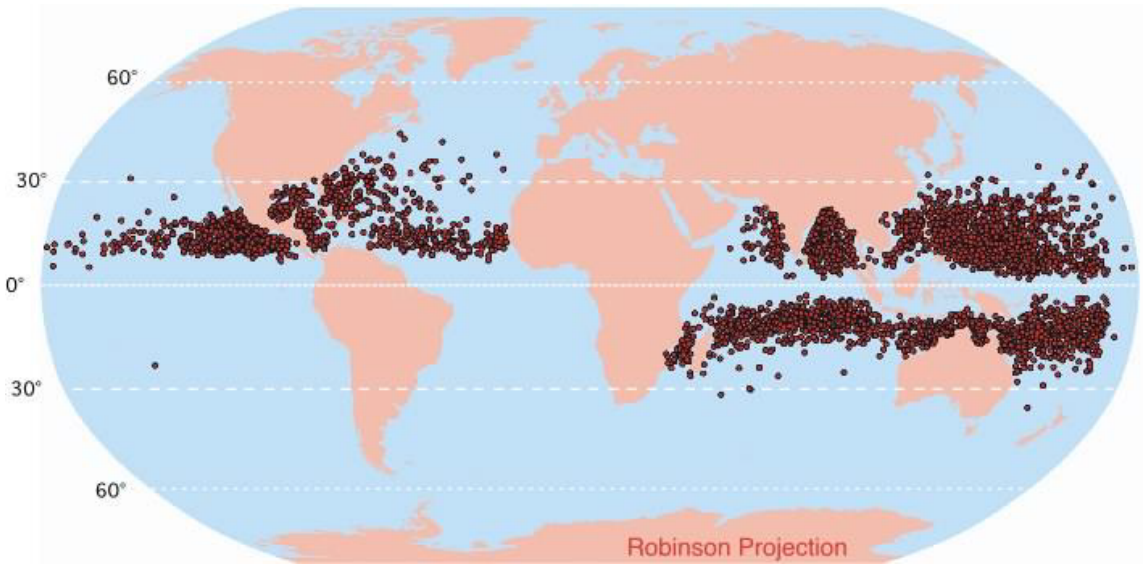


**Figure 1.4**: Global distribution of hurricanes, indicated by brown dots *(Pidwirny, 2006a)*

## 1.3 The cyclogenesis of tropical cyclones

The cyclogenesis of a TC starts with the development of a tropical disturbance, which develops into a tropical depression that grows into a tropical storm and ends with a TC (or hurricane or typhoon, depending on the region). A tropical disturbance consists of many thunderstorms, which develop over various regions of the tropics (Pidwirny, 2006a). For a tropical disturbance to grow to a tropical depression it must have significant cyclonic circulation, which enhances the thunderstorms development through additional latent heat energy and moisture. This allows the tropical disturbance to intensify, and at a point, the thunderstorms begin to move cyclonically toward the storm's eye. A tropical disturbance becomes a tropical depression when a storm has a sustained wind speed between 10.3 m $s^{-1}$ and 17.5 m $s^{-1}$ (Pidwirny, 2006a; Landsea, 2011a). A tropical depression turns into a tropical storm when the eye has a lower surface pressure and the winds range between 17 m $s^{-1}$ and 33 m $s^{-1}$ (Landsea, 2011a). The final stage of cyclogenesis is a TC (or hurricane), where the sustained wind speeds exceed 32.8 m $s^{-1}$. Hurricanes are usually classified into five categories based on their intensity according to the Saffir-Simpson scale (Table 1.1), where

Category 1 is the weakest and Category 5 is the strongest (Marshak, 2008). The extent of damage caused during each category is indicated in Table 1.1.

**Table 1.1**: The Saffir-Simpson hurricane wind scale classification

| Category | Wind speed (m $s^{-1}$) | Central pressure (hPa) | Extent of damage | Example |
|---|---|---|---|---|
| 1 | 33.1 – 42.5 | > 980 | Very dangerous winds will produce some damage | Hurricane Dolly (2008) |
| 2 | 42.8 – 49.2 | 965 – 980 | Extremely dangerous winds will cause extensive damage | Hurricane Catarina (2004) |
| 3 | 49.4 – 57.8 | 945 – 965 | Devastating | Hurricane Ivan (2004) |
| 4 | 58.1 – 69.7 | 920 – 945 | Catastrophic | Hurricane Charley (2004) |
| 5 | 70 + | < 920 | Catastrophic | Hurricane Andrew (1992) |

*Source: NASA: Earth Observatory (2000); Pidwirny (2006a); Schott et al. (2012a); Schott et al. (2012b)*

Once a TC is formed, it is given a name by the World Meteorological Organization. The World Meteorological Organization has developed six separate lists of TC names in alphabetical order, alternating between male and female names (Zimmermann, 2012). The separate lists are for the Atlantic, Eastern North Pacific, Central North Pacific, and other basin names. For example, hurricane names from 2016 to 2021 can be found on the National Oceanic and Atmospheric Administration (NOAA) National Hurricane Center website (http://www.nhc.noaa.gov/aboutnames.shtml). By convention, the names in the lists are recycled and rotated every six years. As such, the names given to hurricanes in 2016 will be reused in 2022. However, if a particular storm was deadly or caused a huge damage, the name is retired. For example, because of their devastating impact in 2005, Hurricanes Rita, Wilma, and Katrina's names have been removed from the list (Zimmermann, 2012).

TCs dissipate when they make landfall due to (i) a lack of warm SSTs or moist tropical air aloft, (ii) friction, and (iii) unfavourable large-scale flow aloft. When a TC moves into cooler waters, the low-level air flow becomes cool, thereby displacing the temperature gradient between the surface and upper air level, and the storm weakens. The source of warm, moist air is also lost when a TC moves over land and away from a water and heat source. Furthermore, the land surface (such as vegetation or buildings) creates friction increasing the vertical wind shear throughout the storm's core and reducing the sustained winds and

surface circulation, and thereby weakening and, later, destroying the storm by disrupting the deep convection within the storm's core (NOAA, 1999; Landsea, 2014; Landsea and Aberson, 2014). Strong upper-level winds can cause a TC to dissipate as the latent heat is dispersed and the source of moisture is cut off (NOAA, 1999; NASA: Earth Observatory, 2000). However, landfall over a very moist area (such as a bay, lake, or swamp) or interaction with a mid-latitude frontal system can result in a brief intensification of the TC prior to dissipation, as the surface evaporation remains unchanged (NOAA, 1999; Landsea and Aberson, 2014).

### 1.4 Socio-economic impacts of tropical cyclones

TCs are usually associated with devastating socio-economic impacts when they make landfall (see Table 1.2). The impacts are most prominent along the coast and over islands in the Pacific Ocean, where TCs are the most common. The Pacific basin has varying TC seasons. The Northeast Pacific season begins mid-May or early June to the end of November – with the peak season occurring late August or early September. The Central Pacific season is from the beginning of June to the end of November (like the Atlantic). The Northwest Pacific TC season is continual through the year – peaking late August or early September. The Southwest or Australian Pacific TC season occurs during late October or early November to early May – with peak season occurring late February or early March (NOAA, 2016). The average number of TCs to develop in the Pacific Basin each year ranges from roughly 5 to 17, depending on the area in the basin (see Table 1.2). Hurricane Manuel caused widespread flooding and mudslides in Mexico, killing 123 people (Pasch and Zelinsky, 2014). Super Typhoon Haiyan affected more than 16 million people and left 4 million homeless in the southern Philippines in 2013 (Singer, 2014). TC Audrey in 1964 caused extensive damage in Queensland, Australia, as a result of flooding (Australian Government: Bureau of Meteorology, *n.d.*).

The Indian basin also experiences differing TC seasons according to location therein. The North Indian basin sees peak TC activity in both May and November with severe storms (exceeding 33 m $s^{-1}$ winds) occurring mainly from April to June, as well as from late September to early December. The Southwest and Southeast or Australian Indian region, on the other hand, begins late October or early November peaking from mid-January and mid-

February to early March (NOAA, 2016). The average number of TCs for the period 1981 to 2011 (with sustained winds greater than 17 m $s^{-1}$) in the North Indian basin is 4.8, while the Southwest Indian basin averages 9.3 (Landsea and Delgado, 2016). On the other hand, the average number of hurricanes, typhoons, or severe TCs in the North Indian basin is 1.5 and in the Southwest Indian basin is 5 (Landsea and Delgado, 2016). The Bangladesh Cyclone of 1970 caused hundreds of thousands of people to die due to the associated storm surge in low-lying deltas (Landsea, 2013). In 2009, severe TC Laurence (category-5 in strength) caused considerable damage to local properties in Darwin, Australia. Over a thousand cattle died and heavy rains caused minor flooding and road closures (Australian Government: Bureau of Meteorology, 2017). More recently, in mid-February 2017, TC Dineo hit the Southwest Indian basin, and brought exceptionally heavy rains. The resultant flooding caused the death of seven people (Hill and Nhamire, 2017).

The Atlantic basin TC season (97% of TC activity) is from the beginning of June to the end of November, with August through October being the peak season, experiencing 78% of storm days and 96% of these storms being category 3 to 5 (NOAA, 2016). On occasion, TCs do occur out of season during May or December in the Atlantic basin (NOAA, 2016). Landsea (2016) tabulated the number of hurricanes making landfall or producing hurricane winds along the North American coastline from 1851 to 2015. The number of TCs to develop annually in the Atlantic basin ranges from 1 to 28 storms a year (Landsea, 2015). In 2005, 28 named storms (tropical storms, hurricanes and subtropical storms) were identified. 15 of these storms were identified as hurricanes (ranging from a category-1 to a category-5 on the Saffir-Simpson hurricane wind scale). The average number of named storms for the period 1968 to 2015 is 11.8, while the average number of hurricanes for the same period is 6.2 (Landsea, 2015). Hurricane Andrew struck the Bahamas, Florida and Louisiana in 1992 resulting in the loss of billions of US dollars, while Hurricane Katrina in 2005, struck the Bahamas, Florida, Louisiana, Mississippi, and Alabama, and is considered the most destructive hurricane to hit the North American coastline to date (Landsea, 2013).

**Table 1.2**: The average number of TCs for each basin for the period 1981 to 2011, and the extent of damage caused thereof

| Basin | Average | | Extent of damage |
|---|---|---|---|
| | Tropical storm or stronger (sustained winds > 17 m $s^{-1}$) | Hurricane, typhoon, or severe TC (sustained winds > 33 m $s^{-1}$) | |
| Atlantic | 12.1 | 6.4 | • Hurricane Andrew (1992): US$26.5 billion in losses<br>• Hurricane Katrina (2005): US$40.6 billion in insured losses and an estimated US$108 billion in total losses |
| NE/Central Pacific | 16.6 | 8.9 | • Hurricane Manuel (2013): 123 deaths in Mexico |
| NW Pacific | 26.0 | 16.5 | • Super Typhoon Haiyan (2013): 6300 people died |
| Australian SW Pacific | 9.9 | 5.2 | • TC Audrey (1964): extensive damage to stock and fencing |
| N Indian | 4.8 | 1.5 | • Bangladesh Cyclone (1970): 300 000 people died |
| SW Indian | 9.3 | 5.0 | • TC Dineo (2017): 7 people died |
| Australian SE Indian | 7.5 | 3.6 | • Severe TC Laurence (2009): 1500 cattle killed |

*Source:* abridged from *Landsea and Delgado (2016); Landsea (2013); Pasch and Zelinsky (2014); Singer (2014); Australian Government: Bureau of Meteorology (2017); Hill and Nhamire (2017); Australian Government: Bureau of Meteorology (n.d.)*

In contrast to other basins, only three TCs are reported over the South Atlantic Ocean (SAO) in recorded history, because the climate of the region is generally unfavourable for the formation of TCs (discussed further in Section 1.6). However, Hurricane Catarina, the first ever-recorded category-2 hurricane in the SAO in recorded history, reached category-1 status on 26 March 2004 and made landfall in Brazil on 28 March 2004 with devastating impacts. It affected half a million people across 23 cities (Silva Dias et *al.*, 2006). Eleven people died (mostly fishermen) and seven people went missing in small boats along the coastline (Silva Dias et *al.*, 2006). A total of 38 people were injured in Santa Catarina, Southern Brazil alone (Arizona State University – https://wmo.asu.edu/content/first-south-atlantic-tropical-cyclone), in just a few hours on 28 March 2004 (Pereira Filho et *al.*, 2010). Numerous municipalities were affected by severe damage caused by Hurricane Catarina's winds (for instance, see Figure 1.6 and 1.7) mostly to buildings (petrol stations and warehouses) – 40 000 of which were destroyed, while 33 000 homes were destroyed (Pereira Filho et *al.*, 2010; Silva Dias et *al.*, 2006). 95% of these had damage to roofs. Urban infrastructures (electrical, telephonic and roads), agriculture, flora and fauna were also affected and there were also human casualties (Marcelino et *al.*, 2004) – see Figure 1.5. Silva Dias et *al.* (2006) state that the damage to agriculture occurred mostly to corn (90%), banana (70%), and rice fields (25%), totalling about US$40 million. 80% of schools were also suspended for up to two weeks (Silva Dias et *al.*, 2006; Pereira Filho et *al.*, 2010).

8600 people in the industrial and commercial sectors lost their jobs due to the damages thereon (Silva Dias et *al.*, 2006). Overall, Hurricane Catarina caused an estimated half a billion dollars in damage, the equivalent of a quarter of the Brazilian gross industrial product growth in 2004 (Pereira Filho et *al.*, 2010; Veiga et *al.*, 2008). Perhaps the damage caused by Hurricane Catarina was so great because the Brazilian communities were not prepared for such a rare event.

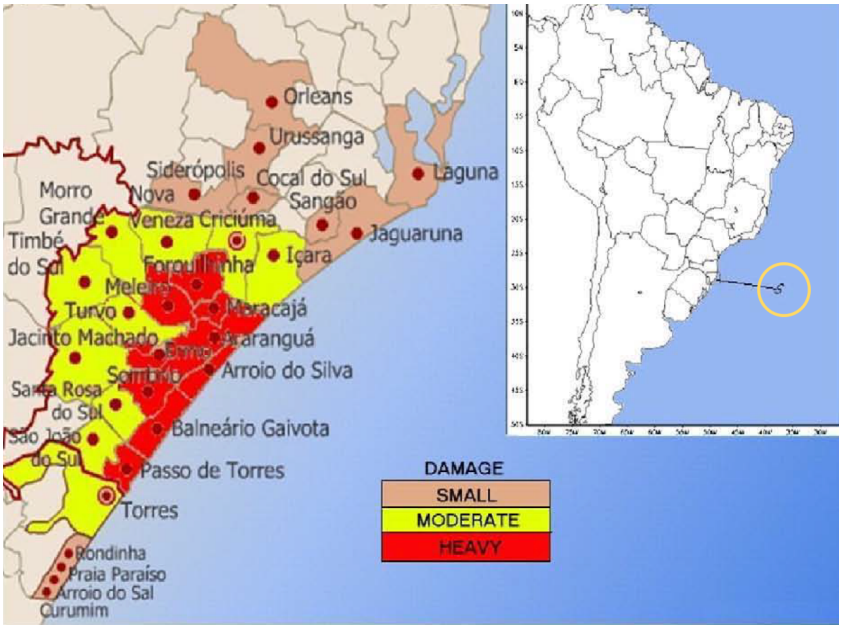


**Figure 1.5**: The extent of damage caused by Hurricane Catarina's landfall on 28 March 2004. The South American map shows the rough area and path of Catarina's landfall, with the yellow circled "S" indicating Catarina's origin *(Pereira Filho et al., 2010: 158)*

**Figure 1.6**: Examples of damage caused by Hurricane Catarina *(Marcelino et al., 2004: 5)*

**Figure 1.7**: Wind damage caused by Hurricane Catarina *(Marcelino et al., 2004: 8)*

## 1.5 Importance of tropical cyclones

Despite their devastating impacts, TCs play a crucial role in maintaining the energy balance in the earth's system. To ensure the upper atmospheric layers maintain equilibrium with the near-surface layers, TCs transport energy and moisture from the lower and upper atmosphere. This occurs when Easterly Waves interrupt the shallow moist layer overlain by drier air, allowing the development of thunderstorms behind the wave. This leads to a deepening of the trough allowing a closed low to form. Latent heat energy combined with surface convergence promotes uplift and the inversion is broken. Heating then occurs throughout the air column thereby encouraging upper air level divergence. This leads to more moist surface air being drawn into the air column and the uplift is intensified. Finally, the strong air pressure drops in the centre due to accelerating wind speeds, and a tropical storm forms. Without this process the atmosphere and surface would remain unstable and imbalanced.

## 1.6 Factors influencing weather and climate over the South Atlantic Ocean and South America

The climate of the SAO has many influencing factors. These range from the South American topography, the El Niño Southern Oscillation (ENSO) and the ITCZ, to the Antarctic Circumpolar Current. The Andes (along the west coast) play a crucial role in acting as a barrier to separate the dry conditions in the west and the moist conditions in the east at

tropical and subtropical latitudes (Garreaud et *al.*, 2008). As such, it obstructs the tropospheric flow of the SAO region and promotes interactions between the tropics and extratropics towards the east (Garreaud et *al.*, 2008). Furthermore, the Brazilian plateau is conducive for development of intense convective storms as the low-level circulation is blocked over subtropical South America. The ENSO, an ocean-atmosphere system, has both a direct and indirect effect on the SAO climate. Its strong direct effect is evident over Peru, coastal Ecuador and northern Chile, while its indirect effect is evident over most of subtropical South America (Garreaud et *al.*, 2008; Paegle and Mo, 2002). The meridional gradient of SSTs over the tropical Atlantic also has a strong impact on the weather and climate of eastern South America (Garreaud et *al.*, 2008). When the SST is warm, droughts are prevalent in north-eastern Brazil.

The Antarctic Circumpolar Current influences the climate of the SAO as it provides cool waters and temperatures to the west and east coasts of South America. Specifically, the Antarctic Circumpolar Current branches off near the southern tip of South America along the Atlantic coast, looping back down and around Antarctica in the Southern Ocean (Przyborski, 2004). This offshoot flowing northwards is called the Falkland Current or the Malvinas Current. It flows northwards adjacent to the South American coastline until it converges with the warm Brazil Current flowing southward (somewhere just north or south of the Rio de la Plata latitude), where the Uruguay and Parana Rivers flow into the SAO (Przyborski, 2004). The convergence of these south and northward flowing currents within a relatively small area results in varying temperatures and salt concentrations.

The Antarctic Oscillation, the leading pattern of tropospheric circulation variability south of 20$^{o}$S (Garreaud et *al.*, 2008), also influences the climate: "The positive phase of the AAO [Antarctic Oscillation] is associated with decreased (increased) surface pressure and geopotential heights over Antarctica (midlatitudes) and a strengthening, poleward shift of the SH westerlies. Opposite conditions prevail during the negative phase" (Garreaud et *al.*, 2008: 13). Furthermore, positive (negative) phases of the Antarctic Oscillation dominate when convection anomalies and SST resemble a La Niña (El Niño) phase of ENSO (Garreaud et *al.*, 2008). The positive (negative) phase of the Antarctic Oscillation is associated with upper-level anticyclonic (cyclonic) anomaly intensification, the convergence of moisture

weakening (enhancing), and decreasing (increasing) precipitation over south-eastern South America (Silvestri and Vera, 2003). As such, the SAO has strong subsidence and cold SST, as well as strong vertical wind shear (Pereira Filho and Lima, 2006).

The spatial distributions of long-term mean precipitation over South America and the SAO for January and July are shown in Figure 1.8, with low-level winds at 925 hPa superimposed, as well as the ITCZ orientated from the east to the west over northern South America and the extratropical oceans. Northeast Brazil experiences its rainy season when the ITCZ reaches the equator, while the subtropical oceans have nearly absent rainfall as a result of large-scale mid-tropospheric subsidence (Garreaud et *al.*, 2008). This subsidence allows a semi-permanent high-pressure cell to be maintained. Hence, the SAO climate is largely dominated by this high-pressure system in the subtropics (Peterson and Stramma, 1991), and, in general, the synoptic conditions over the region do not favour TC formation (see Section 1.4). The South Atlantic Convergence Zone (SACZ) ranges from roughly 10°N to 30°W (Figure 1.9) and is the dominant summertime cloudiness feature of subtropical South America and the western SAO (Seluchi and Marengo, 2000); specifically, it develops in austral spring and summer (Garcia and Kayano, 2010). Normally the SACZ is a cloud band that appears to either emanate from or merge with the intense convection over the Amazon basin, extending from the tropical South America south-eastward into the SAO (Seluchi and Marengo, 2000; Carvalho et *al.*, 2004; Liebmann et *al.*, 2004).

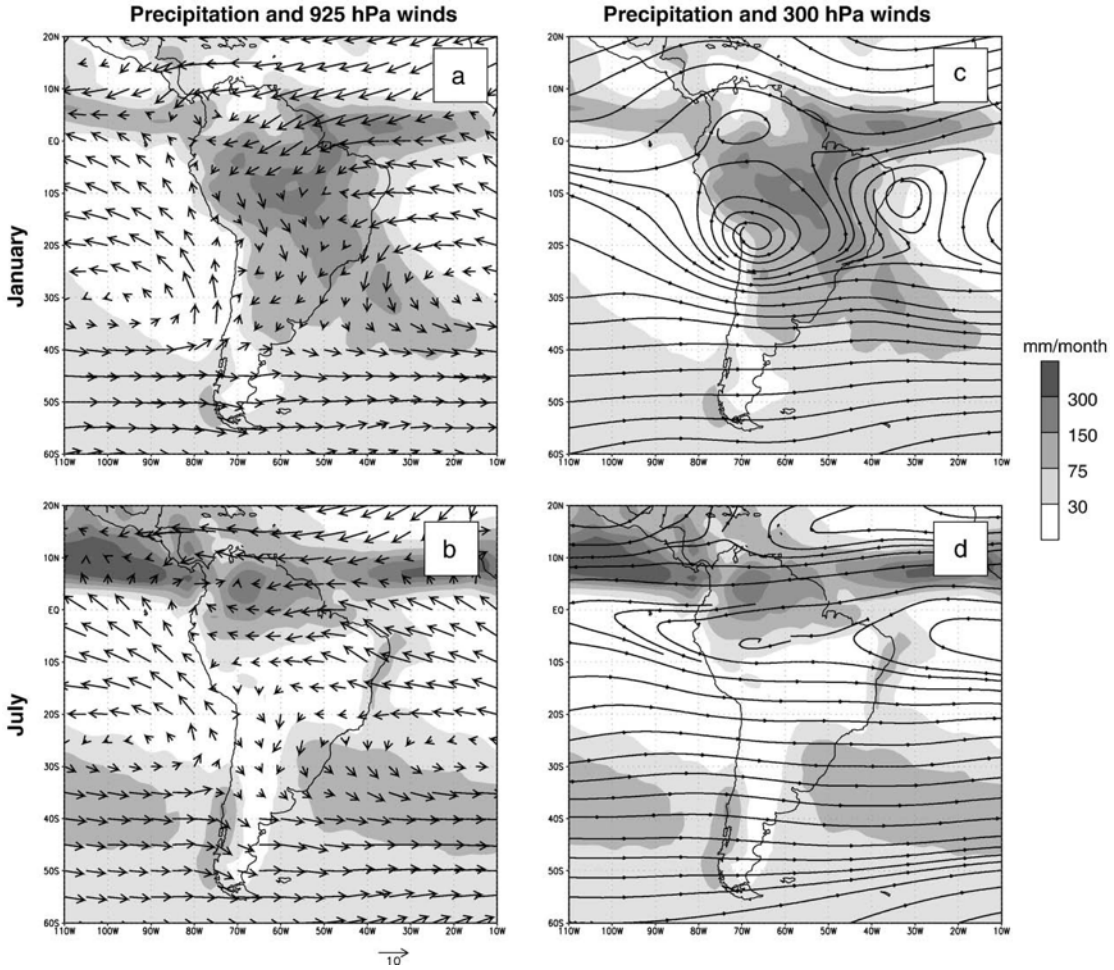


**Figure 1.8**: (a) and (b) January and July long-term Climate Prediction Center Merged Analysis of Precipitation means (mm/month) and wind vectors at 925 hPa. (c) and (d) January and July long-term precipitation means and 300 hPa streamlines *(Garreaud et al., 2008: 4)*

## 1.7 Observing and monitoring tropical cyclones

Prior to World War II, observations and detections of TCs largely depended on reports from islands, ships at sea, or coastal stations (Emanuel, 2003). This meant that many storms would have gone completely undetected, especially storms that did not make landfall. However, World War II brought about military aircraft that were operational from island stations in the Pacific, and carriers were required to locate TCs that could be potentially dangerous to naval operations (Emanuel, 2003). On 27 July 1943, an aircraft was flown into the eye of a hurricane in the Gulf of Mexico to document the hurricane interior for the first time (Emanuel, 2003). The 1940s saw the first radar images, while the 1960s saw the first satellite images of a TC.

However, TCs are now measured either directly or indirectly (NOAA, 1999). The former refers to measurements taken mainly by flying aircraft through the storm, but ships and buoys

are also used, and as soon as the storm is "near and/or on land, Automated Surface Observation Systems (ASOS) provide surface conditions, and radiosondes take upper air measurements" (NOAA, 1999: 2). The latter refers to the use of Doppler radar, which provides hurricane-related weather information as soon as the storm is near shore or has made landfall, and satellite imagery to monitor the storm (NOAA, 1999). Atmospheric models are also used to monitor and forecast the possible future cyclones.

Each of these methods has advantages and disadvantages. For instance, a network of weather stations, buoys, and aircraft measurements can provide the most accurate local observation data (*e.g.* SSTs, air temperature, pressures, wind speeds, and wave conditions (Arruza, 2013)) on TCs, but the spatial resolution of this network is too coarse for effectively studying or monitoring TCs. Doppler radar, on the other hand, can detect precipitation associated with TC activity within an approximate 300 km to 400 km distance of where the radar is situated, and can provide a visualisation of the TCs eye, eye wall and associated rain bands (Arruza, 2013). It also provides information on TC rainfall intensities, TC movement, tornado activity associated with TCs, as well as estimated wind speed within the TC (Arruza, 2013). The network of current radar available is also too sparse. Satellite imagery, on the other hand, provides several hours of data on TC cyclogenesis. For instance, the Geostationary Operational Environmental Satellite's latest satellite (GOES-16) provides high-resolution imagery (Jones, 2017). This provides imagery for locating severe weather, which could result in earlier warning times for severe weather systems associated therewith such as tornadoes (Jones, 2017). This also helps forecasting models in severe weather prediction. However, for better depictions of TC activity over a region, the satellite data needs to be used in conjunction with station and radar measurements.

While TCs are monitored and predicted in other basins, monitoring and prediction thereof across the SAO is lacking due to the rarity of TC activity over the region. Despite the rarity, TC activity forecasting over the SAO is necessary in order to minimize the impacts of possible future TCs on vulnerable coastal communities.

## 1.8 Aim and objective

The aim of this study was to examine the capability of the Weather Research and Forecasting (WRF) model in simulating hurricanes (Catarina and Anita) over the SAO. The objectives were to:

i. understand the characteristics of the hurricanes in observation and reanalysis, including the relationship between hurricanes and the SACZ;
ii. assess how well WRF simulates the hurricanes at different horizontal resolution; and
iii. examine the sensitivity of the simulated hurricanes to the boundary forcing from the reanalysis datasets.

This dissertation is divided into five chapters. Following this introductory chapter, Chapter Two presents a literature review on the characteristics of TCs in the SAO, the relationship between TCs and the SACZ, the influence of climate change on TC activity, and lastly, the use of observational and reanalysis datasets to analyse TCs as well as climate models that have been used to simulate them over the SAO. Chapter Three discusses the data and methodology used in this study, while Chapter Four presents the results and discussions. The conclusion and recommendations for future studies are presented in Chapter Five.

# 2 Literature Review

This chapter reviews the relevant literature relating to TCs. Section 2.1 looks at previous literature on the characteristics of hurricanes over the SAO, focusing on Hurricane Catarina and Hurricane Anita as case studies. Section 2.2 focuses on the relationship between TCs and the SACZ, while Section 2.3 examines the influence of climate change on TCs. The final section, Section 2.4, reviews the studies that have been done on using observational and reanalysis data to study TCs worldwide, as well as examining the literature on simulating TCs.

## 2.1 Characteristics of hurricanes over the South Atlantic Ocean

Previous studies have shown that while the SAO region has experienced several subtropical cyclones (Landsea, 2013), the region along the Brazilian coastline has witnessed only three hurricanes in recorded history. Namely: the Angola TC (a weak tropical storm that developed off the Congolese coast in mid-April in 1991; NOAA, 2016); Hurricane Catarina (an extraordinarily rare category-2 TC that made a landfall off the Santa Catarina coast in mid-March in 2004; McTaggart-Cowan et *al.*, 2006; Pezza and Simmonds, 2006; Silva Dias et *al.*, 2006; Pezza et *al.*, 2009; Vianna et *al.*, 2010; and de Menezes and Vianna, 2011); and Hurricane Anita (a category-1 TC that developed of the coast of Brazil in early-March in 2010 (Dias Pinto et *al.*, 2013)). The characteristics of these hurricanes differ. However, this section will review the literature on the two most prominent hurricanes (Hurricane Catarina and Hurricane Anita), which are focused on in this study.

### 2.1.1 Hurricane Catarina

Hurricane Catarina, the most intense hurricane over the SAO, is also the most studied South Atlantic hurricane. While some studies focus on the cyclogenesis of Catarina (McTaggart-Cowan et *al.*, 2006; Silva Dias et *al.*, 2006), some have tried to understand the cause thereof (Pezza et *al.*, 2009), while others have studied the interaction between Catarina and warm core rings (WCRs) in the SAO (Vianna et *al.*, 2010; de Menezes and Vianna, 2011). Silva Dias et *al.* (2006) explained that Hurricane Catarina developed from a typical baroclinic cyclogenesis caused by an upper-level trough that interacted with a surface frontal system. As the trough cut off from the westerlies, an upper-level low was formed and resulted in a

surface low turning west-northwestward, characterizing a comma cloud system that was embedded in a baroclinic environment. According to Bonatti and Rao (1987), this is a common feature in this region during autumn and spring. However, with the exceptionally unusual favourable conditions (*i.e.* the weak upper level winds and warm SST) the cold-core developed into a subtropical storm, later becoming a tropical storm that intensified into a TC making landfall on the coast of Santa Catarina with winds up to 31 m $s^{-1}$ (McTaggart-Cowan et *al.*, 2006). This TC then developed into Hurricane Catarina with winds up to 41 m $s^{-1}$ (McTaggart-Cowan et *al.*, 2006). McTaggart-Cowan et *al.* (2006) provide a table summarising the cyclogenesis of Hurricane Catarina from 19 to 28 March 2004 (Table 2.1), indicating the locations and intensity of the storm during its various phases.

**Table 2.1**: Evolution of Hurricane Catarina from 19 to 28 March 2004. Abbreviations: extratropical (Ex), hybrid tropical/extratropical (Hy), tropical storm (TS), category-1 hurricane (H1), & category-2 hurricane (H2)

| Day | Hour (UTC) | Lat | Lon | MSLP (hPa) | Wind speed (kt) | State |
|---|---|---|---|---|---|---|
| 19 | 1800[a,b,c] | 27.0°S | 49.0°W | | 25 | Ex |
| 20 | 0000[a] | 26.5°S | 48.5°W | | 25 | Ex |
| 20 | 0600[a] | 25.3°S | 48.0°W | | 30 | Ex |
| 20 | 1200[a] | 25.5°S | 46.0°W | | 30 | Ex |
| 20 | 1800[a,b,c] | 26.5°S | 44.5°W | | 30 | Ex |
| 21 | 0000[a] | 26.8°S | 43.0°W | | 30 | Ex |
| 21 | 0600 | 27.5°S | 42.0°W | | 30 | Ex |
| 21 | 1200[a,c] | 28.7°S | 40.5°W | | 30 | Ex |
| 21 | 1800[c] | 29.5°S | 39.5°W | | 30 | Ex |
| 22 | 0000[a] | 30.9°S | 38.5°W | | 30 | Ex |
| 22 | 0600 | 31.9°S | 37.0°W | | 30 | Ex |
| 22 | 1200[a,c] | 32.3°S | 36.7°W | | 30 | Ex |
| 22 | 1800[b] | 31.5°S | 36.5°W | | 30 | Ex |
| 23 | 0000[a] | 30.7°S | 36.7°W | | 30 | Ex |
| 23 | 0600 | 29.8°S | 37.0°W | 1002 | 30 | Ex |
| 23 | 1200[c] | 29.5°S | 37.5°W | 990 | 30 | Ex |
| 23 | 1800[b] | 29.4°S | 38.1°W | 991 | 35 | Ex |
| 24 | 0000[a] | 29.3°S | 38.5°W | 993 | 35 | Hy |
| 24 | 0600[a] | 29.2°S | 38.8°W | 992 | 35 | Hy |
| 24 | 1200[a,c] | 29.1°S | 39.0°W | 990 | 35 | Hy |
| 24 | 1800[a,c] | 29.1°S | 39.4°W | 990 | 40 | Hy |
| 25 | 0000[a,b] | 29.0°S | 39.9°W | 993 | 40 | Hy |
| 25 | 0600[b] | 28.9°S | 40.4°W | 993 | 45 | TS |
| 25 | 1200[a,c] | 28.7°S | 41.2°W | 994 | 50 | TS |
| 25 | 1800[b] | 28.7°S | 41.9°W | 994 | 55 | TS |
| 26 | 0000[a,c] | 28.7°S | 42.6°W | 989 | 60 | TS |
| 26 | 0600[d] | 28.7°S | 43.1°W | 989 | 65 | H1 |
| 26 | 1200[a,c,d] | 28.8°S | 43.7°W | 982 | 70 | H1 |
| 26 | 1800[a,c,d] | 28.9°S | 44.2°W | 975 | 70 | H1 |
| 27 | 0000[a,d] | 29.1°S | 44.9°W | 974 | 70 | H1 |
| 27 | 0600[a,d] | 29.2°S | 45.6°W | 974 | 75 | H1 |
| 27 | 1200[a,c,d] | 29.5°S | 46.4°W | 972 | 75 | H1 |
| 27 | 1800[a,c,d] | 29.5°S | 47.5°W | 972 | 80 | H1 |
| 28 | 0000[a,d] | 29.3°S | 48.3°W | 972 | 80 | H1 |
| 28 | 0600[d,e] | 29.0°S | 49.7°W | | 85 | H2 |
| 28 | 1200[a,c] | 28.5°S | 50.1°W | | 60 | TS |
| 28 | 1800[a] | 28.5°S | 51.0°W | | 45 | TS |

[a] Infrared satellite imagery was used to estimate location and state.
[b] QuikSCAT imagery was used to estimate location and state.
[c] Visible satellite imagery was used to estimate location and state.
[d] Microwave satellite imagery was used to estimate location and state.
[e] TRMM imagery was used to estimate location and state.

*Source: McTaggart-Cowan et al. (2006: 3034)*

The exceptionally uncommon favourable conditions that produced this rare hurricane have been well debated in the literature (*e.g.* Vianna et *al.*, 2010; de Menezes and Vianna, 2011; Pezza et *al.*, 2009; McTaggart-Cowan et *al.*, 2006). Some studies (Vianna et *al.*, 2010; de Menezes and Vianna, 2011) attributed the formation of Hurricane Catarina to the WCRs (areas of warmer waters) in the SAO at the time of its cyclogenesis. They indicated that the warm SST helped Catarina to gain the latent heat energy needed to develop and maintain itself, thereby achieving a category-2 status (Figure 2.1). de Menezes and Vianna (2011) emphasised that there is a relationship between the cyclogenesis of Catarina (*i.e.* from its formation on 20 March 2004 to the surface structure changes on 23 March, and to the sudden intensification between 26 and 27 March 2004) and WCRs. Hence, de Menezes and Vianna (2011) suggested that, to capture the observed hurricane intensification over the SAO, weather foresting models over the region should be coupled with a high-resolution ocean circulation model. In contrast, other studies (*e.g.* Pezza et *al.*, 2009; McTaggart-Cowan et *al.*, 2006) argued that an environmental blocking combined with a low wind shear, which provides moisture and allows sustained growth, were the key factors for the formation of Catarina. McTaggart-Cowan et *al.* (2006) explained that high vertical wind shear (on average 20 m $s^{-1}$) typically prevents storm development off the south Brazilian coast, but that the vertical wind shear during the formation of Catarina was approximately 10 m $s^{-1}$. Pezza et *al.* (2009) also noted that, although the extra-tropical phase of Hurricane Catarina developed over an area prone to warm-core SST, the dynamic feeding associated with the blocked flow that allowed for the slow modification and build-up of the vortex, played a crucial in the transitioning of Catarina from an extra-tropical phase to TC phase. Hence, they advocated for more studies on anticyclones and blocking events south of the equator, as unusual changes in these features could allow for future hurricanes over the SAO. However, the literature suggests that the formation of Hurricane Catarina is largely due to low wind shear combined with environmental blocking as well as the location of WCRs in the SAO.

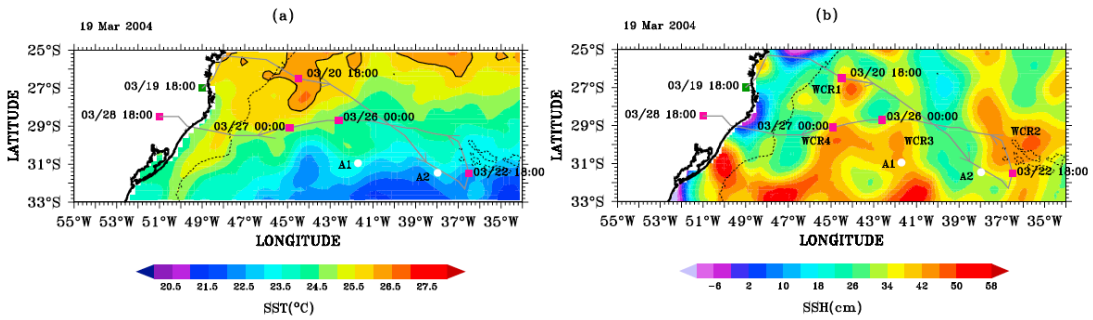


**Figure 2.1**: Hurricane Catarina's trajectory through its lifecycle from 19 March to 28 March 2004. (a) SST on 19th with the Brazil Current clearly visible along the coast and (b) sea surface height data on 19th showing the 4 WCRs crossed by Catarina's trajectory *(Vianna et al., 2010: 8)*

### 2.1.2 Hurricane Anita

Hurricane Anita is less studied than Hurricane Catarina. However, studies (Dias Pinto et *al.*, 2013) indicated that the two hurricanes have some similarities, even though Anita was less intense than Catarina and did not make landfall. Dias Pinto et *al.* (2013) reported that Hurricane Anita formed around the same period of the year as Hurricane Catarina (Catarina: 26 March 2004; Anita: 10 March 2010) and reached categoy-1 status at a similar location as Hurricane Catarina (Catarina: 29°S, 45°W; Anita: 30°S, 48°W). In addition, as with Catarina, the cyclogenesis of Anita's formation involved a dipole blocking in the upper levels, which reduced the vertical wind shear and led to the development of a symmetric eye-like cloudiness structure (Dias Pinto et *al.*, 2013; Dutra et *al.*, 2017). Furthermore, Hurricane Anita formed off the coast of Brazil as a pure ST that later matured into a cold-cored system (Figure 2.2; Dias Pinto et *al.*, 2013; Dutra et *al.*, 2017). Hence, Dias Pinto et *al.* (2013) attributed the formation of Anita to a combination of a dipole-blocking pattern aloft (with the contribution from barotropic energy conversions) and strong turbulent fluxes, while Dutra et *al.* (2013) attributed Anita's formation to horizontal temperature advection and diabatic heating.

However, some studies have also documented a detailed occurrence of Hurricane Anita (*e.g.* Gutro, 2010; NOAA, 2010). For instance, Gutro (2010) reported that the lifecycle of Hurricane Anita spanned 08 to 12 March 2010; and that the system featured maximum sustained winds ranging from 18 m $s^{-1}$ on the 10th, to 21 m $s^{-1}$ on the 11th and 12th, located about 523 km east of Porto Alegre, Brazil in the SAO near 30°S, 45.8°W (Figure 2.2). NOAA (2010) noted that in the upper level analysis for 10 March 2010, Anita appeared as a

closed low near 33°S, 45°W, with an extended short-wave trough to the northwest into Brazil along 20°S, 50°W.

All the studies on TCs over the SAO suggested that the characteristics of Hurricane Catarina and Hurricane Anita at their mature stages differ from that of extra-tropical cyclones. However, they emphasize the need for more studies on the environmental conditions and dynamical processes associated with hurricanes (and even subtropical cyclogenesis) over the region.

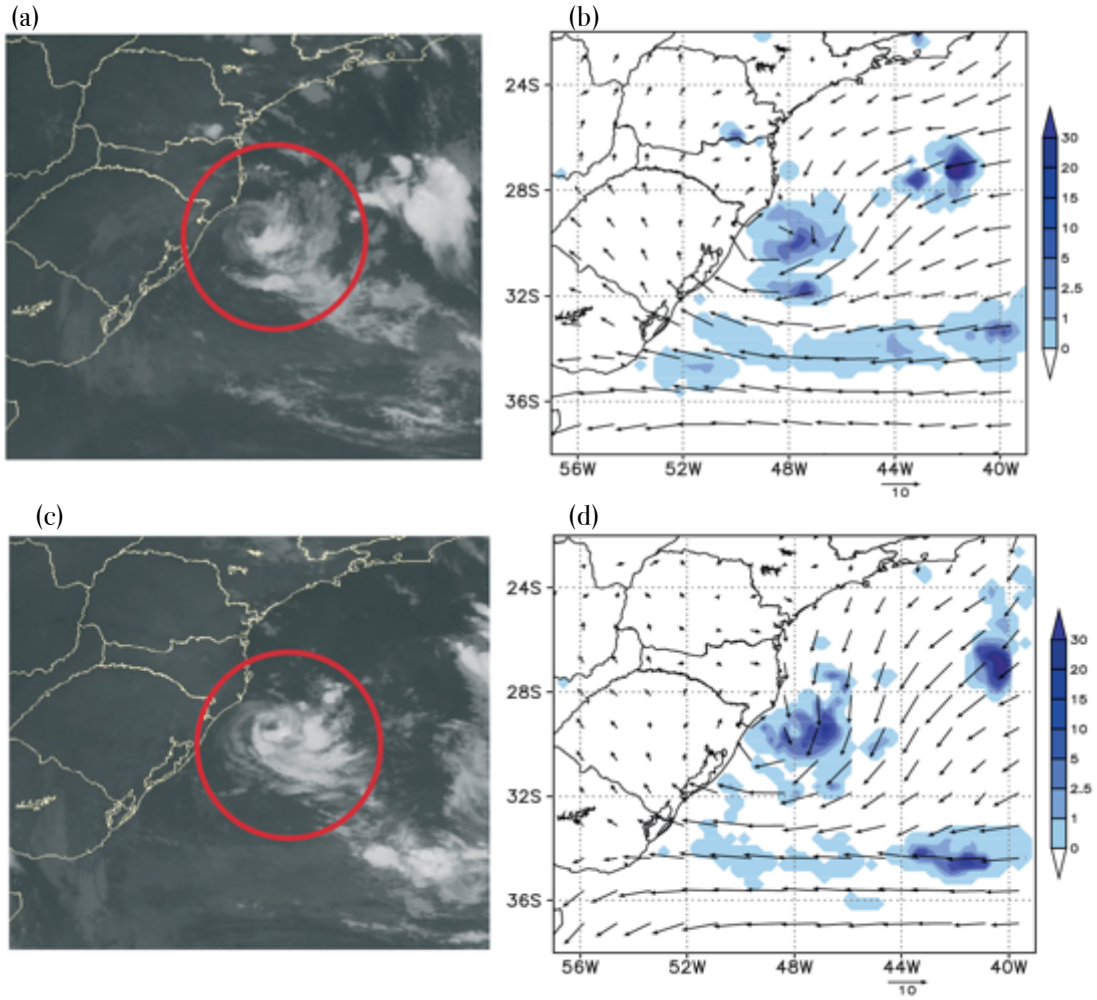


**Figure 2.2**: (a) and (c) showing the convective activity of Hurricane Anita from GOES-12 (IR) at 12am on 10 March 2010, and (b) and (d) showing the accumulated precipitation from TRMM-3B42 (mm/3 hours) overlain by surface winds at 6am on 10 March 2010. The convective activity position associated with Hurricane Anita is highlighted with a red circle (*Dias Pinto et al., 2013: 10877*)

## 2.2 Characteristics of the SACZ and the possible role in hurricane formation

Several studies have discussed the characteristics of the SACZ over the SAO and some have attempted to link the transport of moisture in the SACZ with the formation of hurricanes

(Seluchi and Marengo, 2000; Carvalho et *al.*, 2004; Liebmann et *al.*, 2004). These three studies characterized the SACZ as a cloud band that appears to either emanate from or merge with the intense convection over the Amazon basin, extending from the tropical South America south-eastward into the SAO. Seluchi and Marengo (2000) stated that the SACZ is the dominant summertime cloudiness feature of subtropical South America and the western SAO, while Garcia and Kayano (2010) indicated that the SACZ appears during summer and austral spring. Vasquez (2009) discussed the similarity between the SACZ and the ITCZ (where the northern and southern hemispheric trade winds converge) and indicated that the SACZ descends southwards as a divergence of the ITCZ, because the SACZ is a secondary tropical convergence zone (Vasquez, 2009). Todd et *al.* (2004), who stated that SACZ systems are major regions of moisture convergence, discussed the importance of the SACZ in providing moisture to the surrounding atmosphere. This moisture may be crucial in the formation of hurricanes in the region, which require the convergence of moisture and convection.

Some studies have also documented the relationship between the SACZ and SST anomalies over the SAO. For instance, using an atmospheric general circulation model, Chaves and Nobre (2004) and Robertson and Mechoso (2000) demonstrated that when the SAO SST anomalies are warm (cool), the SACZ intensifies (weakens) and shifts northward. This will have a feedback mechanism on the low-level circulation patterns associated with the SACZ (Doyle and Barros, 2002). Vera et *al.* (2006) noted that SST anomalies, as well as the strength of the tropical convergence zones, large-scale circulations, moisture transport, and the condition of the local land surfaces all influence the variability of precipitation over the SACZ region (Ma et *al.*, 2011). On the other hand, Chaves and Nobre (2004) also found that when the SACZ intensifies the underlying ocean cools as a result of a decreased shortwave solar radiation event. This will create an appearance of cold SST anomalies or the weakening of pre-existing warm SST anomalies (Chaves and Nobre, 2004). However, there is the need for more studies on the relationship between the SACZ and the formation of hurricanes over the SAO.

## 2.3 Impacts of climate change on tropical cyclones

The literature has differing opinions and findings with regards to TC and hurricane formation in a changing climate.

Several studies have found that TC activity is not influenced by climate change. Tsutsui (2002) found that $CO_2$-induced global warming had no effect on the global frequency of TC occurrence; however, it is difficult to identify greenhouse gas-induced changes in TC activity due to the large natural variability of TC frequencies. Furthermore, while $CO_2$-induced warming occurs globally, it is improbable that the changes caused from this will have a uniform effect on local conditions, considering spatial differences in SST anomalies (Tsutsui, 2002). Tsutsui (2002) also pointed out that a change in TC frequency does not necessarily correlate to a change in TC intensity. Similarly, if TC frequency does increase, an increase in TC intensity will not necessarily accompany it. The Intergovernmental Panel on Climate Change (IPCC) also found that confidence is low for TC activity to increase over the observed long term, due to the possible errors in observed data (Holland and Bruyere, 2014).

In contrast to the studies presented in Section 2.3.1, several studies have found that TC activity is influenced by climate change. A study done by Radu et *al.* (2014) looked at the influences of temperature variation on TC size in relation to climate change, specifically with regards to atmospheric temperature and SST variations, and what the potential effects may be in such areas as the SAO. Radu et *al.* (2014)'s study concluded that a profound impact may be seen on TC size because of temperature changes, thereby strongly influencing the early development stages of TC cyclogenesis. Pezza and Simmonds (2005) also looked at SST in relation to hurricane thresholds, stating that there is an increasing probability that when SSTs are relatively close to the hurricane threshold more future TCs will occur in the SAO. However, Oouchi et *al.* (2006) found that TC frequency decreases by 30% globally in a climate warmed by greenhouse gases and increased SSTs. Henson (2005) claimed that SSTs over which Hurricane Catarina formed were slightly cooler than average for the area, regardless of the climate change speculation. In 2012, IPCC concluded that there is a likelihood that intense hurricane frequency will increase because of climate change caused by anthropogenic activities (Holland and Bruyere, 2014). This IPCC finding is reaffirmed by

Chauvin et *al.* (2006) whose experiments look at hurricanes, suggesting that hurricane activity responses to anthropogenic warming are dependent on the pattern of SST anomalies rather than on the grid of the model. In addition, Evans and Braun (2012) state that a region already conducive to cyclogenesis is provided by the combined effects of the warm Brazil Current and the Andes Mountains. As such, and in relation to the SAO, evidence exists suggesting that under global warming conditions Hurricane Catarina, in the SH circulation, could be linked to climate change, as well as there being an increased likelihood of other possible future hurricanes in the region (Pezza and Simmonds, 2005).

Numerous studies also suggest, however, that it is unclear to what extent TC activity will be influenced by climate change. Webster et *al.* (2005) claimed that while there are contradictory findings amongst the global models analysing $CO_2$-induced warming, most climate simulations suggest hurricane intensity may increase but not necessarily hurricane frequency (where there are inconsistencies in the simulations). Knutson et *al.* (2010) take the ideas of Tsutsui (2002) and Webster et *al.* (2005) further, stating that TC intensity will increase by 2100 by 2% to 11% according to high-resolution dynamical models and future projections on theory, while TC frequency will decrease by 6% to 34% according to studies on existing modelling (Knutson et *al.*, 2010). Radu et *al.* (2014) emphasised this uncertainty, finding that while cyclone size is sensitive to temperature variations – as temperature increases so there is an exponential growth of the saturation vapour pressure, which results in an increase in surface fluxes – although this isn't always the case. Radu et *al.* (2014) referenced Lorenz et *al.* (2010) who support this notion, in addition to finding that the surface latent heat flux is an important factor controlling the size of TCs (Radu et *al.*, 2014). Klotzbach (2006) make an important observation regarding TCs and climate change, stating that while their own studies found TC intensity to increase between 1986 and 2005, where SSTs rose by 0.2°C to 0.4°C, their findings could be the result of improved observational technology (as well as other important factors not mentioned) and not necessarily climate change alone.

An interesting paper by Pielke et *al.* (2005) suggested that it is premature to claim that global warming and hurricane impacts are linked. Three reasons have been given, the first is that there has not in fact been a connection made between hurricane behaviour and global

warming. While suggestions have been made, they are not (as yet) definitive. Pielke et *al.* (2005) have acknowledged that this may change in the future. Pielke et *al.*'s (2005) second reason is that should any changes in future hurricane intensities occur and within the context of observed variability, these changes will likely be small. Furthermore, not enough is known about tropical cyclogenesis to provide any answers regarding changes in hurricane frequency. Finally, Pielke et *al.* (2005) state that based on IPCC assumptions, changes in hurricane behaviour are minimalised in relation to the influence of the IPCC's projections of population and wealth growth. And as Frank and Ritchie (2001) pointed out, as coastlines become more vulnerable, due to populations and wealth growth allowing coastlines to become more concentrated, more studies are necessary to understand the processes governing TC intensities and core structures in order to better predict them.

As such, the arguments surrounding TC and hurricane formation in the future range from the refutation that climate change will not have an influence; to confirmation of the influences of climate change already able to be seen; to the middle-ground viewpoint of it being unclear what effects climate change will have on TC and hurricane formation in the future. More climate modelling studies are required to shed more light on the impacts of climate change on TC frequency, especially over the SAO, where the communities are not used to TC occurrence. An increase in TC frequency over the SAO due to climate change may cause more unexpected devastating havoc to the coastal communities. However, before embarking on future climate projections of TCs over the SAO, more studies are needed to examine the capability of atmospheric models in simulating TCs over the SAO.

## 2.4 Monitoring and modelling tropical cyclones

Various models have been used in simulating TCs and hurricanes globally, and while there are many studies that discuss these, only the studies relevant to this study are discussed (Liu et *al.*, 1997; Pezza and Simmonds, 2005; Bonatti et *al.*, 2006; McTaggart-Cowan et *al.*, 2006; Pezza and Simmonds, 2006; Walsh et *al.*, 2007; Veiga et *al.*, 2008; Pezza et *al.*, 2009; da Rocha and Caetano, 2010; Vianna et *al.*, 2010; Dias Pinto et *al.*, 2013; and Radu et *al.*, 2014).

### 2.4.1 Observation and reanalysis data

Several observational and reanalysis datasets have been used to study TC activity in the SAO. Dias Pinto et *al.* (2013) analysed Hurricane Anita in terms of its dynamical and synoptic analysis by using Global Forecasting System (GFS) operational analysis at $1^{o}$ x $1^{o}$ resolution, 3B42 Tropical Rainfall Measuring Mission (TRMM-3B42) precipitation data at $0.25^{o}$ x $0.25^{o}$ horizontal resolution, and ERA-Interim (ERAINT) reanalysis data at a $1.5^{o}$ x $1.5^{o}$ horizontal resolution. Vianna et *al.* (2010) provided a study on the interactions of Hurricane Catarina and WCRs, using numerous multi-satellite-derived high-resolution products to do so. These include "three microwave-based SST data sets, multisatellite collinear data of sea surface height (SSH) anomalies, significant wave heights and wind speeds, four QuikSCAT ocean surface wind vector products (including the 12.5 km resolution swath data), daily fields of absolute objectively analyzed SSH and corresponding geostrophic currents, and Argo floats" (Vianna et *al.* 2010: 1). Like Vianna et *al.* (2010), McTaggart-Cowan et *al.* (2006) analysed Hurricane Catarina using multiple data sources – satellite data from Brazil, the University of Wisconsin-Madison, the American Navy, and NASA. National Centers of Environmental Prediction (NCEP) GFS data was used at a resolution of $1^{o}$ x $1^{o}$, the NCEP National Center for Atmospheric Research (NCAR) Reanalysis (NNRA) at a resolution of $2.5^{o}$ x $2.5^{o}$, and NOAA's Optimum Interpolation SST also at a resolution of $1^{o}$ x $1^{o}$. Pezza and Simmonds (2006) made use of sea-level pressure obtained from the European Centre for Medium-Range Weather Forecasts (ECMWF) at a resolution of $0.5^{o}$ x $0.5^{o}$, SST and upper level variables at $1^{o}$ x $1^{o}$ resolution, as well as NCEP/Department of Energy (NCEP/DOE) reanalysis data for the atmospheric indices at a $2.5^{o}$ x $2.5^{o}$ resolution; in order to study Hurricane Catarina and its associated vertical wind shear and high-latitude blocking. Veiga et *al.* (2008) provided a study on Hurricane Catarina and the environmental energetics associated with its transition, making use of NCEP/NCAR operational model analysis six-hourly data at a resolution of $1^{o}$ x $1^{o}$. Veiga et *al.* (2008) noted that the central pressure of Hurricane Catarina is underestimated by most datasets, even when analysed at a resolution of $0.5^{o}$ x $0.5^{o}$. This highlights the need to make use of multiple data types in conjunction with multiple resolutions in order to obtain the most accurate findings of rare phenomena such as Hurricane Catarina and Hurricane Anita.

### 2.4.2 Climate models

In comparison to Section 2.4.1, few studies using climate models have been undertaken in the SAO, looking at Hurricane Catarina and Hurricane Anita. Pezza et *al.* (2009) looked at Hurricane Catarina in terms of a climate perspective and how it was associated with large-scale circulation. As such, they used the ECMWF operational model and NCEP/DOE at resolutions of $0.5^{o}$ x $0.5^{o}$ and $2.5^{o}$ x $2.5^{o}$ respectively – making use of the mean sea level pressure (MSLP) and atmospheric indices. Similarly, Radu et *al.* (2014) looked at the influences of temperature variation on TC size, using Hurricane Catarina as a case study, in relation to climate change. They used the Advanced Research WRF model (version 3.2.1) and ERAINT at a resolution of $1.5^{o}$ x $1.5^{o}$ for the boundary conditions to do so, as well as using a horizontal resolution of 3.3 km and nesting the model domain at 10 km and 30 km horizontal resolutions. Pezza and Simmonds (2005) made use of the ECMWF operational model in conjunction with NCEP/DOE reanalysis dataset to look at Hurricane Catarina in relation to climate change. The ECMWF operational model utilised SSTs and upper level variables at a resolution of $1^{o}$ x $1^{o}$, while the NCEP/DOE utilised atmospheric indices at a resolution of $2.5^{o}$ x $2.5^{o}$. Bonatti et *al.* (2006) – who used the operational CPTEC (the Center for Weather Prediction and Climate Studies; Santos et *al.*, 2008) global model with resolutions at 68 km, 45 km and 23 km, as well as SST from NCEP, and various convective parameterization schemes – found that the global model's high resolution was incapable of improving winds at the surface as well as the intensity of Hurricane Catarina at a low pressure. Furthermore, Bonatti et *al.* (2006) stated that it is necessary to make use of mesoscale models that are non-hydrostatic, account for the microphysics of clouds and have higher resolutions – high resolutions are therefore critical for providing a properly defined precipitation field because they show better defined topography. Bonatti et *al.* (2006) called for a more in-depth analysis and the use of relevant parameterizations in order to study Hurricane Catarina's scale and intensity. However, more studies are also needed on the relationship between horizontal resolution and boundary forcing in simulating hurricanes over the SAO.

### 2.4.3 Threshold criteria and parameterization

Studies have shown that climate models can generate TCs. However, Walsh et *al.* (2007) explained that while there are few disagreements that climate models can generate TCs,

various studies discussing TC simulations have differing criteria identifying the threshold between tropical depressions and TCs (see Table 2.2). Liu et *al.* (1997) came to a similar conclusion as Walsh et *al.* (2007), 10 years earlier, finding that if the correct features were incorporated into a model run, predictions were possible of hurricane intensity, their tracks and their inner-core structures. For example, in a study by da Rocha and Caetano (2010), it was found that the Kuo cumulus parameterization scheme was sensitive to high resolutions simulations, as they examined the role of the Kuo and Kain-Kritsch cumulus parameterization schemes on the development of cyclones over subtropical SAO. da Rocha and Caetano (2010)'s findings suggested that the scheme was not as sensitive to horizontal grid resolution. They also noted that the cumulus scheme used by Kuo and Low-Nam (1990) operated separately from diabatic heating associated with the rapid deepening of cyclones in the North Atlantic Ocean (da Rocha and Caetano, 2010). da Rocha and Caetano (2010) claimed that Brazilian operational forecast models failed to forecast Hurricane Catarina, as the cyclogenesis associated with Catarina poses a challenge over the region for numerical weather forecasting. As such, more studies are needed in the SAO to ensure appropriate forecasting is provided to the coastal communities of South America.

**Table 2.2**: Various criteria identified by previous studies of the minimum threshold for TCs, used in modelling studies. "T" means temperature anomaly and "V" means wind speed in relation to the surrounding environment (hPa)

| Study | Model horizontal resolution (km) | Wind speed ($m\ s^{-1}$) | Vorticity ($s^{-1}$) | Warm core temperature anomaly (K) | Structure or location | Duration (days) |
|---|---|---|---|---|---|---|
| Bengtsson et al. (1982) | ~200 | 25 at 850 hPa | $7 \times 10^{-5}$ at 850 hPa | — | <30° latitude | — |
| Broccoli and Manabe (1990) | ~300 (R30) | 17 at surface | — | — | <30° latitude | — |
| Haarsma et al. (1993) | ~300 | — | $3.5 \times 10^{-5}$ at 850 hPa | T250 > 0.5<br>T500 > −0.5<br>T250 − T850 > −1 | — | 3 |
| Bengtsson et al. (1995) | ~125 (T106) | 15 | $3.5 \times 10^{-5}$ at 850 hPa | T700 + T500 + T300 > 3 | T300 > T850<br>V850 > V300 | 1.5 |
| Tsutsui and Kasahara (1996) | ~300 (T42) | $V900 > 17.2$ | Cyclonic at 900 hPa | Thickness criterion | V200 < 10 | 2 |
| Walsh and Watterson (1997) | 125 | 6 and 10 at 10 m (area average) | $2.0 \times 10^{-5}$ at 850 hPa | T700 + T500 + T300 > 0 | T300 > T850<br>V850 > V300 | 2 |
| Krishnamurti et al. (1998) | ~300 (T42) | 15 at 850 hPa | $3.5 \times 10^{-5}$ at 850 hPa | T700 + T500 + T300 > 3 | V850 > V300 | 1 |
| Vitart et al. (1997) | ~300 (T42) | 17 | $3.5 \times 10^{-5}$ at 850 hPa | $T_{200\text{-}500} > 0.5$<br>Thickness criterion | — | 2 |
| Vitart et al. (1999) | ~300 (T42) | 17 | $3.5 \times 10^{-5}$ at 850 hPa | $T_{200\text{-}500} > 0.5$<br>Thickness criterion | — | 2 |
| Walsh and Katzfey (2000) | 125 | 5 at 10 m (area average) | $1 \times 10^{-5}$ at 850 hPa | T700 + T500 + T300 > 0 | T300 > T850<br>V850 > V300 | 1 |
| Vitart and Anderson (2001) | ~300 (T42) | 17 | $3.5 \times 10^{-5}$ at 850 hPa | $T_{200\text{-}500} > 0.5$<br>Thickness criterion | — | 2 |
| Nguyen and Walsh (2001) | 125 | 5 at 10 m (area average) | $1 \times 10^{-5}$ at 850 hPa | T700 + T500 + T300 > 0 | T300 > T850<br>V850 > V300 | 1 |
| Sugi et al. (2002) | ~125 (T106) | 15 at 850 hPa | $3.5 \times 10^{-5}$ at 850 hPa | Mean of (T850 + T700 + T500 + T300) > 3 | V850 > V300 | 2 |
| Tsutsui (2002) | ~300 (T42) | — | — | Thickness condition between 200 and 700 hPa | <40° latitude | — |
| Camargo and Zebiak (2002) | ~300 (T42) | Basin dependent | Basin dependent | | | |
| Walsh et al. (2004) | 30 | 17 at 10 m | $1 \times 10^{-5}$ at 850 hPa | T700 + T500 + T300 > 0 | T300 > T850<br>V850 > V300 | 1 |
| McDonald et al. (2005) | ~300 and ~120 | — | $5 \times 10^{-5}$ at 850 hPa | — | <30° latitude | — |
| Oouchi et al. (2006) | ~20 | 17 at 850 hPa | $3.5 \times 10^{-5}$ at 850 hPa | T700 + T500 + T300 > 1.5 | V300−V850 <3 $ms^{-1}$ or <35° latitude | 1.5 |

*Source: Walsh et al. (2007: 2308)*

While these studies are crucial to TC and hurricane research, none of them have investigated how model resolution and boundary forcing could alter the characteristics of simulated hurricanes, specifically that of Hurricane Catarina and Hurricane Anita. Hence, the focus of this study is to address the extent to which model resolution and boundary forcing influence WRF model simulations of hurricanes.

# 3 Study Area, Data and Methodology

This chapter provides a thorough description of the study area, datasets and methodology used in this study. It discusses the observational and reanalysis datasets used, as well as those used in the WRF simulation. The convective parameterisation schemes used in the WRF simulation are discussed. The chapter concludes with a look at the methodology using each dataset type.

## 3.1 Study area

The study area for this project is the domain of the SAO. The region described extends from the Brazilian coastline to the Southern African coastline, covering the Brazilian and Angolan Basins as well as the northern section of the Argentinian and Cape Basins (Encyclopædia Britannica, Inc. 2017). It covers 0°N to 39°S and 53°W to 24°E (Figure 3.1). The domain has been chosen based on the trajectory of both Hurricane Catarina and Hurricane Anita – Hurricane Catarina moving from roughly 28.5°S, 42°W to 28.5°S, 50°W and Hurricane Anita travelling from roughly 25°S, 42.5°W to 38°S, 32°W. However, the domain exceeds these trajectories to ensure that the boundary conditions of the nested domains did not interfere with the WRF modelling of each hurricane. These are then resized accordingly for each nested WRF domain (Figure 3.2).

The Tropic of Capricorn runs through the centre of the study domain. The SAO typically has cool waters due to the interaction between the Antarctic Circumpolar Current and the Brazil Current, influencing the weather and climate of the region – see Chapter One, section 1.6 for a more in-depth discussion thereof. While the Brazilian coastline is tropical (with cool summers and warm winters; Meyer, 2010), the Southwestern African coastline varies – ranging from tropical to moderate tropical to desert in Angola (Nations Encyclopedia. 2017), to sub-tropical in Namibia (with moderate summers and winters; InfoNamibia, 2017), to Mediterranean and desert in South Africa (along the western coast of South Africa; obtained from the Government of South Africa website: http://www.gov.za/aboutsa/geography-and-climate).

## 3.2 The data

Three types of data are analysed for this study: observation (two are used), reanalysis (three are used), and atmospheric model simulation datasets. All the datasets are analysed over the study domain. The time periods examined in this study are 12 March 2004 to 04 April 2004 (for Hurricane Catarina) and 8 March 2010 to 12 March 2010 (for Hurricane Anita). The observation datasets are used to evaluate the performance of the reanalyses and model simulation datasets in representing the two hurricanes.

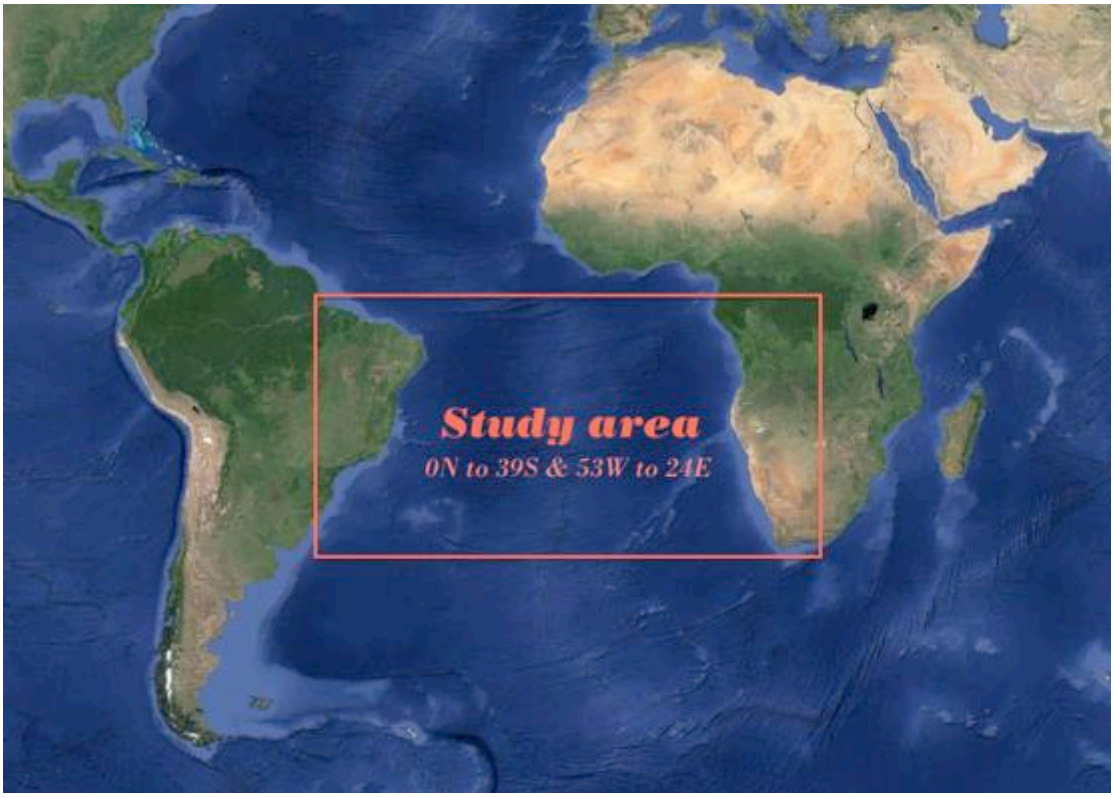


**Figure 3.1**: Map outlining the study area *(Google Earth, 2013)*

### 3.2.1 Observational datasets

The first observation dataset is the International Best Track and Archive for Climate Stewardship (IBT; Knapp et *al.*, 2010), obtained from NOAA's National Centers for Environmental Information website (https://www.ncdc.noaa.gov/ibtracs/). IBT, which consists of TC track data (*e.g.* surface pressure and wind speed), provides information on the distribution, frequency, and intensity of TCs worldwide (Knapp et *al.*, 2010). The second observation dataset is TRMM and is obtained through the Goddard Distributed Active Archive Center (Huffman et *al.*, 2007). TRMM is a satellite product that provides rainfall estimates based on certain merged microwave infrared estimates at three-hour intervals and

0.25° x 0.25° grid spacing for the period 1998 to 2008 (Huffman et *al.*, 2007). The two observation datasets complement each other because while IBT provides information on the location and intensity of the hurricanes, TRMM shows the spatial distribution of the systems and associated intensity. However, none of the observed datasets have information on the vertical structure of the hurricanes.

### 3.2.2 Reanalysis datasets

The two reanalysis datasets analysed are the ECMWF ERAINT reanalysis (http://apps.ecmwf.int/datasets/data/interim-full-daily/levtype=sfc/; Dee et *al.*, 2011) and the NCEP Climate Forecast System Reanalysis (hereafter CFSR; http://dx.doi.org/10.5065/D69K487J; Saha et *al.*, 2010). Both datasets provide atmospheric variables data (*e.g.* 2-dimensional precipitation; 3-dimensonal specific humidity and winds, *etc.*), but at different horizontal resolutions. While the ERAINT data are at 0.75° x 0.75° horizontal grid resolution, CFSR data are at 0.5° x 0.5° horizontal grid resolution. These reanalyses are used for three purposes in this study. First, their capability to represent the characteristics of the hurricanes (their intensity and spatial structure) and the associated rainfall is evaluated against the observation. Secondly, the reanalysis data are used to complement the observed data to study the synoptic winds and moisture fields associated with the hurricanes; especially in studying the relationship between the hurricanes and the SACZ. Lastly, they are used to provide the initial condition and lateral boundary forcing data for the atmospheric model.

### 3.2.3 Atmospheric model, model set-up, and simulations

The WRF model (the Advanced Research WRF Model and the Nonhydrostatic Mesoscale Model; Dudhia, 2016; Skamarock, 2008) is used to perform all the hurricane simulations in this study. The WRF model is a mesoscale numerical weather prediction system used for atmospheric research (Evans et *al.*, 2012). It can be used to simulate the atmospheric conditions (or the dynamical downscaling of global atmospheric data) over a region of interest (Evans et *al.*, 2012); in our case, the SAO. However, being a limited area model, WRF requires a boundary forcing dataset to update the model with atmospheric conditions around the simulation region. Here ERAINT and CFSR provided the boundary forcing datasets. In other words, WRF is used to dynamically downscale ERAINT and CFSR data

over the SAO during the study periods (12 March to 04 April 2004 for Hurricane Catarina and 8 to 12 March 2010 for Hurricane Anita).

The WRF model has two options for dynamic cores and several options for physics parametrization options. The model set-up options used in this study are similar to that of Radu et *al.* (2014). The Kain–Fritsch cumulus parametrization scheme (Kain and Fritsch, 1993; Kain, 2004) is used for convection representation; as well as the Thompson scheme (Hall et *al.*, 2005) for parametrization of microphysical processes, the Rapid Radiative Transfer Model scheme (Mlawer et *al.*, 1997) for long-wave radiation, and Dudhia (1989) implementation for short-wave radiation. The surface layer is parametrized with a similarity scheme based on Monin–Obukhov (Monin and Obukhov, 1954) with Carslon–Boland (Carlson and Boland, 1978) viscous sub-layer and standard similarity functions, while the planetary boundary layer processes are represented with the Yonsei University scheme (Hong et *al.*, 2006).

The model was applied to perform 12 simulations (Table 3.1). The first six simulations are for Hurricane Catarina while the other six are for Hurricane Anita. Two of the Catarina simulations (CEW30 and CCW30) covered $0^{o}$ to $45^{o}$S and $90^{o}$W to $0^{o}$ at a 30 km resolution, but forced with different boundary condition datasets (ERAINT and CFSR, respectively). The next two simulations (CEW10 and CCW10), which covered a smaller domain ($11^{o}$S to $36.5^{o}$S and $69.5^{o}$W to $14^{o}$W) at a higher 10 km resolution, are forced (*i.e.* nested) with the larger domain simulations (EWRF30 and CWRF30, respectively). The last two simulations (CEW03 and CCW03) have the highest resolutions (≈3.3 km), and cover $15^{o}$S to $31^{o}$S and $59^{o}$W to $24.5^{o}$W, and are forced with CEW10 and CCW10, respectively. The six Anita simulations (AEW30, ACW30, AEW10, ACW10, AEW03, and ACW03) have the same configurations as that of Catarina.

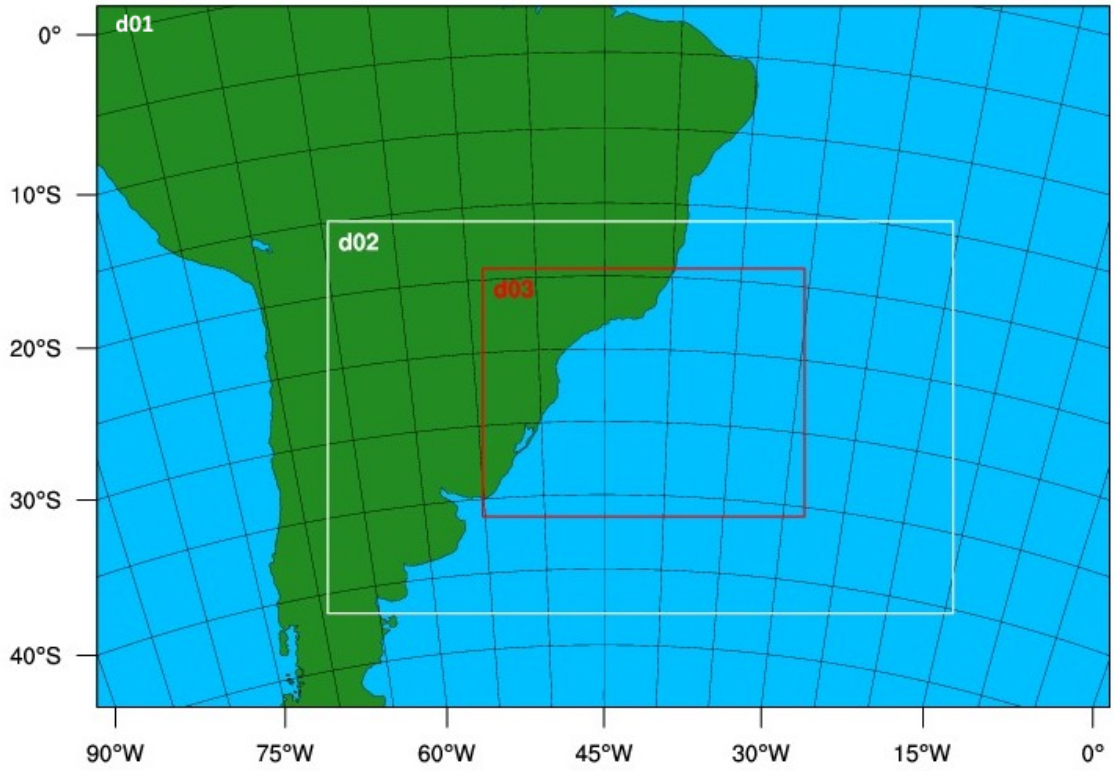


**Figure 3.2**: Nested WRF domain where d01 is at 30 km, d02 is at 10 km, and d03 is at 3.3 km resolutions, for Hurricane Catarina and Hurricane Anita simulations

**Table 3.1**: WRF simulations of Hurricane Catarina and Hurricane Anita

| | Hurricane Catarina | | | Hurricane Anita | |
|---|---|---|---|---|---|
| (1) | CEW03 | Catarina forced with ERAINT at ≈3.3 km resolution | (7) | AEW03 | Anita forced with ERAINT at ≈3.3 km resolution |
| (2) | CEW10 | Catarina forced with ERAINT at 10 km resolution | (8) | AEW10 | Anita forced with ERAINT at 10 km resolution |
| (3) | CEW30 | Catarina forced with ERAINT at 30 km resolution | (9) | AEW30 | Anita forced with ERAINT at 30 km resolution |
| (4) | CCW03 | Catarina forced with CFSR at ≈3.3 km resolution | (10) | ACW03 | Anita forced with CFSR at ≈3.3 km resolution |
| (5) | CCW10 | Catarina forced with CFSR at 10 km resolution | (11) | ACW10 | Anita forced with CFSR at 10 km resolution |
| (6) | CCW30 | Catarina forced with CFSR at 30 km resolution | (12) | ACW30 | Anita forced with CFSR at 30 km resolution |

## 3.3 Methodology

The analysis methods are targeted toward addressing the set objectives in Chapter One. The observation (*i.e.* IBT) and reanalyses (*i.e.* ERAINT and CFSR) are analysed to study the characteristics of the hurricanes and the relationship between the hurricanes and the SACZ. The characteristics considered are the tracks, intensity (using wind speed and surface pressure as the proxy), the pressure-wind relationship, and the spatial-temporal distribution

of rainfall patterns associated with the hurricanes. Following Radu et *al.* (2014)'s approach, the location of the lowest surface pressure is used to identify the location of the hurricanes at every 6-hour interv*al.* The precipitation and moisture flux fields during the mature stage of the hurricanes are used to examine the relationship between the hurricanes and the SACZ.

To examine the capability of WRF in simulating the hurricanes at different resolutions, the characteristics of the simulated hurricanes at different resolutions (*e.g.* CEW30, CEW10, and CEW3) are compared with those of the observed hurricanes (*e.g.* Hurricane Catarina). To examine the sensitivity of the simulated hurricanes to the forcing boundary conditions, the characteristics of the model simulated with ERAINT and CFSR reanalyses are compared. The characteristics of the examined hurricanes include the hurricanes' path, the intensity (*i.e.* wind and surface pressure), the associated maximum rainfall, the spatial distribution of the associated rainfall, and the vertical structure.

# 4 Results and Discussion

Chapter Four discusses the results of this study, starting with looking at the characteristics of Hurricane Catarina and Hurricane Anita in the observational and reanalysis data. It discusses the role of the SACZ in the formation of Hurricane Catarina and Hurricane Anita over the SAO. Lastly, this chapter looks at the WRF model simulations (for each hurricane), using ERAINT and CFSR data, and examines how changes in the model's resolutions and boundary conditions may influence the characteristics of the simulated Hurricane Catarina and Hurricane Anita over the SAO.

## 4.1 Characteristics of Hurricane Catarina and Hurricane Anita in observation and reanalyses

### 4.1.1 A comparison of Hurricane Catarina and Hurricane Anita

Hurricane Catarina and Hurricane Anita are distinct in their tracks (Figure 4.1). While Hurricane Catarina travelled westward (from 28.7°S, 43.1°W) and made landfall in Santa Catarina (at 28.5°S, 51.0°W), Hurricane Anita first travelled south (from 25.2°S, 42.6°W), then southwest (from 27.3°S, 42.6°W) towards the coast without making landfall, and southeast (from 29.7°S, 47.5°W) before dissipating over the SAO at 38.1°S, 31.3°W. Furthermore, while both Hurricane Catarina and Hurricane Anita lasted for two and half days as classified hurricanes, Hurricane Anita covered a longer distance than Hurricane Catarina. However, Hurricane Catarina reached category-2 status while Anita only reached category 1. These results are in line with that of previous studies (Pezza and Simmonds, 2005; McTaggart-Cowan et *al.*, 2006; Veiga et *al.*, 2008; Pezza et *al.*, 2009; Silva Dias et *al.*, 2006; Vianna et *al.*, 2010; Evans and Braun, 2012; Dias Pinto et *al.*, 2013; Radu et *al.*, 2014; Dutra et *al.*, 2017). Dias Pinto et *al.* (2013) indicated that Hurricane Anita did not make landfall because of the prevailing environmental conditions during its cyclogenesis. They found that during its transitioning, Hurricane Anita interacted with another extratropical disturbance after the ocean turbulent heat fluxes decreased. As a result, the vertical wind shear increased, forcing of the extratropical disturbance and caused Anita to travel westward over to colder water, thereby forcing the turbulent heat fluxes to decrease further. The southward movement of Anita was the result of it being embedded in another shortwave synoptic system that propagated eastward away from the coastline (Dias Pinto et

*al.*, 2013). Hence, unlike Hurricane Catarina, the unfavourable conditions prevented Hurricane Anita from reaching category-2 status as well as from making landfall.

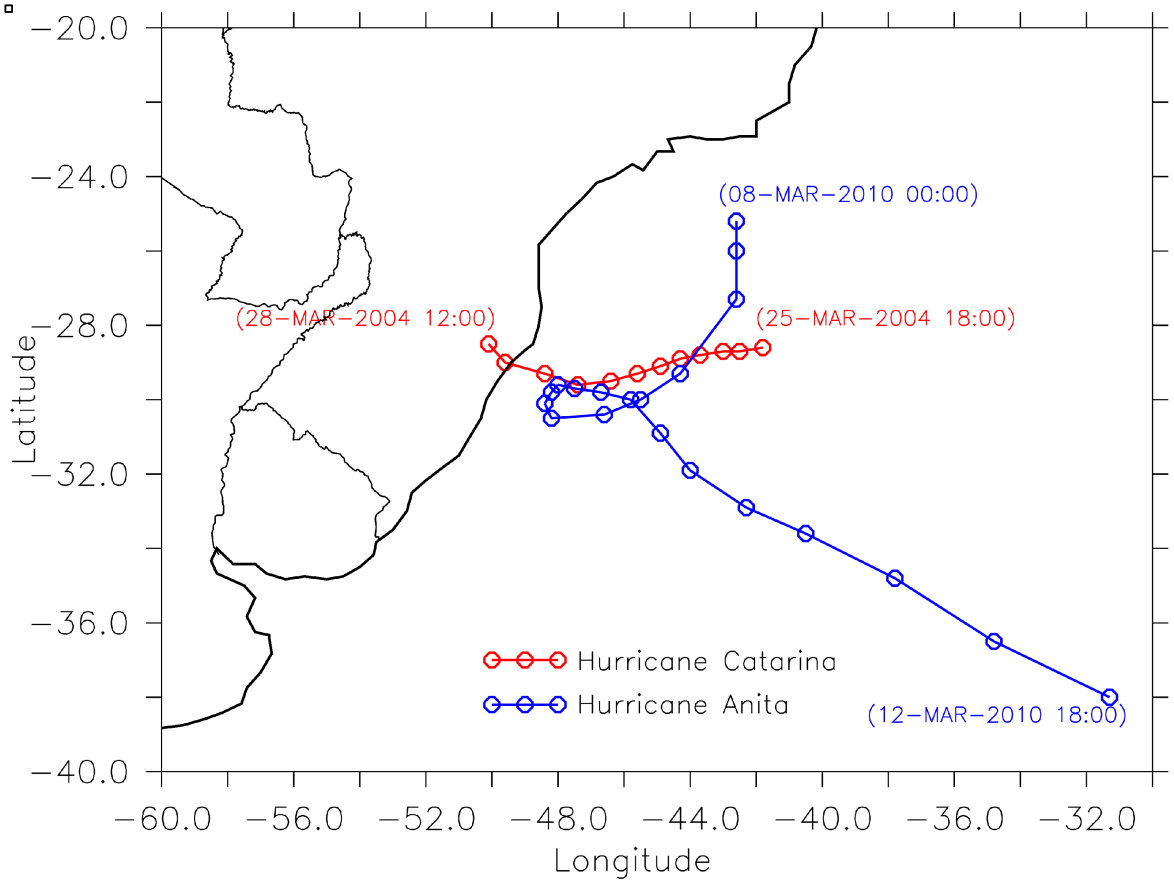


**Figure 4.1**: Observed track of Hurricane Catarina (red) and Hurricane Anita (blue) over the SAO; the locations of each hurricane (from 25 to 28 March 2004 and from 08 to 12 March 2010, respectively) are indicated at 6-hourly intervals

### 4.1.2 Hurricane Catarina in ERAINT and CFSR reanalyses

Both reanalyses realistically represent the track of Hurricane Catarina (with reference to the observational data; Figure 4.2), but with some discrepancies (Figure 4.2a). Nevertheless, CFSR produces a better track than that of ERAINT. While CFSR shows a track with the largest northward bias of approximately 1° at 43°W and the largest southward bias of approximately 1° at 49°W, the track still makes landfall at 29°S, 49.5°W corresponding to the observed track, although 6 hours late. ERAINT, on the other hand, shows a track that maintains a higher northward bias (than that of CFSR) throughout and the track makes no landfall; instead, it moves further north over the ocean as it approaches the coast. The better performance of CFSR over ERAINT in representing the path of Hurricane Catarina may be due to the difference in resolution. The horizontal resolution of CFSR (*i.e.* 0.5° x 0.5°) is higher than that of ERAINT (0.75° x 0.75°); hence convective activity may be stronger in the

former than in the latter. However, the better performance of CFSR here is consistent with various studies that identified CFSR as the best reanalysis for studying the landfall of Hurricane Catarina (*e.g.* Pereira Filho et *al.*, 2010; McTaggart-Cowan et *al.*, 2006).

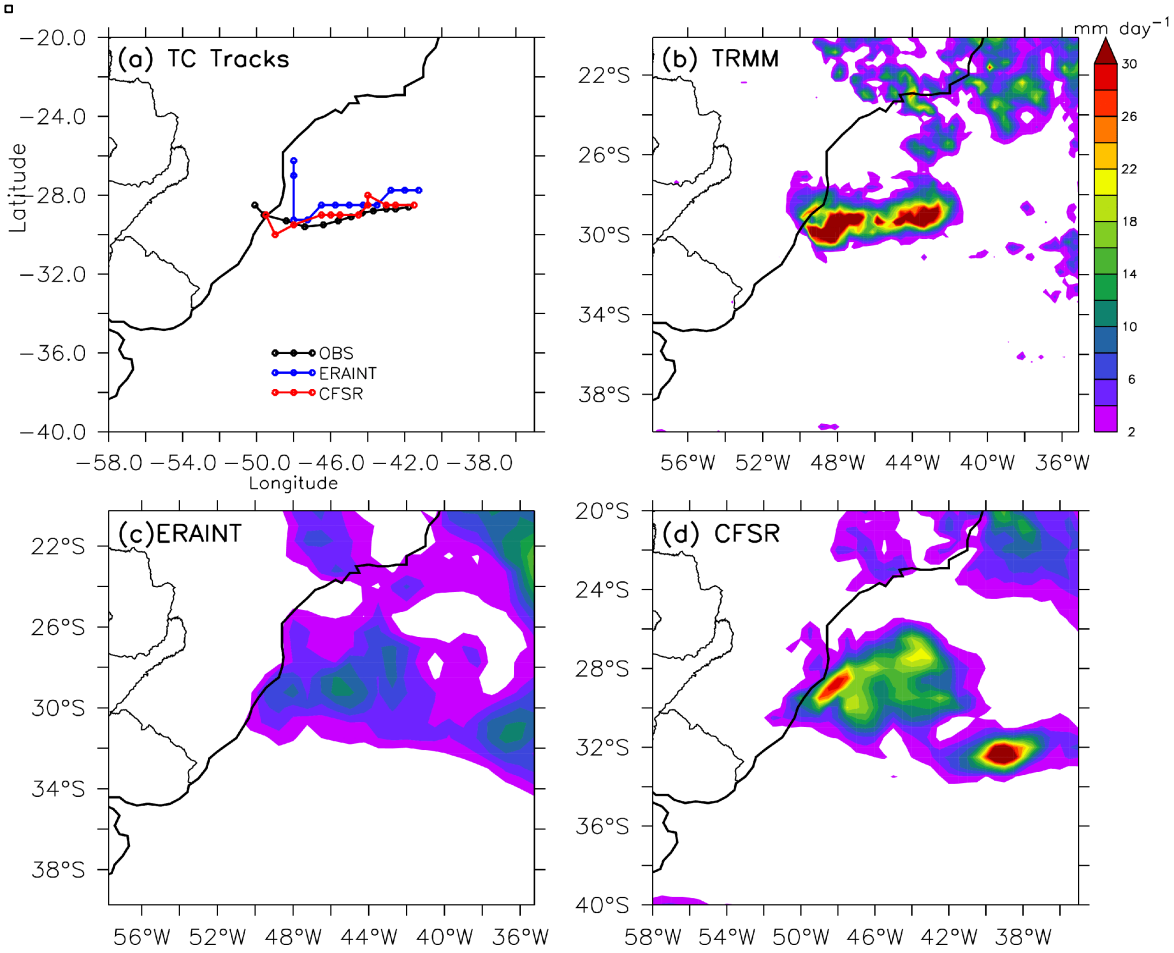


**Figure 4.2**: Characteristics of Hurricane Catarina based on the reanalyses (ERAINT and CFSR) and the observations (IBT and TRMM): (a) the track of Catarina (from 25 to 28 March 2004) as produced by IBT, ERAINT, and CFSR; and the accumulated precipitation (mm day$^{-1}$) over Catarina's lifespan (from 25 to 28 March 2004) as depicted by (b) TRMM, (c) ERAINT and (d) CFSR

Both reanalyses capture the spatial distribution of the accumulated precipitation during the hurricane period, but they underestimate the precipitation intensity (Figure 4.2b, c, and d). Observation and reanalyses demonstrate that the maximum precipitation occurs along the path of Hurricane Catarina, except that, contrary to TRMM observation, the reanalyses produce another maximum precipitation (at around 38°S, 39°W) off Catarina's path. However, the maximum precipitation along the track of the hurricane which is more than 30 mm day$^{-1}$ in TRMM and about 26 mm day$^{-1}$ in CFSR is less than 14 mm day$^{-1}$ ERAINT. Although the maximum precipitation value in CFSR is comparable with the observed value, the aerial coverage of maximum precipitation is smaller than the observed. Hence, the

precipitation from Hurricane Catarina is weaker in the reanalysis than in the observation. The weaker precipitation may be due to the extensive precipitation off the path of Catarina, because the extensive precipitation usually induces a vertical circulation that weakens convection in its surroundings, hence in the hurricane. The temporal distribution of the maximum precipitation from the hurricane further confirms that the reanalyses underestimate the precipitation intensity (Figure 4.3a). With TRMM, the maximum 6-hourly precipitation is up to 24 mm $hr^{-1}$ at 06:00 on 28 March 2004 when Catarina made landfall; but the reanalyses show that it is lower than 4 mm $hr^{-1}$. Pereira Filho et *al.* (2010) found the daily rainfall estimate for the 26 March 2004 to be between 70 mm $day^{-1}$ to 100 mm $day^{-1}$, while Silva Dias et *al.* (2006) found the constant daily rainfall maximum to be greater than 100 mm $day^{-1}$. The former made use of TRMM observational data and various reanalyses, while the latter also made use of TRMM and ECMWF analysis data. The poor performance of the reanalyses in simulating the precipitation intensity may be linked to low resolution and convective parameterization schemes utilised by the reanalyses.

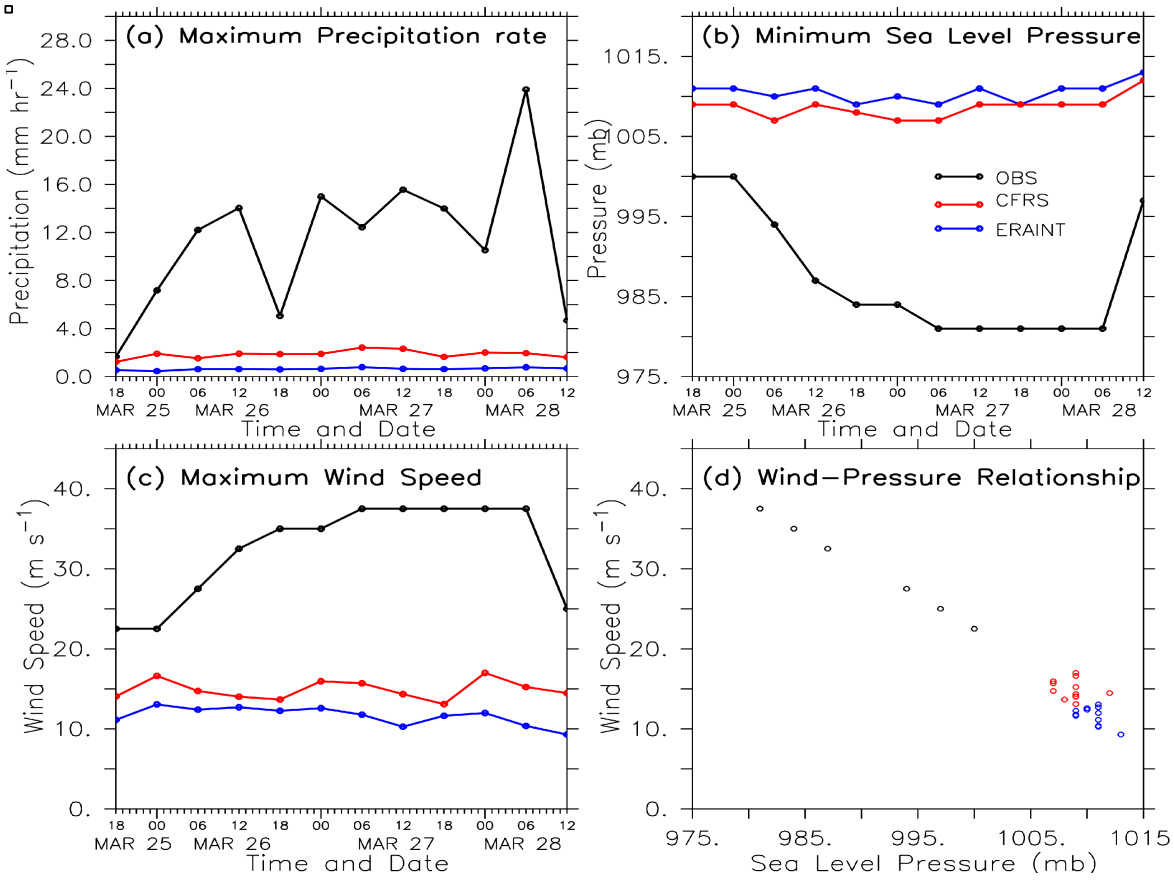


**Figure 4.3**: The temporal variation of (a) maximum 6-hourly accumulated rainfall (mm $hr^{-1}$), (b) minimum sea-level pressure (mb), (c) maximum surface wind speed (m $s^{-1}$), and (d) the wind-pressure relationship for Hurricane Catarina, as depicted by the observations (TRMM or IBT) and the reanalyses (ERAINT and CFSR).

The poor performance of the reanalyses also features in Hurricane Catarina's intensity (Figure 4.3b and c). The IBT observation shows that during the lifecycle of Catarina, the intensity of the system increases (*i.e.* the surface pressure decreases while the wind speed increases) from 18:00 on 25 March (surface pressure ≈1000 mb; wind speed ≈23 m $s^{-1}$) until 06:00 28 March 2004 (surface pressure ≈980 mb; wind speed ≈35 m $s^{-1}$) when Catarina makes landfall. After landfall, the intensity of the hurricane drops drastically (surface pressure ≈998 mb; wind speed ≈25 m $s^{-1}$). In both reanalyses, the hurricane intensity remains almost constant with time; while the surface pressure fluctuates between 1002 mb and 1012 mb, and the wind speed ranges between 9 m $s^{-1}$ and 18 m $s^{-1}$. As Hurricane Catarina does not intensify in the reanalyses and observation, the pressure-wind relationship of the hurricane in the reanalyses does not follow a linear curve as in the IBT observation. Nevertheless, CFSR generally performs better than ERAINT in reproducing the intensity of the hurricane, as the hurricane intensity is much stronger closer to the observed in the former. Silva Dias et *al.* (2006) found the wind speed to be 15 m $s^{-1}$; and McTaggart-Cowan et *al.* (2006) found the wind speed to be 18 m $s^{-1}$ on the 26$^{th}$ and maximum surface winds (during the hurricane's lifetime) of 25 m $s^{-1}$. Alternatively, Pezza and Simmonds (2005) found the sustained surface winds to range from 33 m $s^{-1}$ to 42 m $s^{-1}$ on the 26$^{th}$, Levinson (2005) found the maximum wind speed during landfall to reach 41 m $s^{-1}$, and Pereira Filho et *al.* (2010) found the *in-situ* data collected in the eye of Catarina to be 50 m $s^{-1}$ in a northerly direction. However, McTaggart-Cowan et *al.* (2006) state that on 26 March 2004 it reached 989 hPa and 975 hPa, and Pezza and Simmonds (2005) found category-1 status reached at 974 hPa. Similarly, Vianna et *al.* (2010) estimated a MSLP slightly above 974 hPa during Catarina's most intense stage. As previously mentioned, these studies used different datasets – Pereira Filho et *al.* (2010) made use of TRMM observational data and various reanalyses, while Silva Dias et *al.* (2006) made use of TRMM and ECMWF analysis data. Furthermore, Pezza and Simmonds (2005) made use of the ECMWF operational model and NCEP/DOE, while McTaggart-Cowan et *al.* (2006) used NCEP data, and Vianna et *al.* (2010) made use of NCEP/ECMWF weather prediction models as well as various satellite altimeters.

### 4.1.3 Hurricane Anita in reanalyses

As for Hurricane Catarina, the reanalyses give a credible track for Hurricane Anita (Figure 4.4a). In both reanalyses, the track of Anita closely follows the observed track. They correctly depict that Hurricane Anita initially propagated (in a southwest direction) toward the Brazilian coast, but suddenly moved away (in a south-eastward direction) from the coast, without making landfall. However, CFSR still performs better that ERAINT in reproducing the path. For example, while the latitudinal position of the hurricane at midnight (00:00) on 08 March 2010 is well captured in CFSR, it is about 2° too far northward in the ERAINT plot. In addition, toward the dissipation stage, the bias in the hurricane track is more pronounced in ERAINT than in CFSR. Hence, the location of the dissipation of Hurricane Anita differs amongst the three datasets (TRMM, ERAINT, and CFSR). The observation shows Hurricane Anita to dissipate at 38°S, 31.6°W, but dissipation occurs at 40°S, 32°W in CFSR and at 40.5°S, 36°W in ERAINT. Using TRMM-3B42 and ERAINT data, Dias Pinto et *al.* (2013) also found that Hurricane Anita dissipated at 40°S, 32°W.

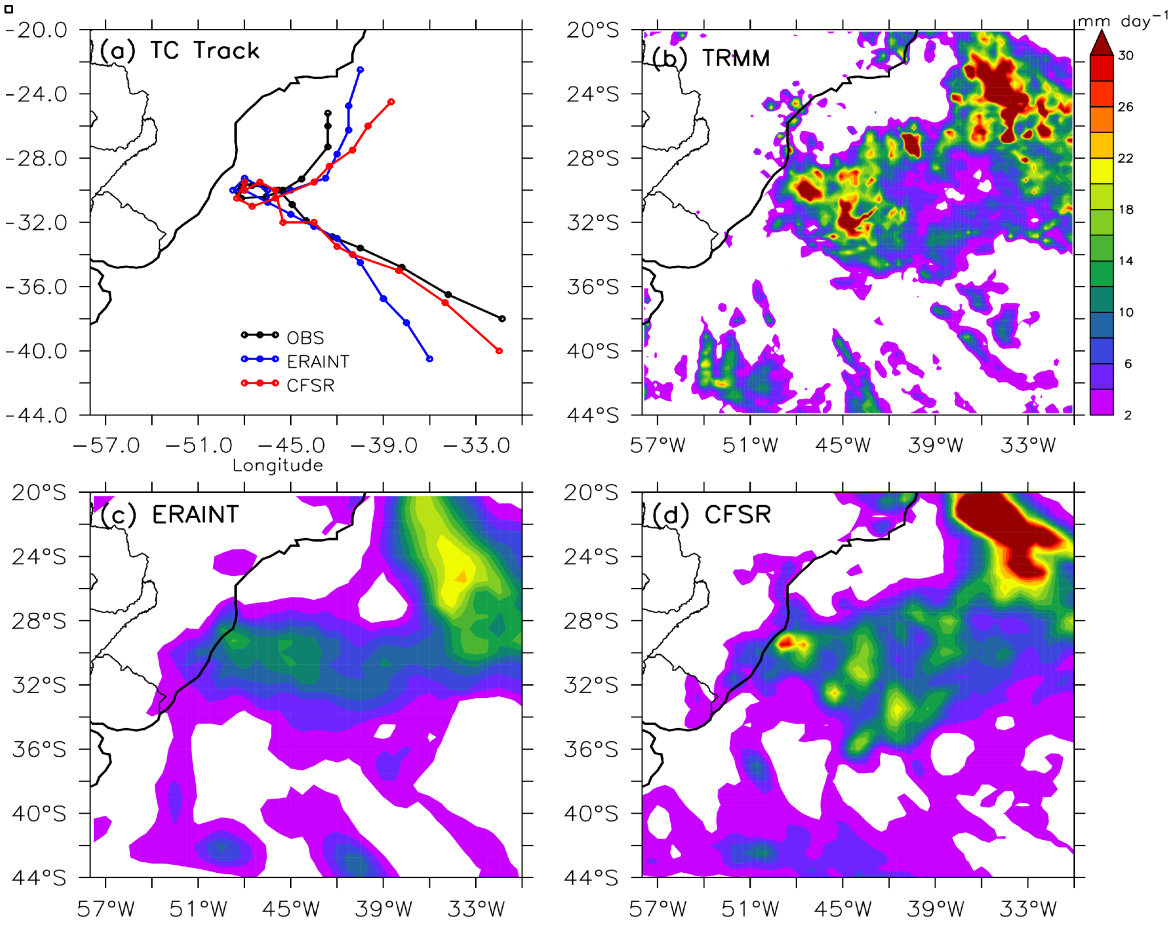


**Figure 4.4**: As in Figure 4.2, but for Hurricane Anita on 10 March 2010

The spatial distribution of the accumulated precipitation during Hurricane Anita is also well reproduced by the reanalyses (Figure 4.4). The three datasets (TRMM, ERAINT, and CFSR) show two areas of maximum precipitation: one is located along the path of Anita and the other is located within the SACZ. However, while TRMM observation shows almost equal magnitudes of precipitation over the two areas, the reanalyses feature more intense precipitation over the SACZ area than over the Anita area. The mechanisms that induce heavy precipitation in these two areas differ. The heavy precipitation over the SACZ area may be attributed to a large-scale convergence of moisture by the trade winds; whereas the heavy precipitation over Anita is due to a smaller-scale convergence and buoyancy induced by the dynamics of the hurricane. The reanalyses feature more precipitation over the SACZ area because they can resolve the large-scale convergence better than the small-scale convergence. In addition, their convective parameterization may not efficiently reproduce the precipitation associated with the vertical movement of the buoyant air parcels (*i.e.* convection) in Anita. Nevertheless, both reanalyses underestimate the precipitation from the hurricane; in this regard, ERAINT performs worse than CFSR. The temporal variation of the maximum 6-hourly accumulated precipitation from Anita is more than 35 mm $hr^{-1}$ in the TRMM observation, but less than 10 mm $hr^{-1}$ in CFSR and less than 5 mm $hr^{-1}$ in ERAINT. This further highlights the influence of reanalysis resolution on representing hurricanes in the SAO. Nevertheless, the discrepancy between observation and reanalyses on hurricane intensity is less pronounced with Hurricane Anita than with Hurricane Catarina (Figure 4.5). This is possibly because Anita is weaker than Catarina and large-scale circulations (which are well resolved in the reanalyses) play a more crucial role in characteristics of Anita than in that of Catarina.

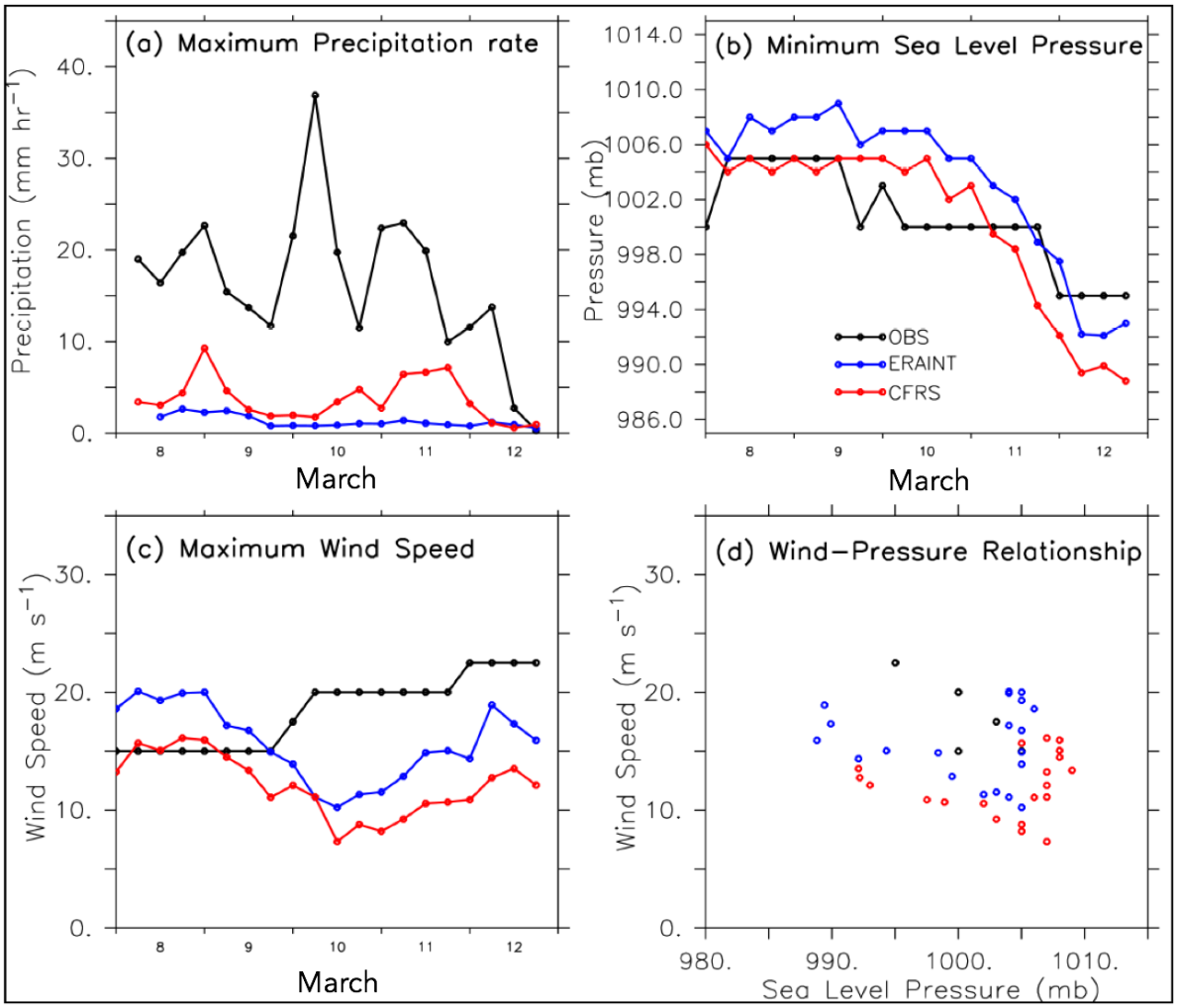


**Figure 4.5**: As in Figure 4.3, but for Hurricane Anita during 8 and 12 March 2010

However, with Anita, the IBT observation shows a stepwise intensification of the system (Figure 4.5). For instance, the surface pressure and wind speed, which are constant (1003 mb and 15 m s$^{-1}$) for about two days, suddenly change (to 1000 mb and 20 m s$^{-1}$) and remain constant for another two days before changing again (to 994 mb and 22 m s$^{-1}$). The reanalyses do not reproduce this stepwise intensification of Anita; instead, they feature a gradual decrease in surface pressure (from 1006 mb to 990 mb) and a linear decrease in wind speed (from 20 m s$^{-1}$ to 10 m s$^{-1}$ in 3 days) followed by an increase in the wind speed for the next 3 days (up to 20 m s$^{-1}$). The stepwise changes in observation produces a linear curve in the wind-pressure relationship, while the changes in the reanalyses do not (Figure 4.5d). The surface pressure and wind speed values shown in Figure 4.5b are closer to values in other studies in the literature. For instance, using TRMM-3B42 and ERAINT data Dias Pinto et *al.* (2013) recorded the surface pressure of the system to be 1012 hPa on 10 March 2010; and using GFS data, NOAA (2010) found it to be 1006 hPa for the same day. With

GOES-12 and TRMM data, Gutro (2010) found the maximum sustained winds to be roughly 17.4 m $s^{-1}$ on 10 March, while Dias Pinto et *al.* (2013) state the surface winds to reach about 10 m $s^{-1}$ on the eastward side strengthening to about 15 m $s^{-1}$ on the 11 March 2010.

In summary, results presented thus far show that while the reanalyses (ERAINT and CFSR) do a good job in reproducing the observed track of Hurricane Catarina and Hurricane Anita and in reporting the associated rainfall patterns, they underestimate the intensity of the hurricanes (*e.g.* surface pressure, wind speed, and precipitation). This underestimation is not surprising given that the resolutions of the reanalyses are too coarse to adequately resolve the hurricane dynamics. However, the reanalyses can be used to provide valuable information on the synoptic-scale conditions associated with the two hurricanes, especially in shedding light on the relationship between the SACZ and the hurricanes.

### 4.1.4 Relationship between the SACZ and hurricanes over the SAO

Figure 4.6, which presents the rainfall and vertically-integrated moisture flux of the reanalyses during the mature stage of Hurricane Catarina and Hurricane Anita, reveals the relationship between the SACZ and the hurricanes. Both reanalyses show not only the presence of the SACZ during both hurricanes, but also indicate that the convective activities in the SACZ are coupled with those in the hurricanes. In addition, the converging moisture along the SACZ feeds into both hurricanes. This is consistent with previous studies (*e.g.* Todd et *al.*, 2004; Garcia and Kayano, 2010) that showed that the convergence moisture flux along the SACZ provides moisture to the surrounding atmosphere. The present study, however, shows that the moisture from the SACZ is transported into Hurricane Catarina and Hurricane Anita. Hence, the SACZ may be a major moisture belt fuelling hurricane activity in the SAO.

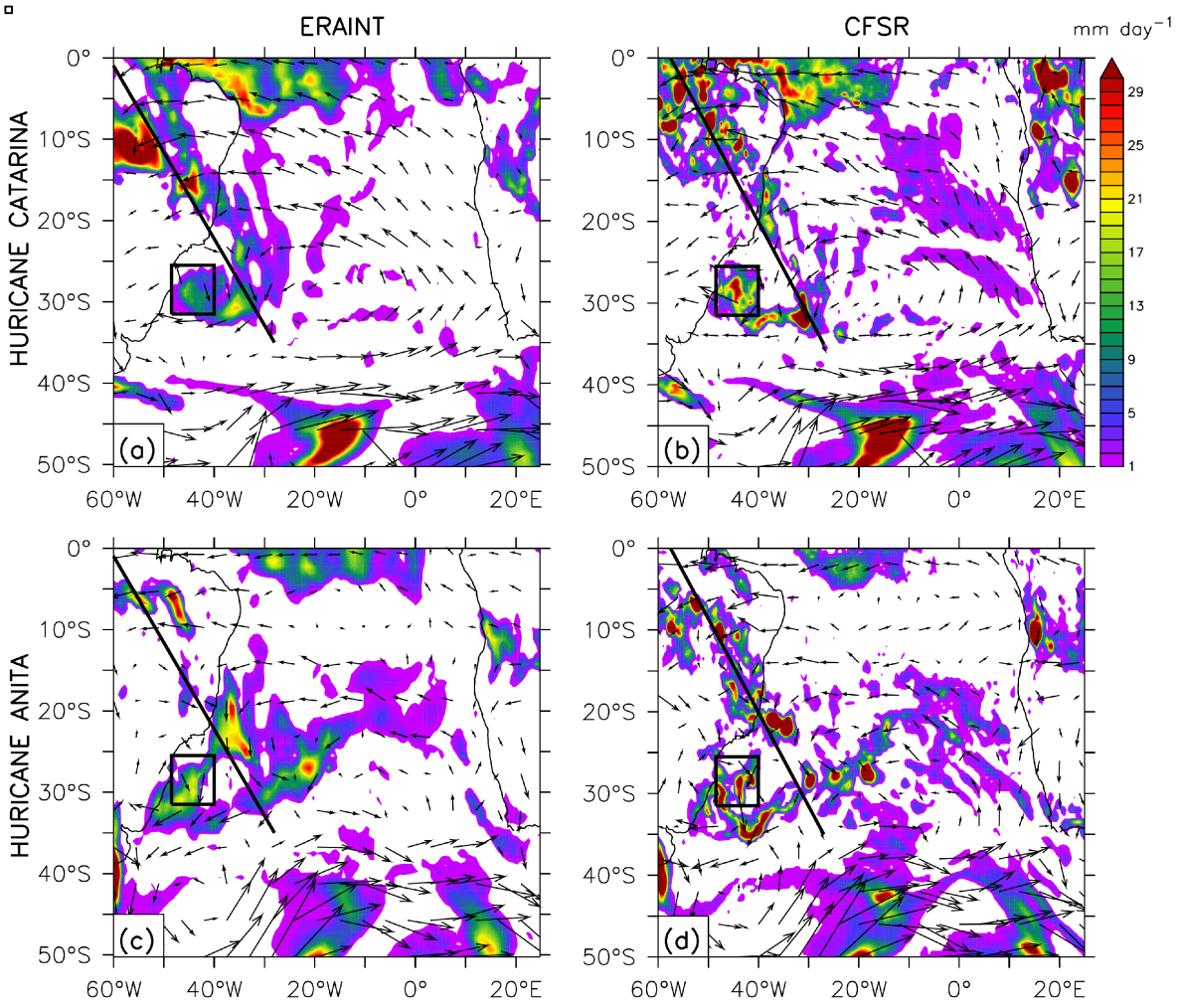


**Figure 4.6**: Precipitation (mm day$^{-1}$) and 850 hPa moisture flux associated with Hurricane Catarina (on 26 March 2004; panels a and b) and Hurricane Anita (on 10 March 2010; panels c and d) as depicted by CFSR (panels b and d) and ERAINT (panels a and c). The location of each hurricane is indicated with a black square, while that of the SACZ is shown with a black line

## 4.2 WRF simulations of Hurricane Catarina

### 4.2.1 Simulations with ERAINT forcing

Figure 4.7 presents the WRF simulations of Hurricane Catarina at different resolutions (*i.e.* CEW30: 30 km; CEW10: 10 km; CEW30: 3.3 km). Note that, as indicated in Chapter 3, CEW30 downscales ERAINT, while CEW10 downscales CEW30, and CEW03 downscales CEW10. In CEW30 and CEW03, the path of the simulated hurricane is located too far south of the observed path but, unlike in ERAINT, the hurricane made landfall (though at about 2° south of the observation). CEW10 gives the best simulation of Hurricane Catarina's path. In this simulation, the path closely follows the observed path and the simulated hurricane made landfall at the same location (and at the same time) as the observed. However, in all the simulations, the spatial distribution of the accumulated precipitation is

similar to those of ERAINT and TRMM, except that the magnitude of the simulated precipitation is higher (and closer to TRMM observation) than what ERAINT offers (compare Figure 4.7 with 4.1). This is better depicted in Figure 4.8a. In this regard, CEW10 still gives the best precipitation because while the maximum precipitation is up to 24 mm $hr^{-1}$ in TRMM observation, it is about 2 mm $hr^{-1}$ in ERAINT, 11 mm $hr^{-1}$ in CEW30, 11 mm $hr^{-1}$ in CEW03, but 17 mm $hr^{-1}$ in CEW10. Nevertheless, all the simulations fail (as ERAINT) in reproducing the temporal variability of the precipitation. For instance, TRMM showed that the precipitation varies from 2 mm $hr^{-1}$ (at 18:00 on 25 March) to about 24 mm $hr^{-1}$ (at 06:00 on 28 March), but all the simulations produce a constant maximum precipitation throughout Catarina's lifetime. This shortcoming may be attributed to parameterization of cloud and precipitation micro-physics in the model.

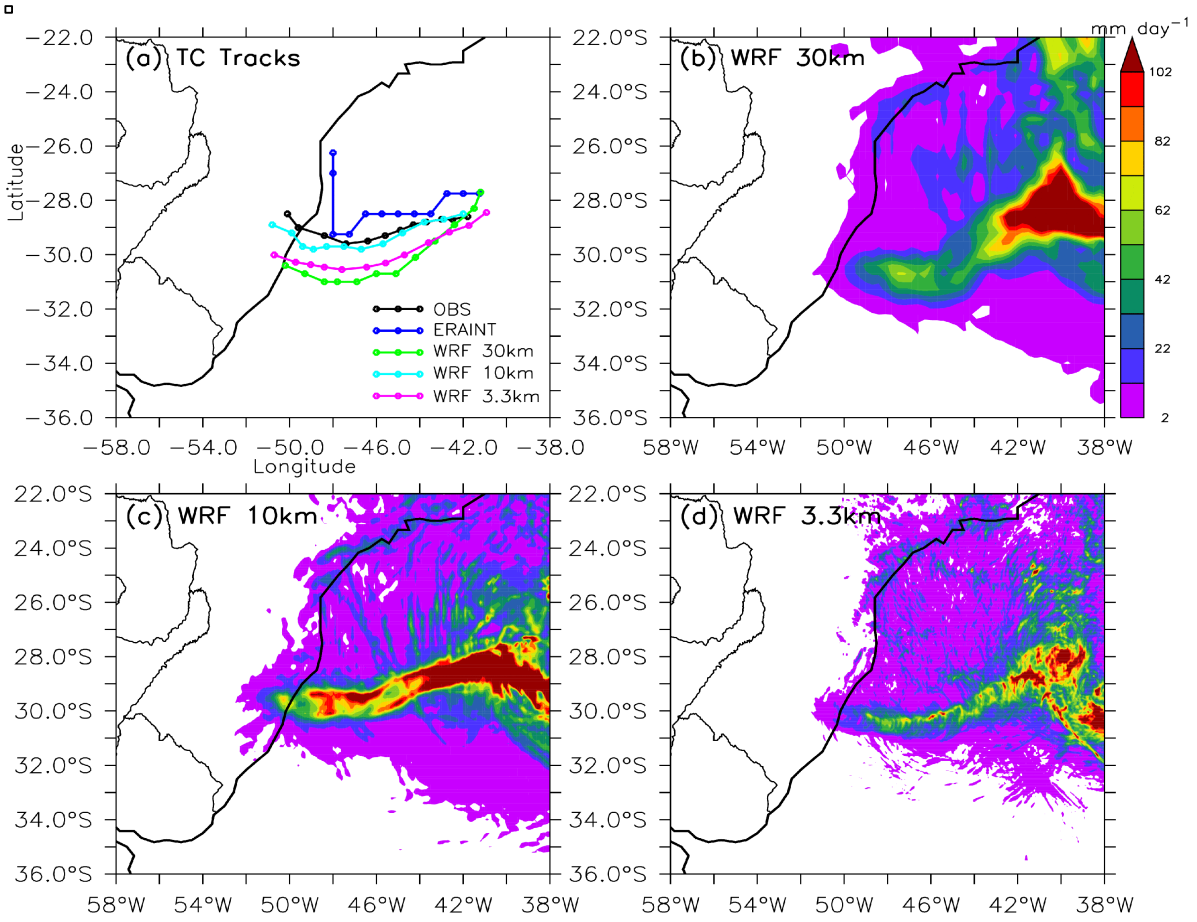


**Figure 4.7**: Sensitivity of Hurricane Catarina's track and associated precipitation in WRF to horizontal grid resolution: (a) the track of the hurricane (from 25 to 28 March 2004) as produced by observation (IBT), ERAINT and WRF simulations at the indicated resolutions. The simulated accumulated precipitation (mm $day^{-1}$) during the hurricane period (from 25 to 28 March 2004) at (b) 30 km, (c) 10 km and (d) 3.3 km resolutions

The WRF simulations improve on the hurricane intensity (surface pressure and wind speed) produced by ERAINT (Figure 4.8b and c). In this respect, CEW10 features the best improvement by producing the closest minimum surface pressure and maximum wind speed to the IBT observation (Figure 4.8d). However, the temporal variability of Hurricane Catarina's intensity is constant throughout the simulation period; whereas, in the observation Catarina intensifies with time. The lack of temporal variability in the simulated hurricane hinders the simulations from producing a linear curve in the wind-pressure plots as depicted in observation. Instead, the wind-pressure plots for each simulation cluster together. For instance, while the plots for CEW30 cluster around a point (1005 mb; 10 m $s^{-1}$), the plots for CEW10 cluster around another point (985 mb; 30 m $s^{-1}$).

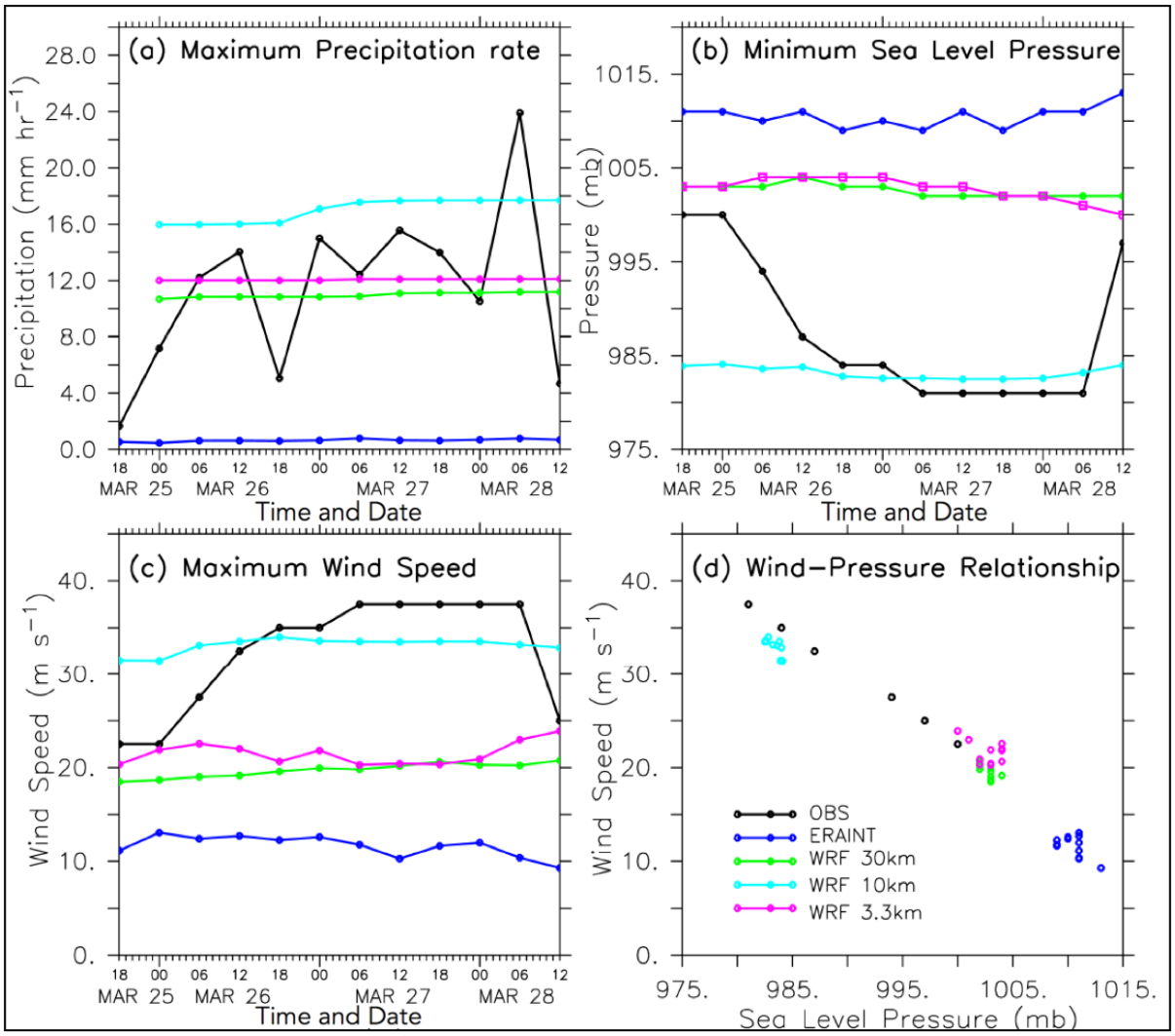


**Figure 4.8**: Sensitivity of Hurricane Catarina's intensity in WRF simulations to horizontal grid resolution

The influence of resolution also features on the horizontal and vertical structure of the simulated Hurricane Catarina (Figure 4.9). While all the simulations (CEW30, CEW10, CEW03) feature a warm-core hurricane system with a cyclonic flow around an eye, CEW10 simulates the hurricane with the warmest core. The simulated hurricane is 5°C warmer than the surrounding atmosphere in CEW10, but is less than 5°C warmer than the surrounding atmosphere in CEW03 and in CEW30. This perhaps explains why CEW10 produced the strongest hurricane than what CEW03 and CEW30 produced. While the hurricane eye and the eye wall (characterized by strong winds around the wall) are better resolved in CEW10 and CEW03 than in CEW30, the wind is strongest in CEW10.

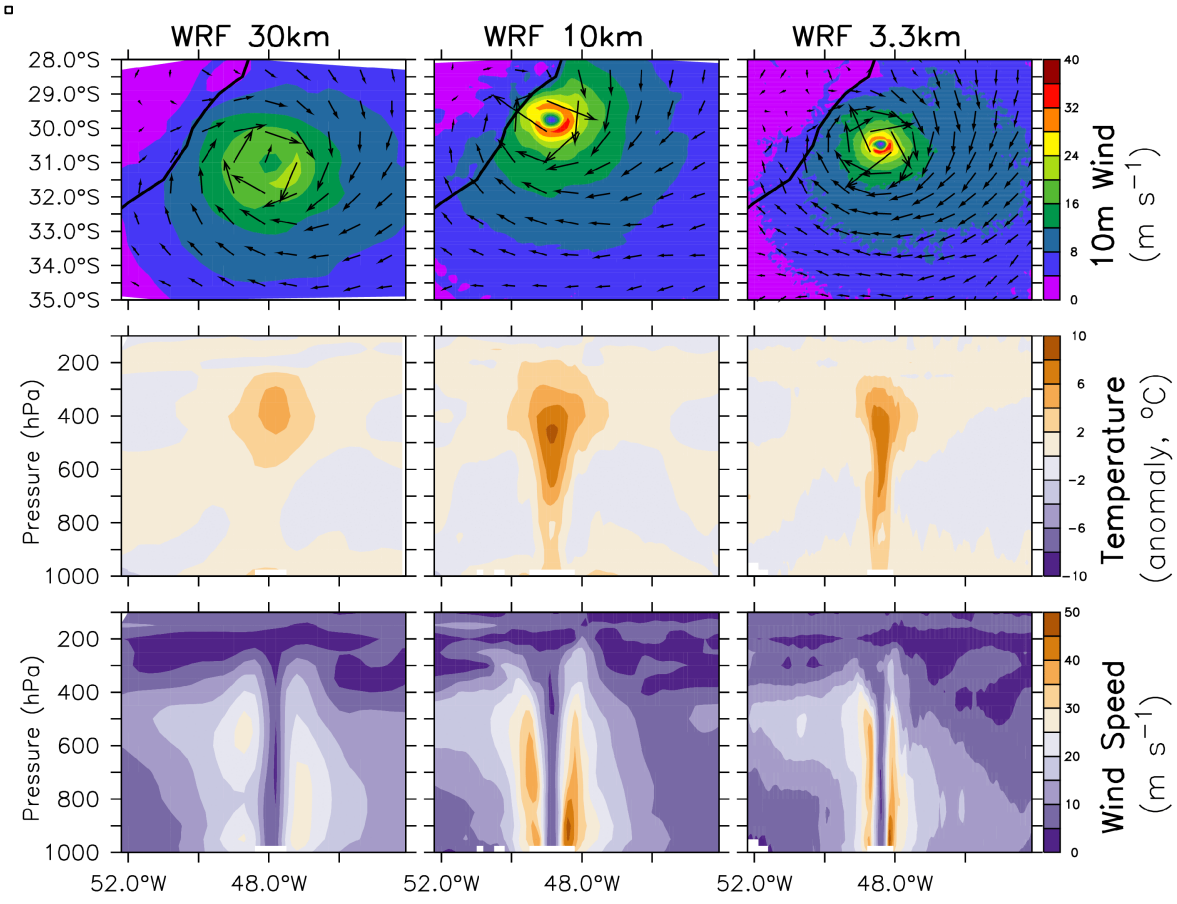


**Figure 4.9**: Sensitivity of Hurricane Catarina's vertical structure in WRF simulations to horizontal grid resolution

The results of the WRF simulations here are comparable with those in Radu et *al.* (2014). Both studies use the same WRF model set-ups (*i.e.* CEW30, CEW10, and CEW03), but Radu et *al.* (2014) only analysed the model results for the highest resolution (CEW03). In their study, CEW03 also simulates the path of Hurricane Catarina south of the observed location; however, the temporal variation of their CEW03 is closer to the observation than

CEW03 is here. However, Radu et *al.* (2014) only analysed CEW03 with the common idea that the highest resolution simulation will produce the best simulation but, the present results show that CEW10 gave a better simulation of the hurricane than CEW03. The reason for this is not clear, but it may be due to the use of convective parameterization in CEW10 and not in CEW03. It could be that, since CEW03 downscales CEW10, the latter might have depleted the simulated atmosphere of the necessary moisture needed for simulating a stronger hurricane in CEW03. Further analysis is needed to pinpoint why CEW10 performs better than CEW03 in simulating Hurricane Catarina, but such analysis is beyond the scope of the present study.

### 4.2.2 Simulations with CFSR forcing

To show the sensitivity of the results in the previous section (*i.e.* Section 4.2.1) to the forcing of the reanalyses, the present section discusses the results of the WRF simulation forced with the CFSR dataset (*i.e.* CCW30: 30 km; CCW10: 10 km; CCW03: 3.3 km). A comparison of Figure 4.10 with Figure 4.7 shows that CCW30 performs worse than CEW30 in simulating Hurricane Catarina's path and in replicating the associated precipitation. For instance, contrary to observation, CCW30 features a hurricane that moved in a southward direction and which made no landfall. Also, the spatial pattern of the accumulated precipitation differs from the TRMM observation (compare Figure 4.10 with 4.2), in that the maximum accumulated precipitation is located further east away from the coast. This implies that, despite the better performance of CFSR (than ERAINT) in representing the hurricane pattern, forcing WRF with CFSR in simulating Catarina produces worse results than forcing it with ERAINT. In fact, the results of CCW30 are worse than that of the forcing reanalysis, meaning that there is no added value in downscaling CFSR results with WRF for simulating the path of Catarina. Although, the magnitude of precipitation is higher and closer to the observation in the WRF simulations than they are in CFSR, the hurricane intensity is similar to that of CFSR (Figure 4.11).

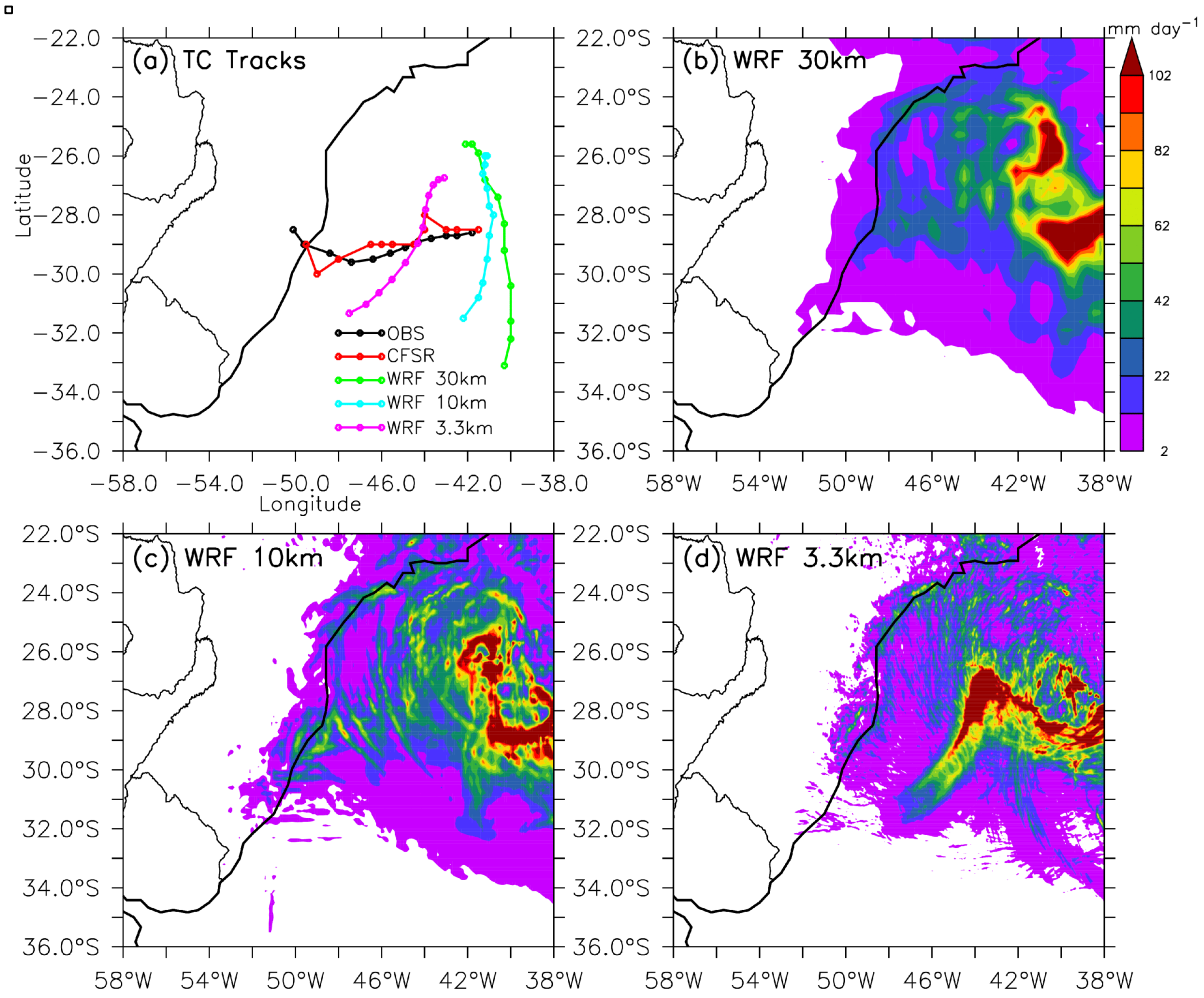


**Figure 4.10**: As in Figure 4.7, but for CFSR

Nevertheless, with the increase in the model resolution (in CCW10 and CCW03), the quality of the simulated Hurricane Catarina improves. For example, the track of the simulated hurricane shifted more westward toward the observed track, although the simulated hurricane did not make landfall, not even in the simulation with the highest resolution (*i.e.* CCW03). The spatial pattern of the accumulated precipitation also improves (CCW03 gave the most comparable pattern to the observation). In addition, the magnitude of the maximum precipitation from the simulated hurricane increased and moved closer to the observed value (Figure 4.11a). Furthermore, the intensity of the simulated hurricane increased with the increase in the model resolution (Figure 4.11b and c). CCW03, which features the most linear plot of the wind-pressure relationship graph (Figure 4.11d), simulated the most intense hurricane.

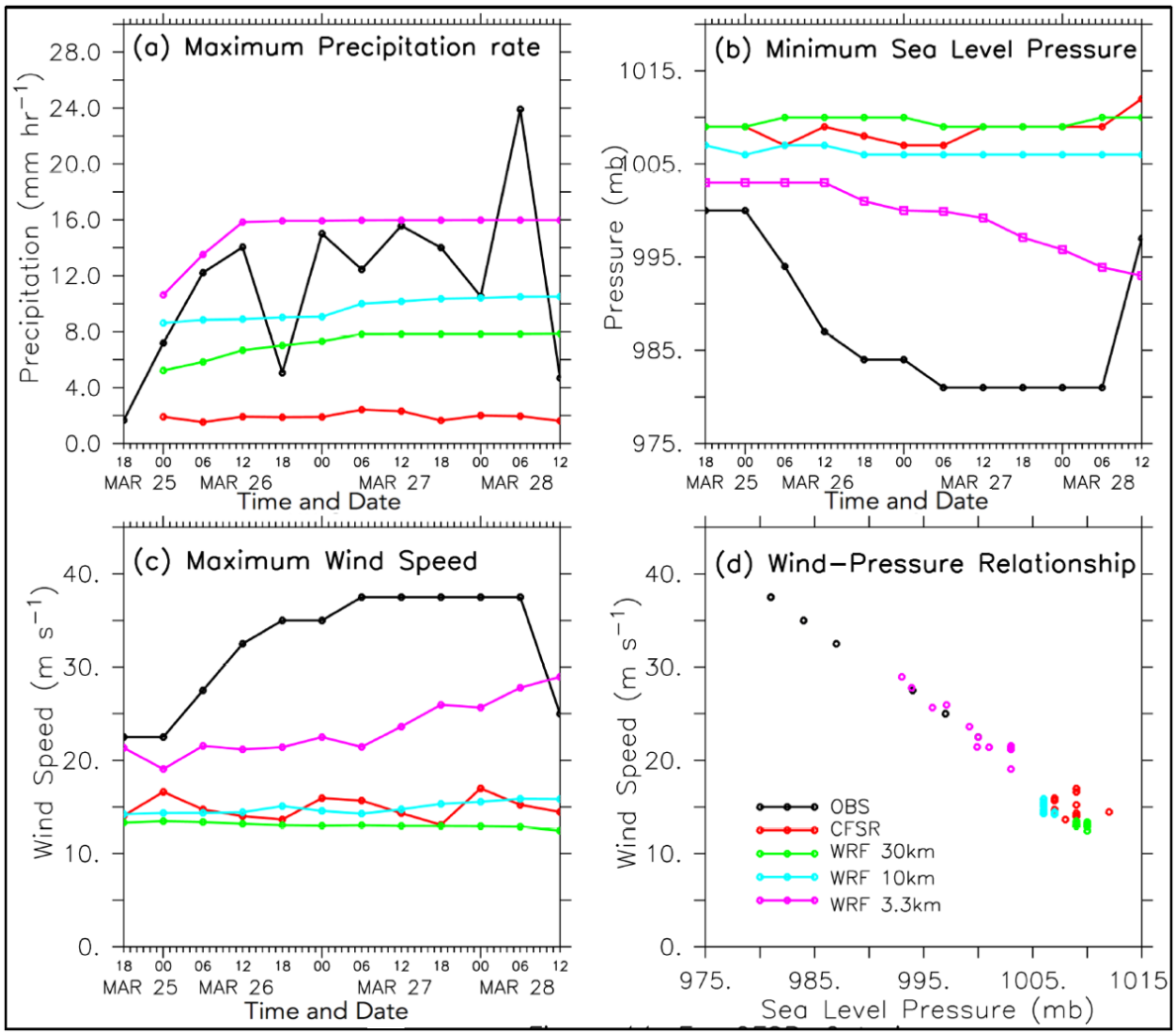


**Figure 4.11**: As in Figure 4.10, but for CFSR forcing

The influence of the resolution on the simulated system is best depicted in the spatial and vertical structure of the hurricane (Figure 4.11). In CCW30 and CCW10, the structure of the simulated system may be best described as a tropical disturbance, because the eye of the system was not well defined, the cyclonic motion around the eye was weak (<10 m/s), and the centre of the system is less than 3°C warmer than the surrounding atmosphere. On the other hand, CCW03 best simulated the warm-core hurricane structure in which the eye was well defined; there was strong cyclonic flow around the eye; the wind speed within the eye wall exceeded up to 40 m s$^{-1}$; the strongest wind was located at the eastern part of the system; and the centre of the hurricane was more than 8°C warmer than the hurricane environment.

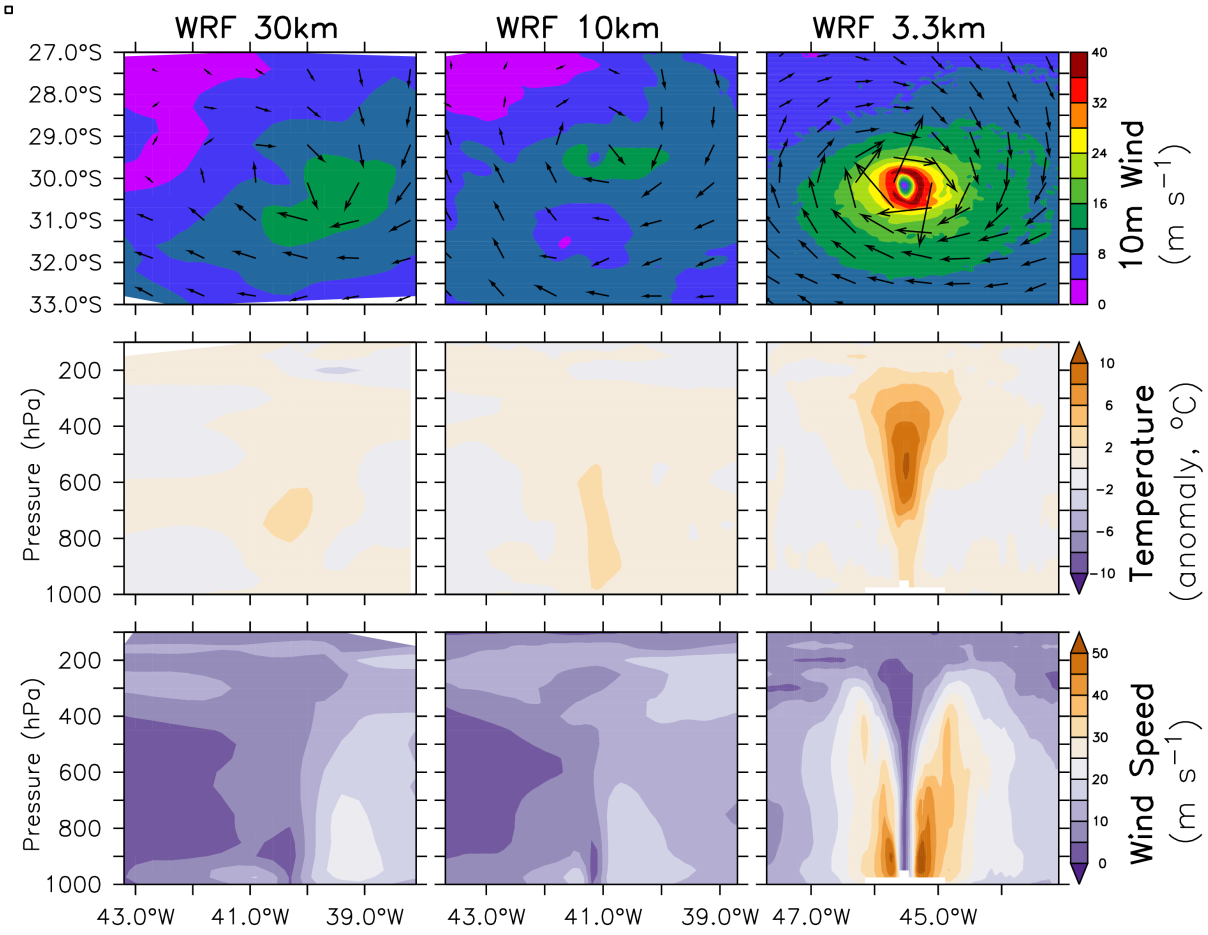


**Figure 4.12**: As in Figure 4.9, but for CFSR forcing

Hence, the results presented indicate that the characteristic of the WRF-simulated Hurricane Catarina is not only sensitive to model resolution, but it is also sensitive to boundary condition forcing. Surprisingly, the results suggest that using a better reanalysis dataset (CFSR) to force the model may not necessarily translate into a better quality simulated hurricane. The reason for this is not clear. Further adjustments and refining the model configuration may be necessary to improve the CFSR-forced simulations; all our attempts to achieve this proved futile. Furthermore, the results indicate that the influence of increasing model resolution on the quality of the simulated hurricane also depends on the boundary forcing. As expected, with CFSR forcing, the highest resolution WRF simulation (CCW03) produced the most accurate representation of the hurricane, but that is not the case with ERAINT forcing, where WRF simulated at a 10 km-resolution (CEW10) featured a better hurricane simulation than that of highest resolution simulation (CEW03). To check whether these results are specific to Hurricane Catarina or not, the next section (Section 4.3) presents the equivalent simulation results for a similar analysis of Hurricane Anita.

## 4.3 WRF simulations of Hurricane Anita

### 4.3.1 Simulations with ERAINT forcing

Figure 4.13 presents the ERAINT-forced WRF simulations of Hurricane Anita at different resolutions (*i.e.* AEW30: 30 km; AEW10: 10 km; AEW03: 3.3 km). The figure shows that none of the simulations capture the track of the hurricane as the IBT observation. In the observation, Anita first travelled south, then southwest (towards the coast), and southeast (away from coast, without making landfall), before dissipating over the ocean. In AEW30 and AEW10 simulations, the hurricane moved south then southeast and dissipated at about 4° south of the observed hurricane. Hence, in both simulations, the track of the simulated hurricane was located too far east and the westward movement of the hurricane was smaller than that of the observation. AEW03 seems to give the best simulation of Anita's track. In this simulation, the hurricane track was similar to the observed track, in that it travelled southwest and reached the same longitude as the observation before travelling eastward. Nevertheless, the westward and eastward legs of the simulated track occurred north of the observed track because the simulated hurricane did not travel far enough southward, making the dissipation of the AEW03 hurricane occur north of the observed paths. Therefore, none of these WRF simulations add value to the ERAINT results in simulating the hurricane track of Hurricane Anita.

Nonetheless, the spatial distribution of the accumulated precipitation is similar to that of TRMM and ERAINT, except that the simulations produced too much precipitation along the coast. Since the simulated hurricane did not move towards AEW30 or AEW10, the rainfall near the coast may not be attributed to Anita in these simulations. In general, the magnitude of the simulated precipitation was higher than what TRMM and ERAINT offered (exceeding 205 mm $hr^{-1}$ in the simulations versus more than 30 mm $hr^{-1}$ in the observation and reanalysis; compare Figure 4.13 with 4.4). This is better depicted in Figure 4.14a. In this regard, AEW10 gives the best precipitation, because while the maximum precipitation was up to 42 mm $hr^{-1}$ in TRMM observation, it was approximately 5 mm $hr^{-1}$ in ERAINT, 20 mm $hr^{-1}$ in AEW30, 33 mm $hr^{-1}$ in AEW03, but 39 mm $hr^{-1}$ in AEW10. Nevertheless, all the simulations fail (as does ERAINT) in reproducing the temporal variability of the precipitation. For instance, TRMM showed that the precipitation varied from 26 mm $hr^{-1}$ (at 03:00 on 8 March) to about 43 mm $hr^{-1}$ (at 03:00 on 10 March), but all the simulations

produce an increasingly linear maximum precipitation throughout the lifetime of Hurricane Anita.

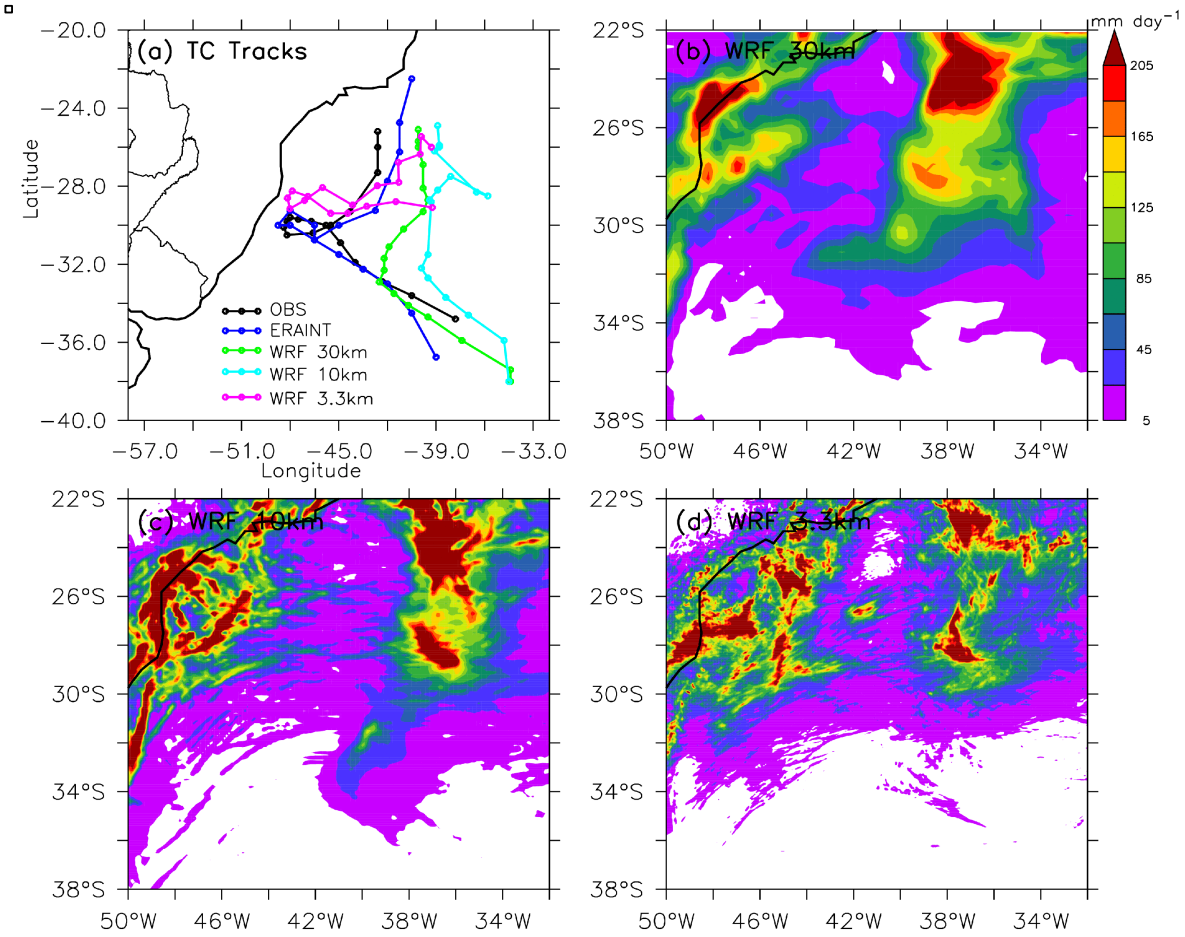


**Figure 4.13**: As in Figure 4.7, but for Hurricane Anita

The WRF simulations improve on Hurricane Anita's intensity (surface pressure, but not wind speed) produced by ERAINT (Figure 4.14b and c). In this respect, AEW03 features the best improvement by producing the closest minimum surface pressure to the IBT observation; because while the minimum surface pressure was at 1000 mb in IBT observation, it was about 993 mb in ERAINT, 986 mb in AEW30, 985.5 mb in AEW10, but 998 mb in AEW03 (Figure 4.14b). The IBT observation showed a stepwise intensification of the maximum wind speed. For instance, the wind speed was constant (15 m $s^{-1}$) for about two days, suddenly changed (20 m $s^{-1}$) and then remained constant for another two days before changing again (to 22 m $s^{-1}$). The simulations do not reproduce this stepwise intensification of Anita; instead they featured a fluctuating change in wind speed with different maximum values (AEW30: 29 m $s^{-1}$, AEW10: 31 m $s^{-1}$, AEW03: 25 m $s^{-1}$). The

lack of temporal variability in the simulated hurricane hinders the simulations from producing a linear curve in the wind-pressure plots as the observation features (Figure 4.14d). Instead, the wind versus pressure plots for each simulation cluster around the observation. For instance, while the plots for AEW30 and AEW10 have a spatially-distributed cluster around 993 mb versus 24 m $s^{-1}$, the plot for AEW03 cluster around 1005 mb versus 19 m $s^{-1}$.

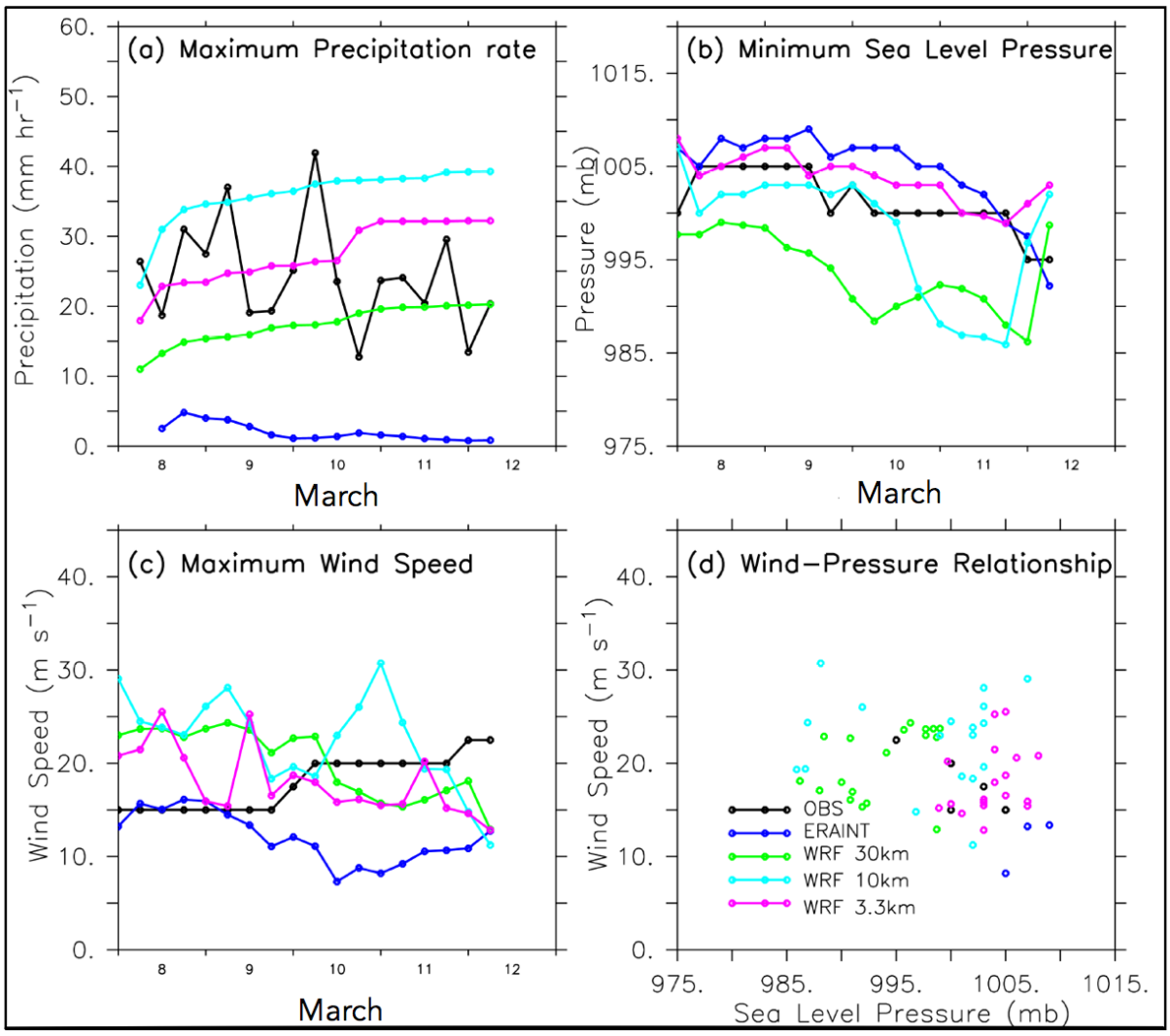


**Figure 4.14**: As in Figure 4.8, but for Hurricane Anita

At the mature stages (*i.e.* lowest surface pressure), none of the simulated systems can be regarded as a TC (Figure 4.15). Although they all feature cyclonic flow around a low centre, the low is too wide to be regarded as an eye of a hurricane. Also, the cyclonic wind is too weak (<20 m $s^{-1}$ in the three simulations). In AEW30 and AEW10, the warm core of the system was too broad and the values very weak (<5°C warmer than the surrounding atmosphere), possibly because the upper-level wind of the system was too strong (>40 m $s^{-1}$) and such a

strong upper-level wind will not allow the system to mature into a hurricane. This is consistent with the results of Dias Pinto et *al.* (2013) who found that the unfavourable conditions prevented Hurricane Anita from reaching category-2 status. However, in AEW30, the system only formed a shallow warm-core system. Hence, in comparison with the simulated Hurricane Catarina, Anita is poorly simulated by WRF. This may be because the environment of the former is more favourable to the formation of TCs than the other. Hence, the added value of the WRF simulations to ERAINT is more considerable for Catarina, than for Anita.

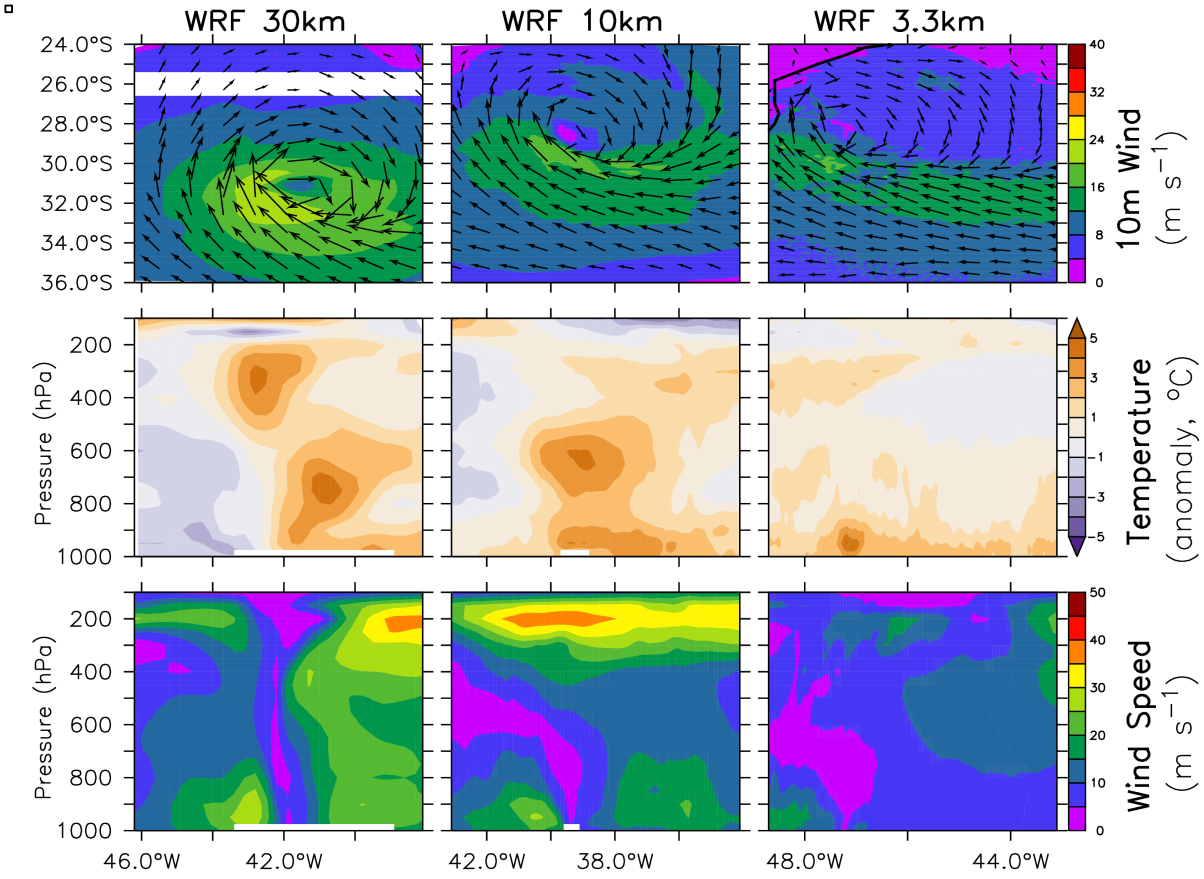


**Figure 4.15**: As in Figure 4.9, but for Hurricane Anita

### 4.3.2 Simulations with CFSR forcing

With CFSR forcing, WRF simulations of Hurricane Anita at different resolutions (*i.e.* ACW30: 30 km; ACW10: 10 km; ACW03: 3.3 km) feature some similarities with the simulations with ERAINT forcing (Figure 4.16), but there are some notable differences. For example, in ACW30 and ACW10, the hurricane tracks are located further eastward of their position in AEW30 and AEW10, respectively. Although, the simulation with the highest resolution (*i.e.* ACW03) gives better results than those of AEW30 and ACW10, the location

of the hurricane track also occurred further north in ACW03 than in AEW03. This means that, in producing the hurricane track, CFSR forcing produces worse simulations than that of ERAINT forcing; this is consistent with what was found in the Hurricane Catarina simulations (Section 4.2.2). However, the differences between ERAINT forcing and CFSR forcing are less distinct in the pattern of the accumulated precipitation (Figure 4.16), the hurricane intensity (Figure 4.17), and the hurricane structure (Figure 4.18).

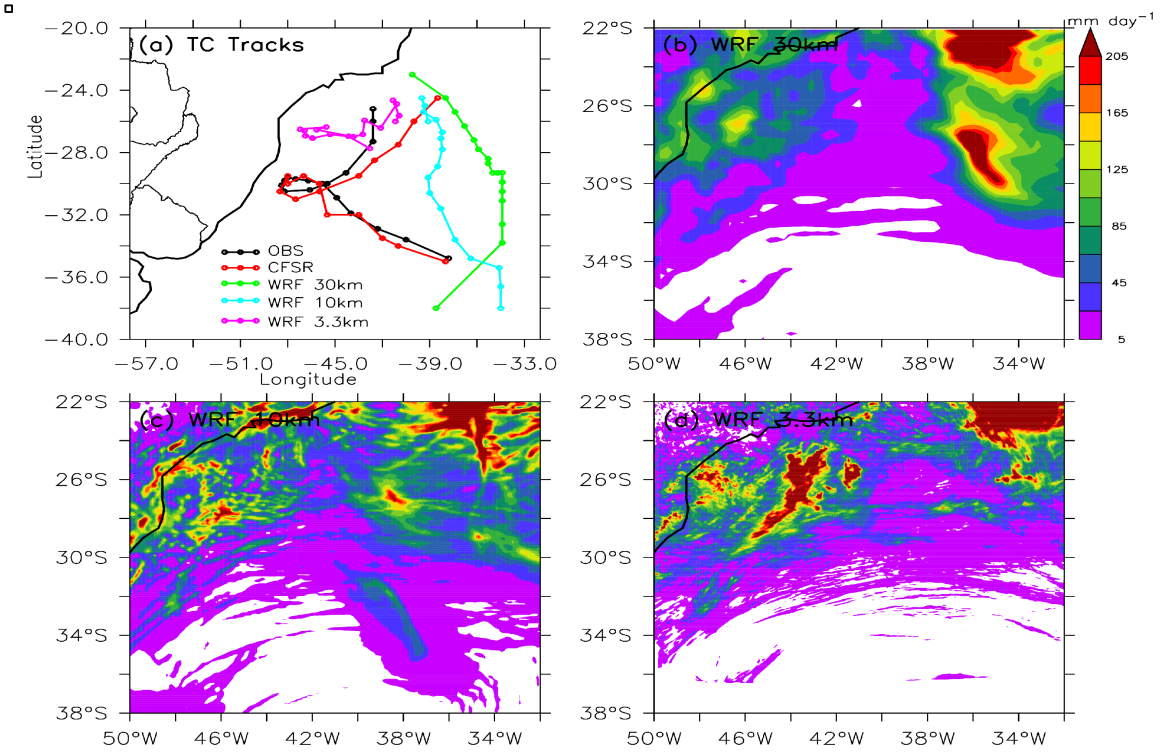


**Figure 4.16**: As in Figure 4.10, but for Hurricane Anita

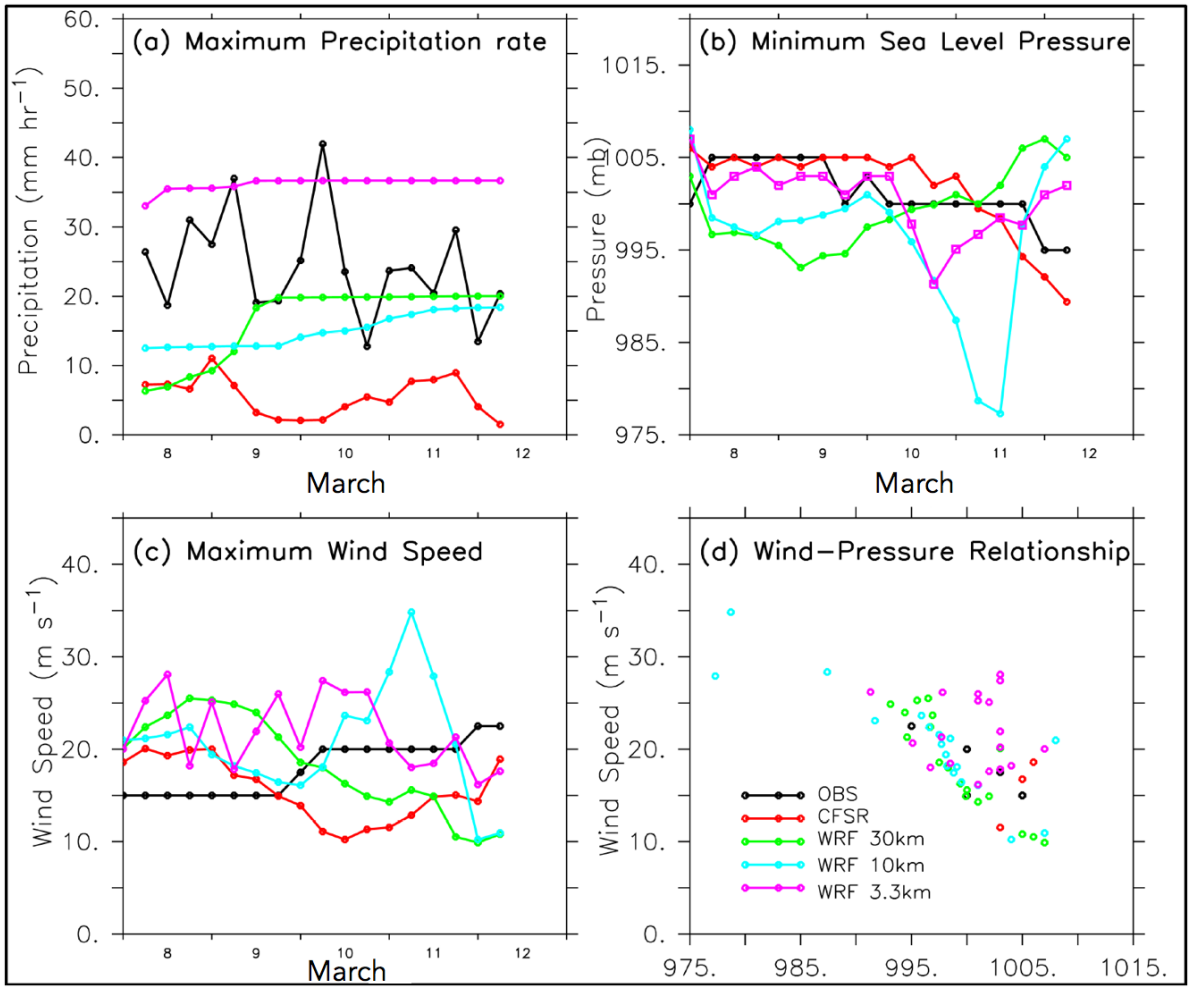


**Figure 4.17**: As in Figure 4.11, but for Hurricane Anita

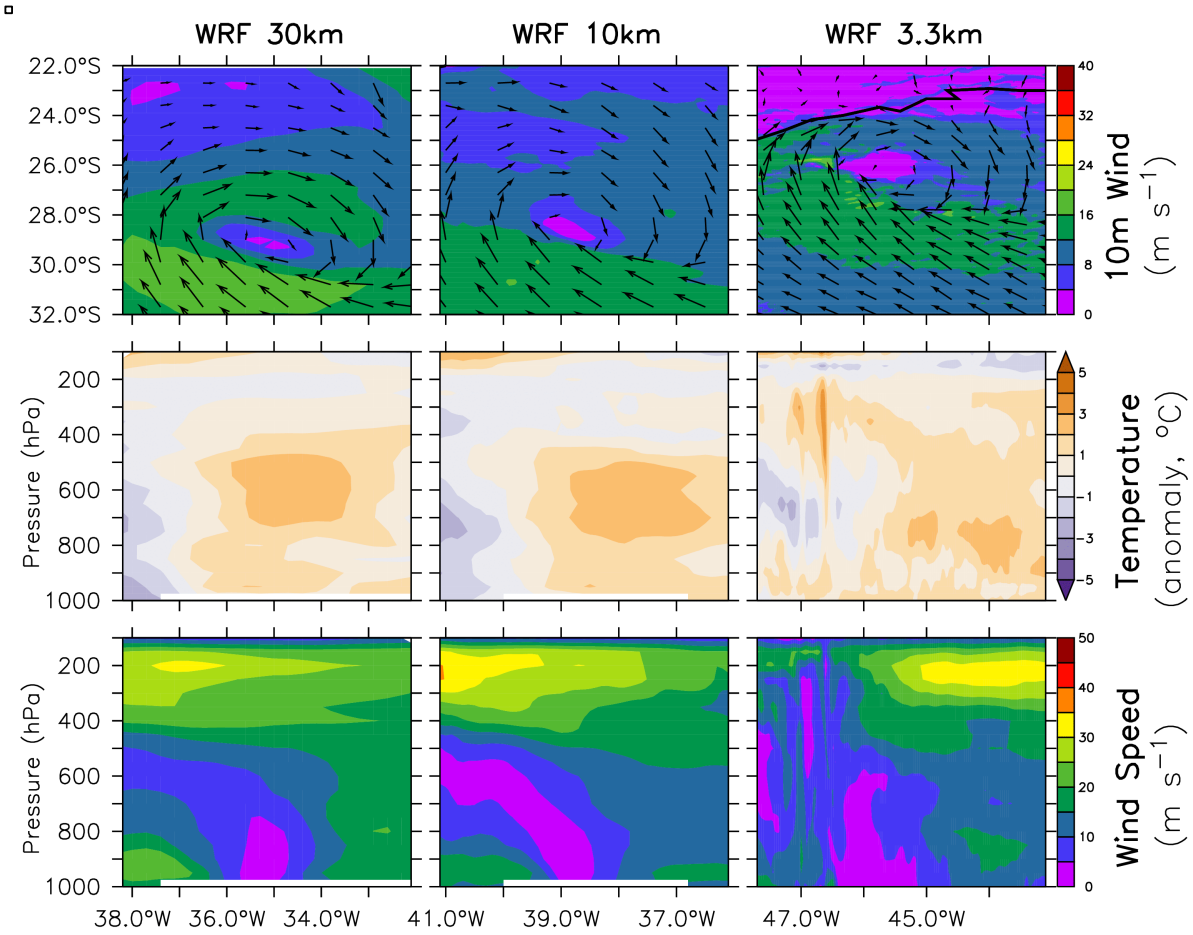


**Figure 4.18**: As in Figure 4.12, but for Hurricane Anita

# 5 Conclusion and Recommendations

## 5.1 Summary

As part of the efforts towards obtaining reliable tools in providing early warning systems on hurricane occurrences and studying the impacts of climate on hurricanes over the coastal communities of the SAO, this study has investigated the characteristics of observed and simulated hurricanes over the SAO. The objectives of the study were to examine the characteristics of two hurricanes (Catarina and Anita) over the SAO, the relationship between the SACZ and the two hurricanes, the capability of an atmospheric model (WRF) in simulating the hurricanes, and the sensitivity of the simulated hurricanes to horizontal resolution and boundary condition forcing. The characteristics of the hurricanes considered in the study include the path of each hurricane, their intensity (*i.e.* surface pressure, wind speed and rainfall), as well as their vertical and horizontal structures.

To achieve these objectives, observation (IBT and TRMM), reanalysis (ERAINT and CFSR), and atmospheric model simulation (WRF) datasets were analysed over the lifecycle periods of the two hurricanes (25 to 29 March 2004 and 8 to 12 March 2010). To investigate the role of resolution on the characteristics of the simulated hurricanes, the WRF simulations were performed at three resolutions (30 km, 10 km and 3.3 km). To study the impacts of boundary forcing on the hurricanes' characteristics, the WRF simulations were forced with the two reanalysis datasets. The capability of the reanalyses and the WRF simulations in representing hurricanes were obtained by comparing the results with the observations.

The results of the study can be summarized as follows:

- While Hurricane Catarina and Hurricane Anita have some commonalties, the two systems are distinct in their tracks and intensity. While Catarina travelled westward and made landfall in Santa Catarina, Anita first travelled south, then southwest (towards the coast without making landfall), and then southeast before dissipating over the SAO. Catarina reached category-2 status while Anita only reached category 1. However, Anita propagated faster than Catarina did.
- The CFSR reanalysis produced a better representation of both hurricanes than what ERAINT produced. In the CFSR results, the tracks and intensity of the hurricanes

were closer to the observation than they were in the ERAINT results. Nevertheless, both reanalyses underestimated the intensity of Hurricane Catarina and failed to capture the temporal variability of its intensity. The shortcomings of these reanalyses may be related to their horizontal resolution.

- Both reanalyses showed the presence of the SACZ during the active stages of both hurricanes and indicated that the convective activities in the SACZ are linked with the hurricanes. This suggests that the convergence of moisture along the SACZ may provide the moisture needed to fuel both hurricanes.
- WRF provides a realistic simulation of both hurricanes, but the model simulated the characteristics of Hurricane Catarina better than it simulated the characteristics of Hurricane Anita.
- The simulation of the hurricanes with WRF was sensitive to both horizontal resolution and boundary condition forcing. For both hurricanes, the model simulated a better track with ERAINT forcing than with CFSR forcing. This means that using a better reanalysis as the boundary forcing may not necessarily improve the quality of the simulated hurricane. With CFSR forcing, the quality of the simulated hurricane increased with the higher resolution, but with ERAINT forcing, the 10 km WRF simulation performed better than 30 km and 3.3 km simulations. This suggests that with ERAINT forcing, the 10 km simulation may be WRF's optimum resolution for simulating and studying the characteristics of Hurricane Catarina. However, for all resolutions and with all boundary forcing, the WRF simulations failed to reproduce the temporal variation of Hurricane Catarina as observed.

## 5.2 Recommendations

The results presented in this study can be reinforced in many ways. For example, early hurricane warning systems require multi-simulation ensembles from many models. There is therefore a need to test the robustness of the results presented in this study with more simulations. For instance, as the present study only used forcing data from two reanalyses, using forcing data from more reanalyses and from global climate models will make the information more robust in terms of the impacts of boundary forcing on the WRF simulations. Similarly, using more observational datasets will ensure limitations thereof do not influence the study analysis. In addition, only the WRF model was used in the present

study. Extending the study to other regional models will help establish the sensitivity of the results presented here to limited areas or regional climate models. Furthermore, while the present study focused on the impact of resolution, the simulated hurricanes (*e.g.* Hurricane Catarina) may also be sensitive to the actual model and the microphysics used in its configuration. The performance of the highest resolution simulation (*e.g.* CEW03 and CCW03) might improve by optimising the parameters of the microphysics parameterization or by using other microphysics. Nevertheless, the simulations that will implement these recommendations would require massive computational resources, which may not be available in developing countries like Brazil, where the coastal communities may be impacted by the future hurricanes from SAO.

Moreover, the present study has only focussed on STs that transitioned into hurricanes over the SAO; meanwhile, there were many STs that did not develop into TCs over the basin. More studies on why these STs did not transition into TCs, and the possibility of them doing so under projections of a warmer climate, will be helpful in preparing the SAO coastal communities for the possible impacts climate change may have on TC-related risks in the future. Such studies may also consider the influence of further expansions of the Hadley cells on the transition of STs to hurricanes.

Nevertheless, the present study has shown that the quality of hurricane simulations with WRF depends on the model horizontal resolution and on the dataset used for the lateral forcing. It showed that while the simulation with the highest resolution may not necessarily give the best simulation, the simulation with a better boundary forcing may not automatically produce a better simulation of the hurricane either. The results of this study have implications for using WRF for hurricane forecasting and for studying the impacts of future climate change on hurricanes over the SAO.

# References


Arizona State University. World Weather/Climate Extremes Archive. (unknown date). *First identified South Atlantic hurricane*. [Online]. Available: https://wmo.asu.edu/content/first-south-atlantic-tropical-cyclone (accessed 24 April 2016)

Arruza, T. The Weather Company. 2013. Hurricane safety and preparedness: *Tracking hurricanes*. [Online]. Available: https://weather.com/safety/hurricane/news/tracking-hurricanes-20120330 (accessed 22 February 2017)

Australian Government: Bureau of Meteorology. 2017. *Severe Tropical Cyclone Laurence*. [Online]. Available: http://www.bom.gov.au/cyclone/history/laurence09.shtml (accessed 28 February 2017)

Australian Government: Bureau of Meteorology. (unknown date). *Tropical Cyclone Audrey*. [Online]. Available: http://www.bom.gov.au/cyclone/nt/Audrey1964.shtml (accessed 28 February 2017)

Bonatti J. P., and Rao, V. B. 1987. Moist baroclinic instability of North Pacific and South American intermediate-scale disturbances. *Journal of the Atmospheric Sciences of the American Meteorological Society*, 44 (18): 2657 – 2667

Bonatti J. P., Rao V. B., and Silva Dias P. L. 2006. On the westward propagation of Catarina storm. *International Conference on Southern Hemisphere Meteorology and Oceanography*, 8: 1659 – 1675

Bureau of Meteorology. 2017. Tropical Cyclones: About Tropical Cyclones: *What is a Tropical Cyclone?* [Online]. Available: http://www.bom.gov.au/cyclone/about/ (accessed 28 January 2017)

Carlson, T. N. and Boland, F. E. 1978. Analysis of urban-rural canopy using a surface heat flux/temperature model. *Journal of Applied Meteorology*, 17 (7): 998 – 1013

Carvalho L. M. V., Jones C., and Liebmann B. 2004. The South Atlantic Convergence Zone: Intensity, form, persistence, and relationships with intraseasonal to interannual activity and extreme rainfall. *Journal of Climate of the American Meteorological Society*, 17 (1): 88 – 108

Chaves, R. R. and Nobre, P. 2004. Interactions between sea surface temperature over the South Atlantic Ocean and the South Atlantic Convergence Zone. *Geophysical Research Letters*, 31 (3): 1 – 4

Chauvin F., Royer J-F., and Déqué M. 2006. Response of hurricane-type vortices to global warming as simulated by ARPEGE-Climat at high resolution. *Climate Dynamics*, 27 (4): 377 – 399

da Rocha, R. P. and Caetano, E. 2010. The role of convective parameterization in the simulation of a cyclone over the South Atlantic. *Atmósfera*, 23 (1): 1 – 23

de Menezes, V. V. and Vianna, M. L. 2011. *A multisatellite data study of the interactions of Hurricane Catarina (2004) with the mesoscale structures of the Southwestern Atlantic Ocean upper-layer*. [Online]. Available: http://www.dsr.inpe.br/sbsr2011/files/p1351.pdf (accessed 31 January 2017)

Dee D. P., Uppala S. M., Simmons A. J., Berrisford P., Poli P., Kobayashi S., Andrae U., Balmaseda M. A., Balsamo G., Bauer P., Bechtold P., Beljaars A. C. M., van de Berg L., Bidlot J., Bormann N., Delsol C., Dragani R., Fuentes M., Geer A. J., Haimberger L., Healy S. B., Hersbach H., Hólm E. V., Isaksen L., Kållberg P., Köhler M., Matricardi M., McNally A. P., Monge-Sanz B. M., Morcrette J.-J., Park B.-K., Peubey C., de Rosnay P., Tavolato C., Thépaut J.-N., and Vitart F. 2011. The ERAINT reanalysis: configuration and performance of the data assimilation

system. *Quarterly Journal of the Royal Meteorological Society*, 137 (656): 553 – 597

Dias Pinto J. R., Reboita M. S., and da Rocha R. P. da. 2013. Synoptic and dynamical analysis of subtropical cyclone Anita (2010) and its potential for tropical transition over the South Atlantic Ocean. *Journal of Geophysical Research: Atmospheres*, 118 (19): 10870 – 10883

Doyle, M. E. and Barros, V. R. 2002. Midsummer low-level circulation and precipitation in subtropical South America and related sea surface temperature anomalies in the South Atlantic. *Journal of Climate of the American Meteorological Society*, 15 (23): 3394 – 3410

Dudhia, J. 1989. Numerical study of convection observed during the winter monsoon experiment using a mesoscale two-dimensional model. *Journal of the Atmospheric Sciences of the American Meteorological Society*, 46 (20): 3077 – 3107

Dudhia, J. 2016. *WRF Modeling System Overview*. [Online]. Available: http://www2.mmm.ucar.edu/wrf/users/tutorial/201601/overview.pdf (accessed 11 May 2016)

Dutra L. M. M., da Rocha R. P., Lee R. W., Peres J. R. R, and de Camargo R. 2017. Structure and evolution of Subtropical Cyclone Anita as evaluated by heat and vorticity budgets. *Quarterly Journal of the Royal Meteorological Society*, 143 (702): 1 – 21

Emanuel, K. 2003. Tropical cyclones. *Annual Review of Earth and Planetary Sciences*, 31: 75 – 104

Encyclopædia Britannica, Inc. 2017. *Atlantic Ocean: with depth contours and submarine features*. [Online]. Available: https://www.britannica.com/place/Atlantic-Ocean#ref408452 (accessed 21 May 2017)

Evans J. L. and Braun A. 2012. A climatology of subtropical cyclones in the South Atlantic. *Journal of Climate of the American Meteorological Society*, 25 (21): 7328 – 7340

Evans J. P., Ekström M., and Ji F. 2012. Evaluating the performance of a WRF physics ensemble over south-east Australia. *Climate Dynamics*, 39 (6): 1241

Frank, W. M. and Ritchie E. A. 2001. Effects of Vertical Wind Shear on the Intensity and Structure of Numerically Simulated Hurricanes. *Monthly Weather Review of the American Meteorological Society*, 129 (9): 2249 – 2269

Garcia, S. R. and Kayano, M. T. 2010. Some evidence on the relationship between the South American monsoon and the Atlantic ITCZ. *Theoretical and Applied Climatology*, 99 (1): 29 – 38

Garreaud R. D., Vuille M., Compagnucci R., and Marengo J. 2008. Present-day South American climate. *Palaeogeography, Palaeoclimatology, Palaeoecology – An International Journal for the Geo-Sciences*, 281 (3 – 4): 180 – 195

Google Earth 7.1.1.1888. 2013. *Study Area polygon from 0N to 39S and 53W to 24E*. [Online]. Available: http://www.google.com/earth/index.html (accessed 27 September 2013)

Government of South Africa. 2017. *Geography and climate*. [Online]. Available http://www.gov.za/about-sa/geography-and-climate (accessed 21 May 2017)

Gutro, R. 2010. NASA's Goddard Space Flight Center: Hurricanes/tropical cyclones: Hurricane season 2010: *Tropical Storm 90Q (Southern Atlantic)*. [Online]. Available:

http://www.nasa.gov/mission_pages/hurricanes/archives/2010/h2010_90Q.html (accessed 22 February 2015)

Hall W. D., Rasmussen R. M., and Thompson G. 2005. The new Thompson microphysical scheme in WRF. Preprints, *2005 WRF/MM5 User's Workshop*, Boulder, CO, NCAR, 6.1.

Henson, B. 2005. *What was Catarina? Forecasters, researchers debate nature of Brazil's mystery storm*. [Online]. Available: http://www.ucar.edu/communications/quarterly/summer05/catarina.html (accessed 07 September 2014)

Hill, M. and Nhamire, B. Business Live. 2017. *Tropical cyclone Dineo pounds Mozambique, nears SA*. [Online]. Available: https://www.businesslive.co.za/bd/world/africa/2017-02-17-tropical-cyclone-dineo-pounds-mozambique-nears-sa/ (accessed 28 February 2017)

Holland, G. and Bruyere, C. L. 2014. Recent intense hurricane response to global climate change. *Climate Dynamics*, 42 (3): 617 – 627

Hong S. Y., Noh Y., and Dudhia J. 2006. A new vertical diffusion package with an explicit treatment of entrainment processes. *Monthly Weather Review of the American Meteorological Society*, 134 (9): 2318 – 2341

Huffman G. J., Adler R. F., Bolvin D. T., Gu G., Nelkin E. J., Bowman K. P., Hong Y., Stocker E. F., and Wolff D. B. 2007. The TRMM Multisatellite Precipitation Analysis (TMPA): Quasi-global, multiyear, combined-sensor precipitation estimates at fine scales. *Journal of Hydrometeorology of the American Meteorological Society*, 8 (1): 38 – 55

InfoNamibia. 2017. *Climate and weather of Namibia*. [Online]. Available: http://www.info-namibia.com/info/namibia-weather (accessed 21 May 2017)

Jones, J. CNN: Extreme Weather. 2017. *The newest high-resolution weather images from space are here*. [Online]. Available: http://edition.cnn.com/2017/01/23/us/weather-first-images-goes-16/index.html (accessed 22 February 2017)

Kain J. S. 2004. The Kain–Fritsch convective parameterization scheme: An update. *Journal of Applied Meteorology of the American Meteorological Society*, 43 (1): 170 – 181

Kain J. S. and Fritsch J. M. 1993. Convective parameterization for mesoscale models: The Kain–Fritsch scheme. *The Representation of Cumulus Convection in Numerical Models, Meteorological Monograph of the American Meteorological Society*, 24 (46): 165 – 170

Klotzbach, P. J. 2006. Trends in global tropical cyclone activity over the past twenty years (1986–2005). *Geophysical Research Letters: An AGU Journal*, 33 (10): 1 – 4

Knapp K. R., Kruk M. C., Levinson D. H., Diamond H. J., and Neumann C. J. 2010. The International Best Track Archive for Climate Stewardship (IBTrACS): Unifying tropical cyclone best track data. *Bulletin of the American Meteorological Society*, 91 (3): 363 – 376

Knutson T. R., McBride J. I., Chan J., Emanuel K., Holland G., Landsea C., Held I., Kossin J. P., Srivastava A. K., and Sugi M. 2010. *Nature Geoscience*, 3: 157 – 163

Kuo Y.H. and Low-Nam S. 1990. Prediction of nine explosive cyclones over the western Atlantic Ocean with a regional model. *Monthly Weather Review of the American Meteorological Society*, 118 (1): 3 – 25

Landsea, C. NOAA: Hurricane Research Division. 2011a. *Subject: A1) What is a hurricane, typhoon, or tropical cyclone?* [Online]. Available: http://www.aoml.noaa.gov/hrd/tcfaq/A1.html (accessed 21 February 2017)

Landsea, C. NOAA: Hurricane Research Division. 2011b. *Subject: A6) What is a sub-tropical cyclone?* [Online]. Available: http://www.aoml.noaa.gov/hrd/tcfaq/A6.html (accessed 21 February 2017)

Landsea, C. NOAA: Hurricane Research Division. 2013. *Subject: E9) Which tropical cyclones have caused the most deaths and most damage?* [Online]. Available: http://www.aoml.noaa.gov/hrd/tcfaq/E9.html (accessed 24 February 2017)

Landsea, C. NOAA: Hurricane Research Division. 2014. *Subject: A15) How do tropical cyclones form?* [Online]. Available: http://www.aoml.noaa.gov/hrd/tcfaq/A15.html (accessed 21 February 2017)

Landsea, C. NOAA: Hurricane Research Division. 2015. *Subject: E11) How many tropical cyclones have there been each year in the Atlantic basin? What years were the greatest and fewest seen?* [Online]. Available: http://www.aoml.noaa.gov/hrd/tcfaq/E11.html (accessed 24 February 2017)

Landsea, C. and Aberson, S. NOAA: Hurricane Research Division. 2014. *Subject: C2) Doesn't the friction over land kill tropical cyclones?* [Online]. Available: http://www.aoml.noaa.gov/hrd/tcfaq/C2.html (accessed 21 February 2017)

Landsea, C. and Delgado, S. NOAA: Hurricane Research Division. 2016. *Subject: E10) What are the average, most, and least tropical cyclones occurring in each basin?* [Online]. Available: http://www.aoml.noaa.gov/hrd/tcfaq/E10.html (accessed 24 February 2017)

Levinson, DH. 2005. State of the climate in 2004. *Bulletin of the American Meteorological Society*, 86 (6): 1 – 86

Liebmann B., Kiladis G. N., Vera C. S., Saulo A. C., and Carvalho L. M. V. 2004. Subseasonal variations of rainfall in South America in the vicinity of the low-level jet

east of the Andes and comparison to those in the South Atlantic Convergence Zone. *Journal of Climate of the American Meteorological Society*, 17 (19): 3829 – 3842

Liu Y., Zhang D.-L., and Yau M. K. 1997. A multiscale numerical study of Hurricane Andrew (1992). Part I: Explicit simulation and verification. *Monthly Weather Review of the American Meteorological Society*, 125 (12): 3073 – 3093

Lorenz D. J., DeWeaver E. T, and Vimont D. J. 2010. Evaporation change and global warming: The role of net radiation and relative humidity. *Journal of Geophysical Research: Atmospheres – an AGU Journal*, 115 (D20): 1 – 13

Ma H.-Y., Ji X., Neelin J. D., and Mechoso C. R. 2011. Mechanisms for precipitation variability of the eastern Brazil/SACZ convective margin. *Journal of Climate of the American Meteorological Society*, 24 (13): 3445 – 3456

Marcelino, E. V., de Oliveira Marcelino, I. P. V., and de Moraes Rudorff, F. 2004. *Cyclone Catarina: Damage and vulnerability assessment*. Natural Disaster Research Group, Geosciences Department, Santa Catarina Federal University, Florianópolis, Santa Catarina, Brazil. Pg. 1 – 14

Marshak, S. 2008. *Earth: Portrait of a planet*. New York and London: W. W. Norton and Company. Pg.: 706, 707 and 716

McTaggart-Cowan R., Bosart L. F., Davis C. A., Atallah E. H., Gyakum J. R., and Emanuel K. A. 2006. Analysis of Hurricane Catarina (2004). *Monthly Weather Review of the American Meteorological Society*, 134 (11): 3029 – 3053

Meyer, A. 2010. *Brazil Climate*. [Online]. Available: http://www.brazil.org.za/climate.html (accessed 21 May 2017)

Mlawer E. J., Taubman S. J., Brown P. D., Iacono M. J., and Clough S. A. 1997. Radiative transfer for inhomogeneous atmosphere: RRTM, a validated correlated-k model for

the longwave. *Journal of Geophysical Research: Atmospheres: Papers on Climate and Atmospheric Physics*, 102 (D14): 16663 – 16682

Monin, A. S. and Obukhov A. M. 1954. Basic laws of turbulent mixing in the surface layer of the atmosphere. *Contributions of the Geophysical Institute of Academy of Sciences*, USSR, (151), 163 – 187 (in Russian)

NASA: Earth Observatory. 2000. *Hurricanes: The greatest storms on earth*. [Online]. Available: http://earthobservatory.nasa.gov/Features/Hurricanes/Archive/original.pdf (accessed 27 March 2016)

NASA: Earth Observatory. LANCE/EOSDIS MODIS Rapid Response Team. 2014. *Tropical Cyclone Cristina*. [Online]. Available: http://earthobservatory.nasa.gov/IOTD/view.php?id=83863 (accessed 17 February 2017)

Nations Encyclopedia. 2017. *Angloa – Climate*. [Online]. Available: http://www.nationsencyclopedia.com/Africa/Angola-CLIMATE.html (accessed 21 May 2017)

NOAA. U.S. Department of Commerce. 1999. *Hurricane basics*. [Online]. Available: https://www.hsdl.org/?view&did=34038 (accessed 03 October 2013)

NOAA: NCEP: The Hydrometeorological Prediction Center. 2010. *South American Synopsis*. [Online]. Available: http://www.hpc.ncep.noaa.gov/discussions/fxsa20.html and archived at http://www.webcitation.org/5o7vOfDzk on 10 March 2010 (accessed 23 November 2014)

NOAA. National Weather Service: Central Pacific Hurricane Center. 2016. *Tropical cyclone climatology*. [Online]. Available:

http://www.prh.noaa.gov/cphc/pages/FAQ/Climatology.php (accessed 17 February 2017)

Oouchi K., Yoshimura J., Yoshimura H., Mizuta R., Kusunoki S., and Noda A. 2006. Tropical cyclone climatology in a global-warming climate as simulated in a 20 km-mesh global atmospheric model: Frequency and wind intensity analyses. *Journal of the Meteorological Society of Japan*, 84 (2): 259 – 276

Paegle J. N. and Mo K. C. 2002. Linkages between Summer Rainfall Variability over South America and Sea Surface Temperature Anomalies. *Journal of Climate of the American Meteorological Society*, 15 (12): 1389 – 1407

Pasch, R. J. and Zelinsky D. A. National Hurricane Center: Tropical cyclone report. 2014. *Hurricane Manuel*. [Online]. Available: http://www.nhc.noaa.gov/data/tcr/EP132013_Manuel.pdf (accessed 24 February 2017)

Pereira Filho A. J., Pezza A. B., Simmonds I., Silva Lima R., and Vianna M. 2010. New perspectives on the synoptic and mesoscale structure of Hurricane Catarina. *Atmospheric Research*, 95 (2-3): 157 – 171

Pereria Filho A. J. and Lima R. S. 2006. Synoptic and mesoscale analysis of Hurricane Catarina, Brazil. *Proceedings of the 8$^{th}$ International Conference on Southern Hemisphere Meteorology and Hydrology*. Pg. 1901 – 1907

Peterson R. G. and Stramma L. 1991. Upper-level circulation in the South Atlantic Ocean. *Progress in Oceanography*, 26 (1): 1 – 73

Pezza A. B. and Simmonds I. 2005. The first South Atlantic hurricane: unprecedented blocking, low shear and climate change. *Geological Research Letters*, 32 (15): 1 – 5

Pezza A. B. and Simmonds I. 2006. Catarina: The first South Atlantic hurricane and its association with vertical wind shear and high latitude blocking. *International Conference on Southern Hemisphere Meteorology and Oceanography,* 8 (2006): 353 – 364

Pezza A. B., Simmonds I., and Pereiro Filho A. J. 2009. Climate perspective on the large-scale circulation associated with the transition of the first South Atlantic hurricane. *International Journal of Climatology*, 29 (8): 1116 – 1130

Pidwirny, M. Fundamentals of Physical Geography, 2nd Edition. 2006a. *Tropical weather and hurricanes*. [Online]. Available: http://www.physicalgeography.net/fundamentals/7u.html (accessed 29 March 2016)

Pidwirny, M. Fundamentals of Physical Geography, 2nd Edition. 2006b. *The Mid-Latitude Cyclone*. [Online]. Available: http://www.physicalgeography.net/fundamentals/7s.html (accessed 29 January 2017)

Pielke Jr. R. A., Landsea C., Mayfield M., Laver J., and Pasch R. 2005. Hurricanes and global warming. *Bulletin of the American Meteorological Society*, 86 (11): 1571 – 1575

Przyborski, P. NASA Earth Observatory. 2004. *Beautiful blooms in South Atlantic Ocean*. [Online]. Available: http://earthobservatory.nasa.gov/NaturalHazards/view.php?id=5123 (accessed 30 January 2017)

Robertson, A. W. and Mechoso, C. R. 2000. Interannual and interdecadal variability of the South Atlantic Convergence Zone. *Monthly Weather Review of the American Meteorological Society*, 128 (8): 2947 – 2957

Radu R., Toumi R., and Phau J. 2014. Influence of atmospheric and sea surface temperature on the size of hurricane Catarina. *Quarterly Journal of the Royal Meteorological Society*, 140 (682): 1778 – 1784

Saha S., Moorthi S., Pan H., Wu X., Wang J., Nadiga S., Tripp P., Kistler R., Woollen J., Behringer D., Liu H., Stokes D., Grumbine R., Gayno G., Wang J., Hou Y., Chuang H., Juang H. H., Sela J., Iredell M., Treadon R., Kleist D., Van Delst P., Keyser D., Derber J., Ek M., Meng J., Wei H., Yang R., Lord S., van den Dool H., Kumar A., Wang W., Long C., Chelliah M., Xue Y., Huang B., Schemm J., Ebisuzaki W., Lin R., Xie P., Chen M., Zhou S., Higgins W., Zou C., Liu Q., Chen Y., Han Y., Cucurull L., Reynolds R. W., Rutledge G., and Goldberg M. Research Data Archive at the National Center for Atmospheric Research, Computational and Information Systems Laboratory. 2010. *NCEP Climate Forecast System Reanalysis (CFSR) 6-hourly products, January 1979 to December 2010.* [Online]. Available: http://dx.doi.org/10.5065/D69K487J (accessed 29 May 2013)

Santos A. F., Mendonça A. M., Bonatti J. P., de Mattos J. G. Z., Kubota P. Y., Freitas S. R., Silva Dias M. A. F., Ramirez E., and Camayo R. 2008. Evaluation of the CPTEC/AGCM wind forecast during the hurricane Catarina occurrence. *Advances in Geosciences – European Geosciences Union*, 14: 317 – 326

Schmaltz, J. NASA: Earth Observatory. 2007. *Subtropical Storm Andrea*. [Online]. Available: http://earthobservatory.nasa.gov/IOTD/view.php?id=7666 (accessed 23 February 2017)

Schmaltz, J. NASA: Earth Observatory. 2011. *Mid-Latitude Cyclone over the United States*. [Online]. Available: http://earthobservatory.nasa.gov/NaturalHazards/view.php?id=52297 (accessed 17 February 2017)

Schott T., Landsea C., Hafele G., Lorens J., Taylor A., Thurm H., Ward B., Willis M., and Zaleski W. 2012a. *Saffir-Simpson hurricane wind scale extended table.* [Online].

Available: http://www.nhc.noaa.gov/pdf/sshws_table.pdf (accessed 28 January 2017)

Schott T., Landsea C., Hafele G., Lorens J., Taylor A., Thurm H., Ward B., Willis M., and Zaleski W. 2012b. *Minor modification to Saffir-Simpson hurricane wind scale for the 2012 hurricane season*. [Online]. Available: http://www.nhc.noaa.gov/pdf/sshws_2012rev.pdf (accessed 28 January 2017)

Silva Dias P. L., Gan M., Beven J. L., Pezza A., Holland G., Pereira A., McTaggart-Cowan R., Diniz F. A., Seluchi M., and Braga H. J. 2006. The Catarina phenomenon. *Tropical Meteorology Research Program Report Series*, 72 (1): 329 – 360. [Online]. Available: http://severe.worldweather.wmo.int/iwtc/document/Topic_2a_Pedro_Silva_Dias.pdf (accessed 02 April 2013)

Silvestri G. E. and Vera C. S. 2003. Antarctic Oscillation signal on precipitation anomalies over southeastern South America. *Geophysical Research Letters: An AGU Journal*, 30 (21): 1 – 4

Singer, M. NOAA: Climate.gov. 2014. *2013 State of the Climate: Record-breaking Super Typhoon Haiyan.* [Online]. Available: https://www.climate.gov/news-features/understanding-climate/2013-state-climate-record-breaking-super-typhoon-haiyan (accessed 28 February 2017)

Seluchi, M. E. and Marengo, J. A. 2000. Tropical-midlatitude exchange of air masses during summer and winter in South America: Climatic aspects and examples of intense events. *International Journal of Climatology*, 20 (10): 1167 – 1190

Skamarock W. C., Klemp J. B., Dudhia J., Gill D. O., Barker D. M., Duda M. G, Huang X.-Y., Wang W., and Powers J. G. 2008. *A description of the Advanced Research WRF Version 3*. NCAR Tech. Note NCAR/TN-475+STR, 113 pp. doi:10.5065/D68S4MVH

Smithson P., Addison K., and Atkinson K. 2008. *Fundamentals of the physical environment*. London and New York: Routledge – Taylor and Francis Group. Pg. 135 – 137, 142 – 144, 167 and 147

Todd M. C, Washington R., and Palmer P. I. 2004. Water vapour transport associated with tropical-temperate trough systems over southern Africa and the southwest Indian Ocean. *International Journal of Climatology*, 24 (5): 555 – 568

Tsutsui, J. 2002. Implications of anthropogenic climate change for tropical cyclone activity: A case study with the NCAR CCM2. *Journal of the Meteorological Society of Japan*, 80 (1): 45 – 65

Vasquez, T. Weatherwise. 2009. *The Intertropical Convergence Zone*. [Online]. Available: http://www.weatherwise.org/Archives/Back%20Issues/2009/Nov-Dec%202009/full-Intertropical-Converge.html (accessed 24 April 2016)

Veiga J. A. P., Pezza A. B., Simmonds I., and Silva Dias P. L. 2008. An analysis of the environmental energetics associated with the transition of the first South Atlantic hurricane. *Geophysical Research Letters: An AGU Journal*, 35 (15): 1 – 6

Vera C., Higgins W., Amador J., Ambrizzi T., Garreaud R., Gochis D., Gutzler D., Lettenmaier D., Marengo J., Mechoso C. R., Nogues-Paegle J., Silva Dias P. L., and Zhang C. 2006. Toward a unified view of the American monsoon systems. *Journal of Climate of the American Meteorological Society*, 19 (20): 4977 – 5000

Vianna M. L., Menezes V. V., Pezza A. B., and Simmonds I. 2010. Interactions between Hurricane Catarina (2004) and warm core rings in the South Atlantic Ocean. *Journal of Geophysical Research: Oceans – an AGU Journal*, 115 (C7): 1 – 19

Walsh K. J. E., Fiorino M., Landsea C. W., and McInnes K. L. 2007. Objectively determined resolution-dependent threshold criteria for the detection of tropical

cyclones in climate models and reanalysis. *Journal of Climate of the American Meteorological Society*, 20 (10): 2307 – 2314

Webster P. J., Holland G. J., Curry J. A., and Chang H.-R. 2005. Changes in tropical cyclone number, duration, and intensity in a warming environment. *Science*, 309 (5742): 1844 – 1846

Zimmermann, K. A. Live Science: Planet Earth. 2012. *Hurricanes, Typhoons and Cyclones: Storms of Many Names*. [Online]. Available: http://www.livescience.com/22177-hurricanes-typhoons-cyclones.html (accessed 29 January 2017)